Absolute Flux Calibration For Prime STIS Echelle Modes With The 0.2x0.2" Slit

Ralph Bohlin
Space Telescope Science Institute
1998 June

ABSTRACT

Point source sensitivity curves for the 0.2x0.2 arcsec entrance aperture are derived for the 12 prime echelle medium and high dispersion modes, which collectively span a wavelength range from 1140Å to 3150Å. The sensitivity for each order is determined from observations of spectrophotometric standard stars by fitting a set of spline nodes to the ratio of the observed count rate divided by the standard star flux. Since both the average absolute sensitivity and the shape of the ripple correction are expected to change smoothly with echelle order number, the effects of spectral features are avoided by masking the strongest absorption lines and then fitting smooth functions of order number.

In general, the uncertainty in the calibration is determined by the number of observations, by the repeatability among the observations, and by the uncertainty of 3% in the absolute fluxes of the standard stars. A 3% repeatability limit is set by the observed drop in the global count rate between a pair of observations of G191B2B with E140M on consecutive orbits, where the spectra were at the same place on the FUV MAMA within 1 pixel. Since most of the echelle modes have only one observation, the above two 3% uncertainties combine in quadrature to a 4% one sigma expectation for the bulk of the coverage. For the worst case at 1151Å, scatter about the average of +10 to -7% is caused by a low signal level that is near the background. There are greater uncertainties for the particular cases of E140H-1234 and E140H-1598. These calibrations are based on BD+75 325, where a plethora of absorption lines at wavelengths below 1900Å, confuses the analysis and causes errors of 10-20% in the relative flux within one order.

1. Analysis Method

Echelle spectrographs are often calibrated with a semi-empirical approach of adjusting grating constants to fit the data, cf. Heap and Brown (1997). Using an entirely empirical method, echelle sensitivity calibrations can be derived by dividing the observed countrates by the known flux of a standard star, as described for STIS low dispersion by Bohlin, Collins, & Gonnella (1998). In practice, there are many absorption lines in the STIS echelle spectra that complicate the analysis. Most of these lines are narrower than the resolution of the standard star spectra, which are from FOS for BD+28 4211 and BD+75 325. Consequently, the reference standard star spectra are smooth with undulations at the few percent level, except for a handful of strong lines. Upon dividing the echelle net countrate spectrum by the standard star flux, the absorption lines still appear as sharp absorption features in these raw sensitivities as illustrated in Figure 1. Since these narrow features in the extracted spectrum typically extend to depths of 10-50% and sometimes reach zero or go negative because of interorder scattered light, the spline curve fits to the raw sensitivities are often biased low, as in Figure 1 near the strong HeII line at 1640.5Å. The trick of binning the high-resolution stis spectra to the lower resolution standard star spectra fails because the STIS sensitivity varies within the standard star resolution element of 1-2Å. For example, even the E140M resolution is ~55 STIS px per FOS standard star resolution element.

Thus, the following procedure is used for deriving order-by-order sensitivities from echelle spectra of stars with standard star reference spectra of lower spectral resolution:

1. For each order m, fit a smooth curve to the unfiltered raw sensitivities with 7 spline nodes (or 9 for E230M), ignoring points with bad data quality. Since the standard star spectrum for G191B2B is a pure hydrogen model with only the Ly-α absorption line, median filter the 1024 point STIS arrays for G191B2B with a 65 point median filter to minimize effects of the many weak absorption lines.

2. For each order, define the average sensitivity, A, as the average of the 7 (or 9) spline nodes; and plot this raw average sensitivity vs. echelle order count. (See section 3 and Figure 3.) Define the best estimate of the actual average sensitivity by a set of spline nodes that fits the log of the valid average sensitivity points within the scatter of the data, in analogy with the low dispersion sensitivity vs. wavelength (Bohlin, Collins, & Gonnella 1998). The strongest lines like Ly-α and seven others invalidate the average sensitivity for a few orders.

3. Enforce continuity in the shape of the ripple correction, R, from order to order by fitting the raw sensitivity of each of the 7 (or 9) sets of spline nodes divided by the average sensitivity from step 2. (See section 3 and Figure 4.) Fit each of these 7 (or 9) relative sensitivity curves with a stiff spline, omitting the same nodes as in step 2, as well as several more strong, narrow absorption lines in BD+28 4211 and

BD+75 325. At the extremes of the wavelength coverage, a few extra spline nodes are often required, because the relative sensitivities often deviate from a smooth fit.

4. The final sensitivity for an observation is S(i,m) = A(m) R(i,m), where i is the node number 0 to 6 (or 0 to 8) and m is the order count number. Write individual sensitivity curves for each observation, in order to average multiple observations per mode and to monitor for secular changes.

Fluxes derived from these echelle sensitivities S(i,m) are generally within a factor of 1-2 of the fluxes derived from pre-launch calibration estimates. GO's should recalibrate their data with the latest IRAF tasks and reference files to get accurate fluxes and ripple corrections.

2. STIS Observations

Spectra of three flux standards, as listed in Table 1, are used to define the echelle mode calibrations. All observations are in the 0.2x0.2 aperture following standard peakup target acquisitions. Relative transmission measurements are used to compute absolute fluxes for other apertures. At the shorter wavelengths, the heavy line blanketing in BD+75 325 causes sensitivity errors of 10-20%, even for the relative flux within one order. One observation (O3ZX10DAQ) of BD+75 325 in E140H-1416 does not appear in Table 1, because the E140H-1416 spectra of BD+28 4211 produce smooth ripple corrections vs. order that differ by the 10-20% from BD+75 325 data. Unfortunately, two short wavelength modes, E140H-1234 and E140H-1598, have only BD+75 325 calibration observations, currently. New observations of the relatively line free stars, G191B2B or BD+28 4211, are needed for these two settings, in order to provide more accurate sensitivity calibrations.

The standard height of 7 pixels is used to extract each spectrum (Leitherer & Bohlin 1998). The background is measured half way between the orders with an extraction height of three pixels and is smoothed twice with a boxcar width of 15 pixels.

Table 1: Echelle Observations of Standard Stars

ROOTNAME	MODE	APERTURE (arcsec)	CENWAV	TARGET	GLOBAL (ct/s)	DATE	PROPID	EXPTIME (s)
O3ZX02X5Q	E140M	0.2X0.2	1425	BD+28D4211	224360	19/09/97	7096	1779.0
O45930030	E140M	0.2X0.2	1425	BD+28D4211	222557	30/12/97	7673	350.0
O4PG02QCQ	E140M	0.2X0.2	1425	G191B2B	65205	17/03/98	7917	2160.0
O4PG02QKQ	E140M	0.2X0.2	1425	G191B2B	63341	18/03/98	7917	3091.0
O45931020	E140M	0.2X0.2	1425	BD+28D4211	225692	20/05/98	7673	350.0
O3ZX02XAQ	E230M	0.2X0.2	1978	BD+28D4211	100793	19/09/97	7096	1136.0
O45930040	E230M	0.2X0.2	1978	BD+28D4211	106387	30/12/97	7673	430.0
O45931040	E230M	0.2X0.2	1978	BD+28D4211	107022	20/05/98	7673	516.0
O3ZX02XEQ	E230M	0.2X0.2	2707	BD+28D4211	103235	19/09/97	7096	1085.0
O45930050	E230M	0.2X0.2	2707	BD+28D4211	104386	30/12/97	7673	365.0
O45931050	E230M	0.2X0.2	2707	BD+28D4211	104103	20/05/98	7673	438.0
O4DD05070	E140H	0.2X0.2	1234	BD+75D325	178318	07/01/98	7657	1000.0
O45930010	E140H	0.2X0.2	1416	BD+28D4211	104787	30/12/97	7673	935.0
O45931030	E140H	0.2X0.2	1416	BD+28D4211	106739	20/05/98	7673	994.0
O4DD05LGQ	E140H	0.2X0.2	1598	BD+75D325	51878	07/01/98	7657	1148.4
O4DD05030	E230H	0.2X0.2	1763	BD+75D325	57282	07/01/98	7657	2799.0
O4DD05020	E230H	0.2X0.2	2013	BD+75D325	85802	07/01/98	7657	2040.0
O4DD05040	E230H	0.2X0.2	2263	BD+75D325	95722	07/01/98	7657	1200.0
O45930020	E230H	0.2X0.2	2263	BD+28D4211	44346	30/12/97	7673	1006.0
O45931010	E230H	0.2X0.2	2263	BD+28D4211	43843	20/05/98	7673	1681.0
O3ZX10DEQ	E230H	0.2X0.2	2513	BD+75D325	78817	15/09/97	7096	603.0
O4DD05050	E230H	0.2X0.2	2762	BD+75D325	53230	07/01/98	7657	1434.0
O4DD05060	E230H	0.2X0.2	3012	BD+75D325	22819	07/01/98	7657	1200.0

3. Results

The stellar reference spectra are from Bohlin (1996) and can be obtained from the Calibration Data Base System (CDBS) at http://www.stsci.edu /ftp/instrument_news/Observatory/cdbs/astronomical_catalogs_alt.html. In order to derive the proper sensitivity calibration, the wavelength scale must be in the instrumental frame of rest, as observed, i.e. with *NO* velocity correction. The standard star spectrum must be shifted to coincide with the observations, i.e. the wavelength scale of the model reference spectrum for G191B2B must be shifted by the radial velocity of the star plus the heliocentric correction for the earth and HST velocity vectors. An observed standard star spectrum (BD+28 4211 and BD+75 325) without radial velocity correction requires only the heliocentric correction for the earth and HST velocity vectors. Consequently, the application of derived sensitivity curves must be to the counts/sec with the instrumental rest frame wavelengths. The observed radial velocity of G191B2B is +22 km/s, which includes the gravitational component (Reid & Wegner, 1988), while the radial velocity of BD+75 325 is -19 km/s 11 (Gould, Herbig, & Morgan 1957).

Figure 2 compares the final 7 node spline fit from step 3 of the calibration procedure with the same point-by-point raw sensitivity as in Figure 1 for order m=90 of E140M. The absorption features in the BD+28 4211 spectrum (light dotted line) do not bias the final result (heavy line), since step 3 enforces continuity in the ripple correction from order to order. The sensitivity from the line-free order m=90 of G191B2B (heavy dashed line) agrees with the BD+28 4211 results within 5%.

The average calibrations vs. order count for each of the 23 observations in Table 1 appear in Figure 3, per step 2 of the calibration procedure. The final fits are the solid lines. Figure 4 is the result of step 3 for each observation in Table 1. The valid sensitivities at each of the raw nodes divided by the average sensitivity are the squares, alternating between open squares for the even nodes (0,2,..) and filled squares for odd nodes (1,3,..). In Figure 4, there are two plots per observation: the first for the first 4 (or 5) nodes from node 0 at the bottom and the second plot for the remaining 3 (or 4) nodes with the last node at the bottom of the plot. The adopted fits are the heavy solid lines and define the final ripple calibration. Because of rapid sensitivity changes at the edges of the MAMA detectors, especially at the extremes of the wavelength coverage, a higher density of spline nodes are often required to define the final fits at the lowest and highest orders. Written at the top of the plots in Figure 4 and tabulated in Table 2 are the rms scatter of the data about the fits for each node. The results for the BD+75 325 observations at the shorter wavelengths, especially E140H-1234 and E140H-1598, have σ values that are much larger than for the other observations. Systematic uncertainty in the smooth fits for these two modes is

~10%. Even for E230H-1763, the large σ's in Table 2 dominate the uncertainty and are caused by the heavy line blanketing that extends to ~1900Å in the standard BD+75 325.

As an internal consistency check, the raw counts for each observation are divided by the above sensitivity corrections S(i,m) and plotted over the standard star flux. The mean ratio and rms scatter σ_m of STIS flux to standard star flux is computed in wavelength bins corresponding to the standard star resolution and appears in columns 5-6 of Table 2. Since the mean ratios lie in the range .995 to 1.00, any systematic bias from the absorption lines is less than 1% on average. A region of heavy line blanketing is illustrated in Figure 5. The STIS flux averaged over the FOS bandpass is plotted as diamonds. The smooth echelle calibration, defined by seven spline nodes per order, reproduces the input calibration flux of the standard star within a 1-2% uncertainty that is dominated by the use of an approximate FOS line profile. The mean ratio of the diamonds to the standard star flux over all wavelengths is 0.998 with an rms scatter of 1.6%. Thus, for most of the echelle sensitivities, the uncertainty is *NOT* limited by the analysis technique but is dominated by the accuracy of the standard star flux and by the photometric repeatability of observations in the small echelle slits.

For the echelle modes with repeat observations, Figure 6 quantifies the scatter about the adopted average calibration. When Figure 5 is made using the average sensitivity for E140M, rather than the S(i,m) defined by the O3ZX02X5Q observation itself, then the STIS fluxes are systematically low by 0-2%, since the relative sensitivity at 97Sep19 (1997.72) in Figure 6 is lower than the final adopted average sensitivity from the five calibration observations with E140M.

4. Uncertainties

After several repeat observations in the same 12 prime echelle modes, the accuracy of the calibrations can be quantified more precisely. Currently, the estimated uncertainty in the echelle flux calibration is ~4% (1σ) from a 3% standard star flux uncertainty and a 3% STIS photometric stability, except for E140H-1234 and E140H-1598 and except for occasional anomalies at the ends of the orders or in the lowest sensitivity regions, where uncertainties are as much as 10-20%. The adopted photometric error of 3% is probably set by stability of the PSF and centering in the small 0.2x0.2 arcsec aperture, since repeatability in low dispersion for the 52x2 arcsec aperture is better than 1%. The observed 3% drop in the countrate for G191B2B in E140M could be caused by a 10-20 milli-arcsec pointing shift or thermal drift from the first observation to the second observation on the succeeding orbit. Entrance slits smaller than 0.2x0.2 are less photometric.

Perhaps, the shape of broad line profiles that extend over a significant fraction of one or more echelle orders is the most important result of an echelle flux calibration. As a guide to the relative precision of this ripple correction, the last nine columns of Table 2

include the 1σ scatter about the fits to the nodes from Figure 4 and step 3 of the calibration procedure. Since each value is the uncertainty at one node position, combining any two of these in quadrature, produces an estimate of the relative flux uncertainty between the two regions of an order.

Table 2: RMS Scatter about the Fits for each Node in Percent

ROOTNAME	MODE	CENWAV	TARGET	MEAN	σ_m	σ 0	for 1	Fits 2	of 3	Nodes 4	5	6	7	8
O3ZX02X5Q	E140M	1425	BD+28D4211	0.998	1.6	3.8	1.3	1.5	1.3	1.3	1.3	2.8		
O45930030	E140M	1425	BD+28D4211	0.998	1.7	5.0	1.3	1.6	1.5	1.3	1.3	2.6		
O4PG02QCQ	E140M	1425	G191B2B	0.996	1.1	1.0	0.6	0.6	0.5	0.6	0.7	1.4		
O4PG02QKQ	E140M	1425	G191B2B	0.996	1.1	1.0	1.2	0.6	0.5	0.5	0.7	1.4		
O45931020	E140M	1425	BD+28D4211	0.998	1.7	3.3	2.0	1.4	1.6	1.3	1.4	2.3		
O3ZX02XAQ	E230M	1978	BD+28D4211	0.999	0.8	2.5	1.4	0.5	0.6	0.8	0.6	1.0	1.2	1.6
O45930040	E230M	1978	BD+28D4211	0.999	1.1	2.3	2.2	0.7	0.5	0.7	0.9	0.9	1.7	1.7
O45931040	E230M	1978	BD+28D4211	0.999	1.0	3.0	1.9	0.5	0.6	0.8	0.6	1.1	1.6	1.7
O3ZX02XEQ	E230M	2707	BD+28D4211	0.999	0.7	1.0	0.4	0.6	0.4	0.5	0.4	0.6	1.0	0.6
O45930050	E230M	2707	BD+28D4211	0.999	0.7	0.9	0.6	0.4	0.5	0.5	0.5	0.5	0.9	0.8
O45931050	E230M	2707	BD+28D4211	1.000	0.7	0.9	0.5	0.5	0.4	0.5	0.4	0.6	0.9	0.9
O4DD05070	E140H	1234	BD+75D325	0.995	3.3	16.3	8.8	9.0	8.2	9.1	8.3	15.0		
O45930010	E140H	1416	BD+28D4211	0.999	1.3	2.5	1.3	1.4	1.3	1.7	1.2	1.9		
O45931030	E140H	1416	BD+28D4211	0.997	1.3	3.4	1.3	1.7	1.3	1.9	1.2	2.4		
O4DD05LGQ	E140H	1598	BD+75D325	0.998	2.9	10.6	5.7	5.4	3.8	5.9	6.7	11.8		
O4DD05030	E230H	1763	BD+75D325	0.995	2.5	8.8	5.1	4.0	3.7	4.4	4.8	9.0		
O4DD05020	E230H	2013	BD+75D325	0.999	0.9	2.5	1.4	1.8	1.9	1.5	1.6	3.8		
O4DD05040	E230H	2263	BD+75D325	0.998	2.2	3.5	2.4	1.9	2.5	4.1	2.9	2.5		
O45930020	E230H	2263	BD+28D4211	0.999	0.9	1.6	0.8	1.0	1.0	1.2	1.3	1.2		
O45931010	E230H	2263	BD+28D4211	0.999	0.8	1.1	0.9	0.8	0.9	1.1	1.6	2.8		
O3ZX10DEQ	E230H	2513	BD+75D325	0.998	1.5	2.0	1.6	1.2	1.5	1.3	1.2	2.3		
O4DD05050	E230H	2762	BD+75D325	0.998	1.2	1.1	0.7	0.7	0.5	0.9	0.9	0.7		
O4DD05060	E230H	3012	BD+75D325	1.000	0.7	0.5	0.9	0.3	0.7	0.6	0.7	0.7		

The uncertainty of the ripple correction in any GO observation can be checked by comparing the flux in the order overlap regions, because there is no correlation in the calibration procedure between the fits at the opposite ends of the orders. Since the ends of the orders are the regions of lowest sensitivity, typical mismatches provide an upper limit to the uncertainties nearer the center of the orders.

5. Future

G191B2B is better than BD+75 325 for echelle calibration, because the heavy line blanketing in BD+75 325 confuses the calibration in comparison with the much lower resolution FOS calibration reference spectrum. The lines in G191B2B are both weaker and sparser. Spectra of G191B2B are on the long range plan in order to provide more accurate calibrations of the E140H modes that currently have only BD+75 325 observations. In addition, a correction will be available for scattered light that currently causes the inter-order background to be too high. After this correction, which is as large as ~10%, is implemented and tested, new echelle sensitivities will be derived. When a statistically significant set of data are available for each mode, the rms scatter as a function of wavelength within each order will provide a more precise estimate of the uncertainty of the STIS echelle flux calibration.

6. Acknowledgements

Claus Leitherer or Nolan Walborn is PI for many of the calibration observations analyzed here. Stefi Baum motivated the work. Bruce Woodgate is STIS PI and encourages cooperation between the STScI and his software team that is led by Don Lindler.

7. References

Bohlin, R. C. 1996, AJ, 111, 1743

Bohlin, R., Collins, N., & Gonnella, A. 1998, Instrument Science Report, STIS 97-14, (Baltimore:STScI).

Gould, N. L., Herbig, G. H., & Morgan, W. W. 1957, PASP, 69, 242.

Heap, S. R., & Brown, T. M. 1997, "1997 HST Calibration Workshop,"

(Baltimore:STScI), p. 114.

Leitherer, C., and Bohlin, R. 1998, Instrument Science Report, STIS 98-09, (Baltimore:STScI).

Reid, N., & Wegner, G. 1988, ApJ, 335, 953.

8. FIGURE CAPTIONS

1. Example of a spline node fit to the raw sensitivities for order m=90 of E140M in the O3ZX02X5Q observation of BD+28 4211. Raw sensitivities are the light dotted line. The 7 spline nodes that define the heavy solid line fit are the diamonds. The fit is badly biased downward by the strong HeII 1640.5Å line.

2. Final fit for order m=90 of Figure 1, demonstrating the similar fits for BD+28 4211 (heavy solid line) and G191B2B (heavy dashed line). The 7 spline nodes that define each fit are the diamonds. The similarity of the shape of the two final fits in a case with and without a strong line provides confidence in the robustness of the calibration technique.

3. Average absolute flux calibrations for the 23 observations in Table 1 for the 12 different echelle prime settings. The solid line defines the fit to the filled squares, which are the average sensitivities for each order. The diamonds are for orders that are heavily contaminated by strong absorption lines and are not used in the fitting procedure. The bottom panel shows the residual of the fit for each square, while the number of spline nodes used for the fit and the residual rms scatter is written at the bottom of the top panel. The abscissa, Order Count, is not the echelle order number but is just a count of the orders, beginning with zero at the longest wavelength order for each mode.

4. The valid raw sensitivities at each of the nodes divided by the average sensitivity are the squares, alternating between open squares connected by a light solid line for the even nodes (0,2,..) and filled squares connected by a light dotted line for odd nodes (1,3,..). Small diamonds are individual nodes that are ignored in the fits due to absorption line contamination. There are two plots per observation: the first for the first 4 (or 5) nodes from node 0 at the bottom and the second plot for the remaining 3 (or 4) nodes with the last node at the bottom of the second plot. The adopted fits are the heavy solid lines and define the final ripple calibration. Because of rapid sensitivity changes at the edges of the MAMA detectors, especially at the extremes of the wavelength coverage, a higher density of spline nodes are often required to define the final fits at the lowest and highest orders. Written at the top of the plots are the rms scatter of the data about the fits for each node.

5. Sample calibrated echelle flux distribution alternating between dashed and solid for alternate orders) and the FOS standard star flux distribution (heavy solid line). Diamonds represent the echelle flux for each FOS point as averaged over an approximate FOS line-spread function. Agreement in the overlap regions of adjacent echelle orders is good to a few percent. Echelle orders m=114-117 correspond to order count i=28-31.

6. Evaluation of the calibration observations in the five modes with more than one observation. Sensitivities relative to the average for the odd numbered nodes vs. time, where the sensitivities for each order are the diamonds connected by solid lines that increase in thickness with order number. The first order (light dotted line) and the last order (heavy dashed line) may deviate from the general trends of the other orders because of limiting sensitivities or detector edge effects. Since the two observations of G191B2B in E140M are from consecutive orbits, these sensitivities are all at the same time (1998.22) as indicated by the position of the star name. Nodes are numbered 0 to 6 (or 0-8 for E230M), so that node 3 (or 5) is the central node for each order.

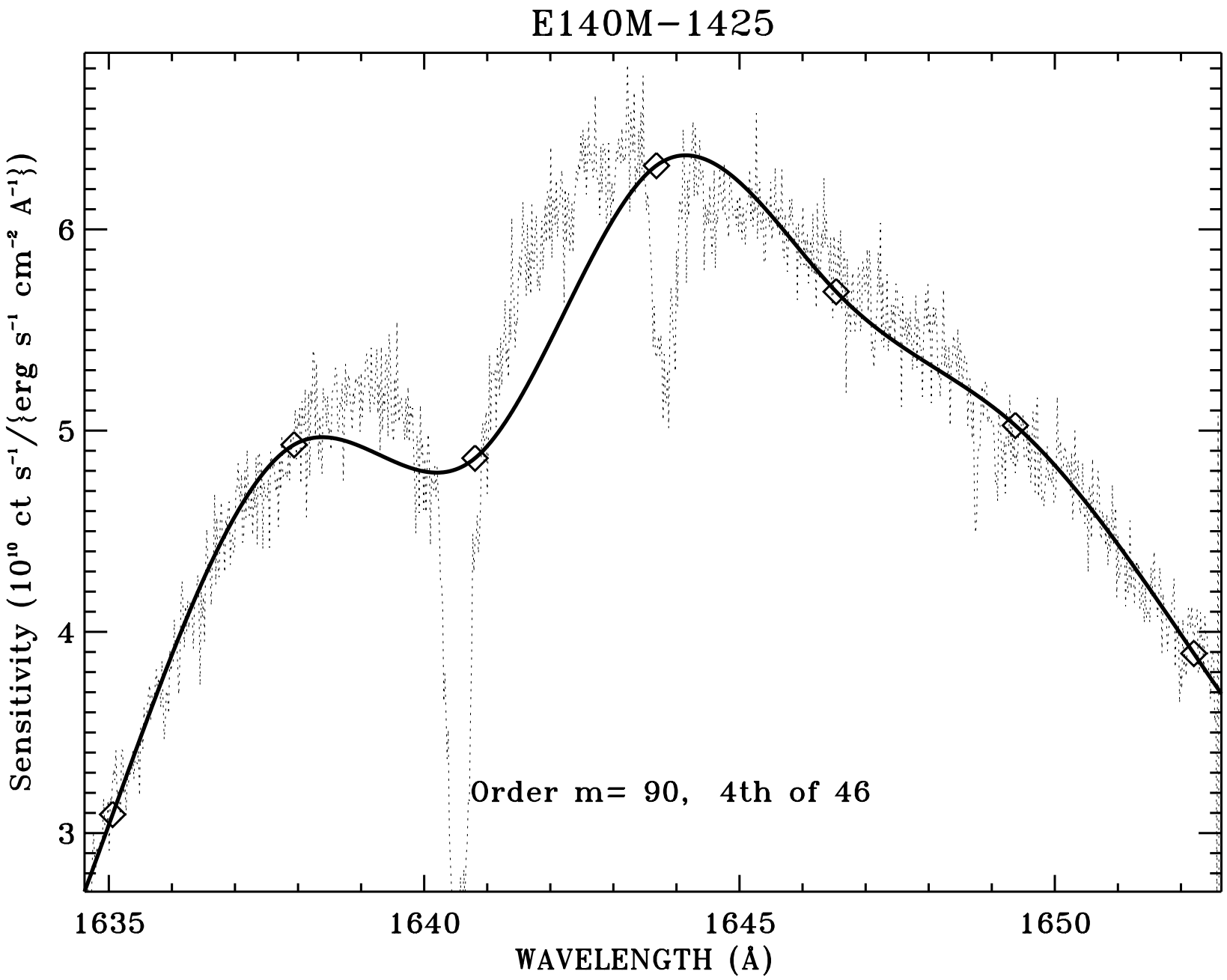

Fig. 1

BOHLIN: echsens 3-Jun-1998 14:42

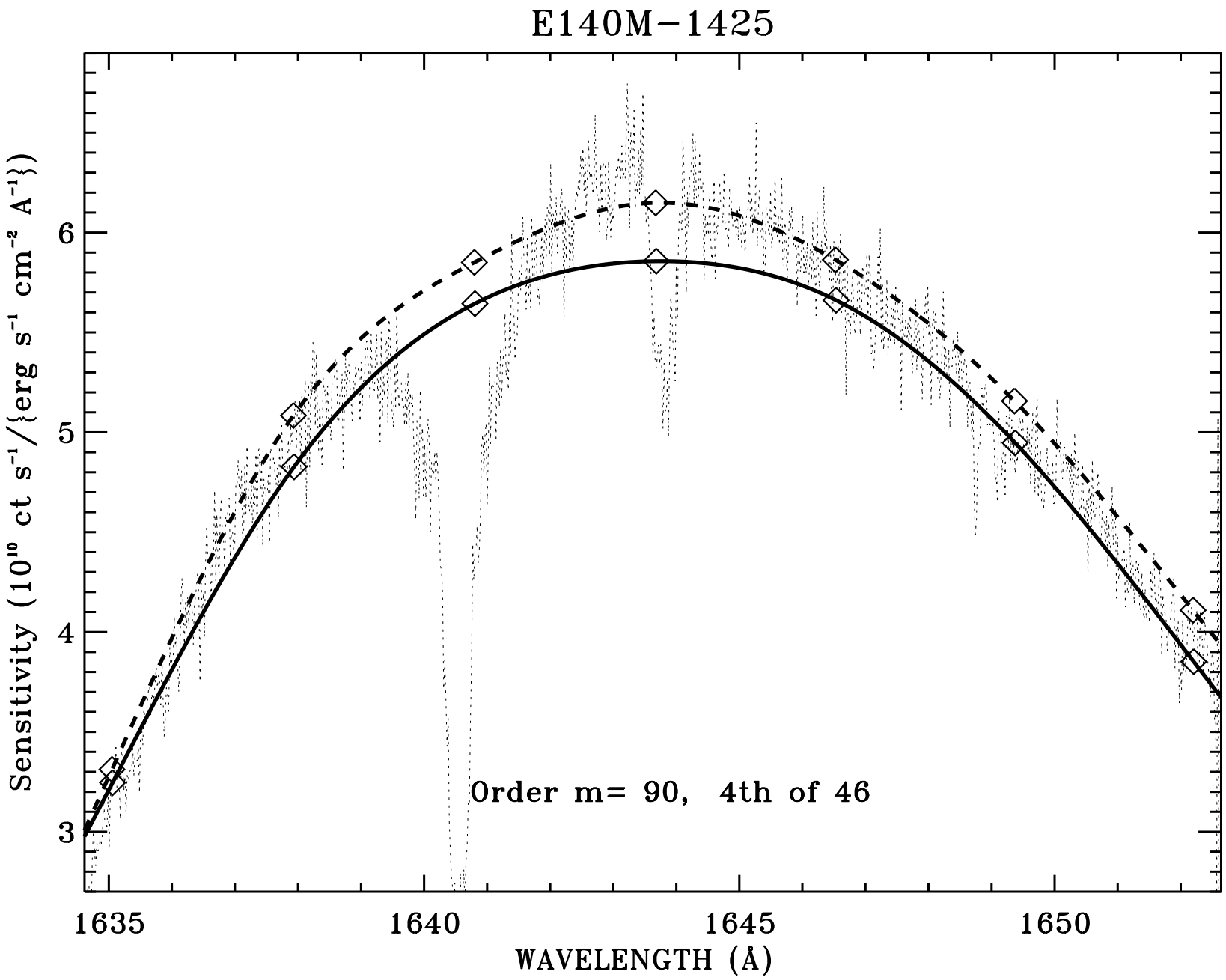

Fig. 2

BOHLIN: echfig2 3-Jun-1998 14:32

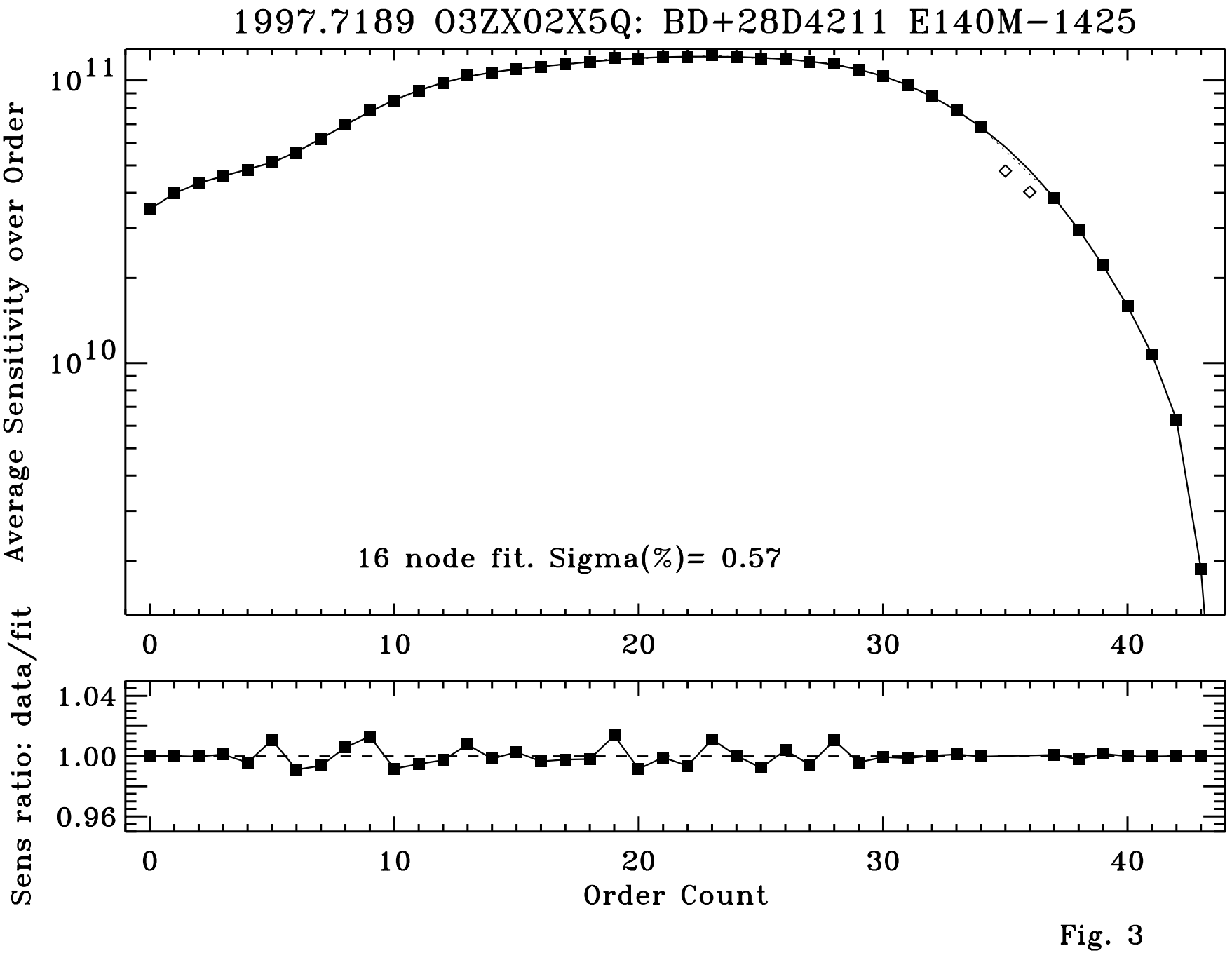

Fig. 3

BOHLIN: echsens 3-Jun-1998 15:26

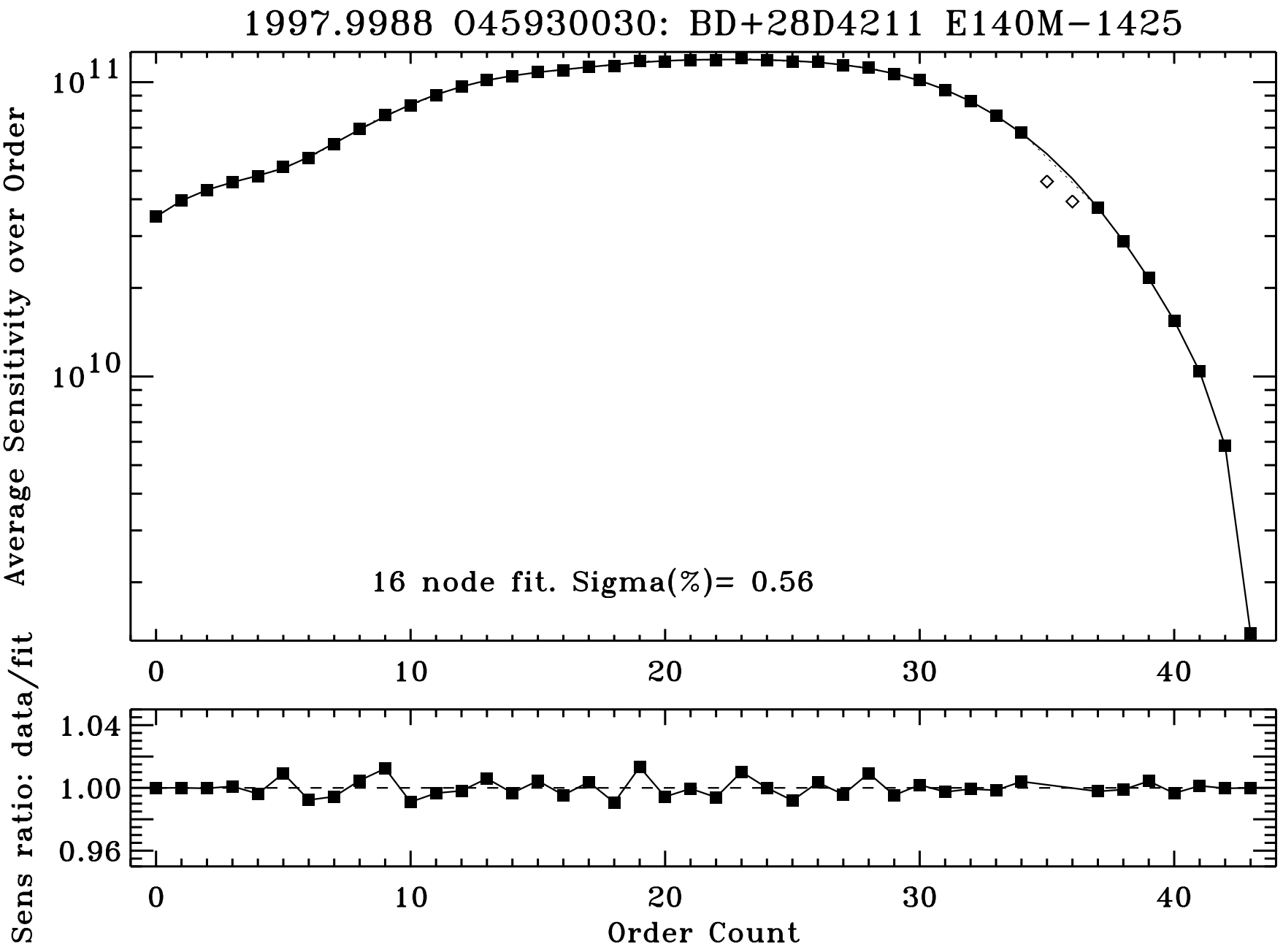
1997.9988 045930030: BD+28D4211 E140M-1425
Average Sensitivity over Order
10^{11}
10^{10}
16 node fit. Sigma(%)= 0.56
0
10
20
30
40
Sens ratio: data/fit
1.04
1.00
0.96
0
10
20
30
40
Order Count
BOHLIN: echsens 3-Jun-1998 15:26

Fig. 3 (cont.)

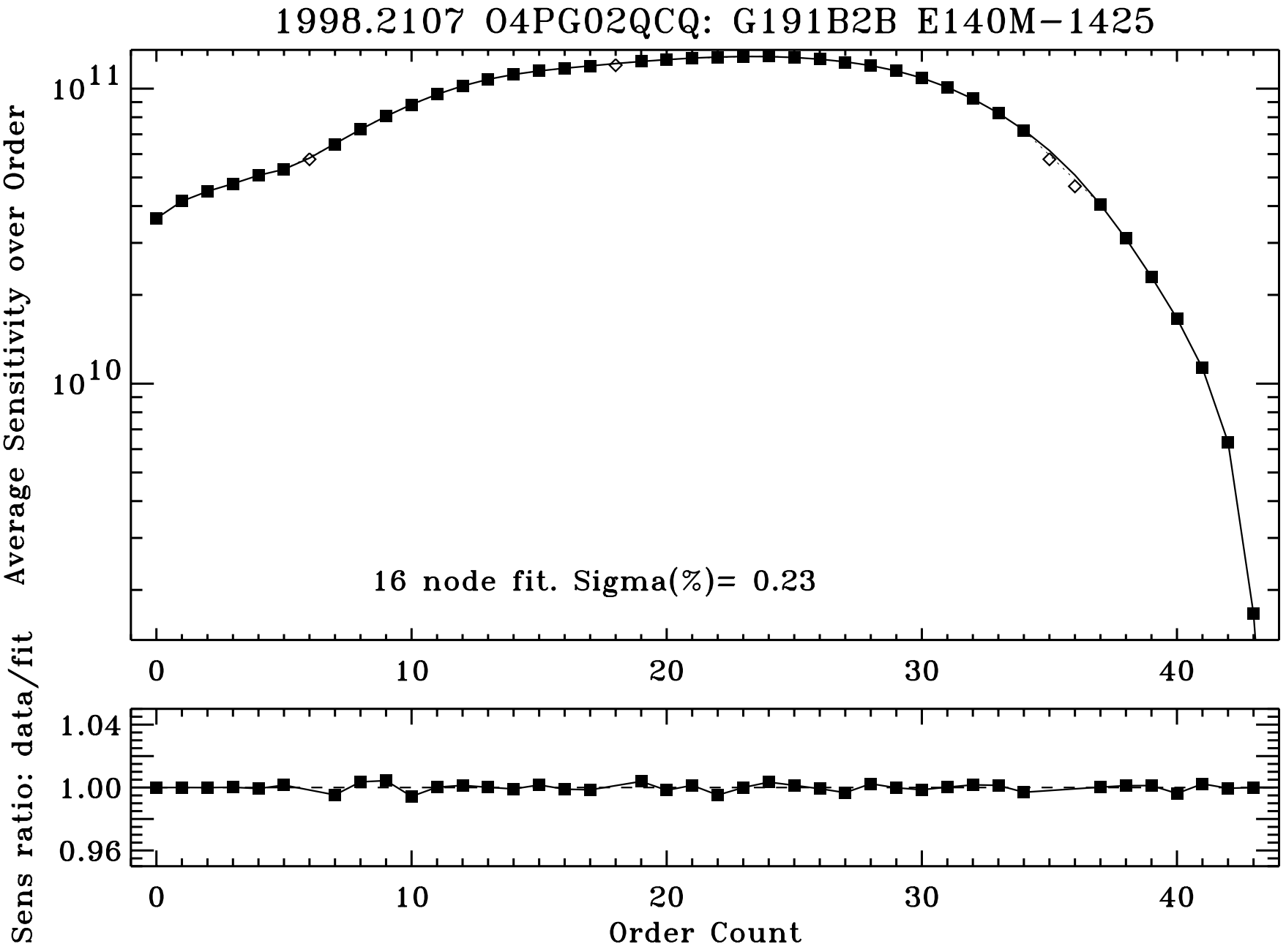

Fig. 3 (cont.)

BOHLIN: echsens 3-Jun-1998 15:26

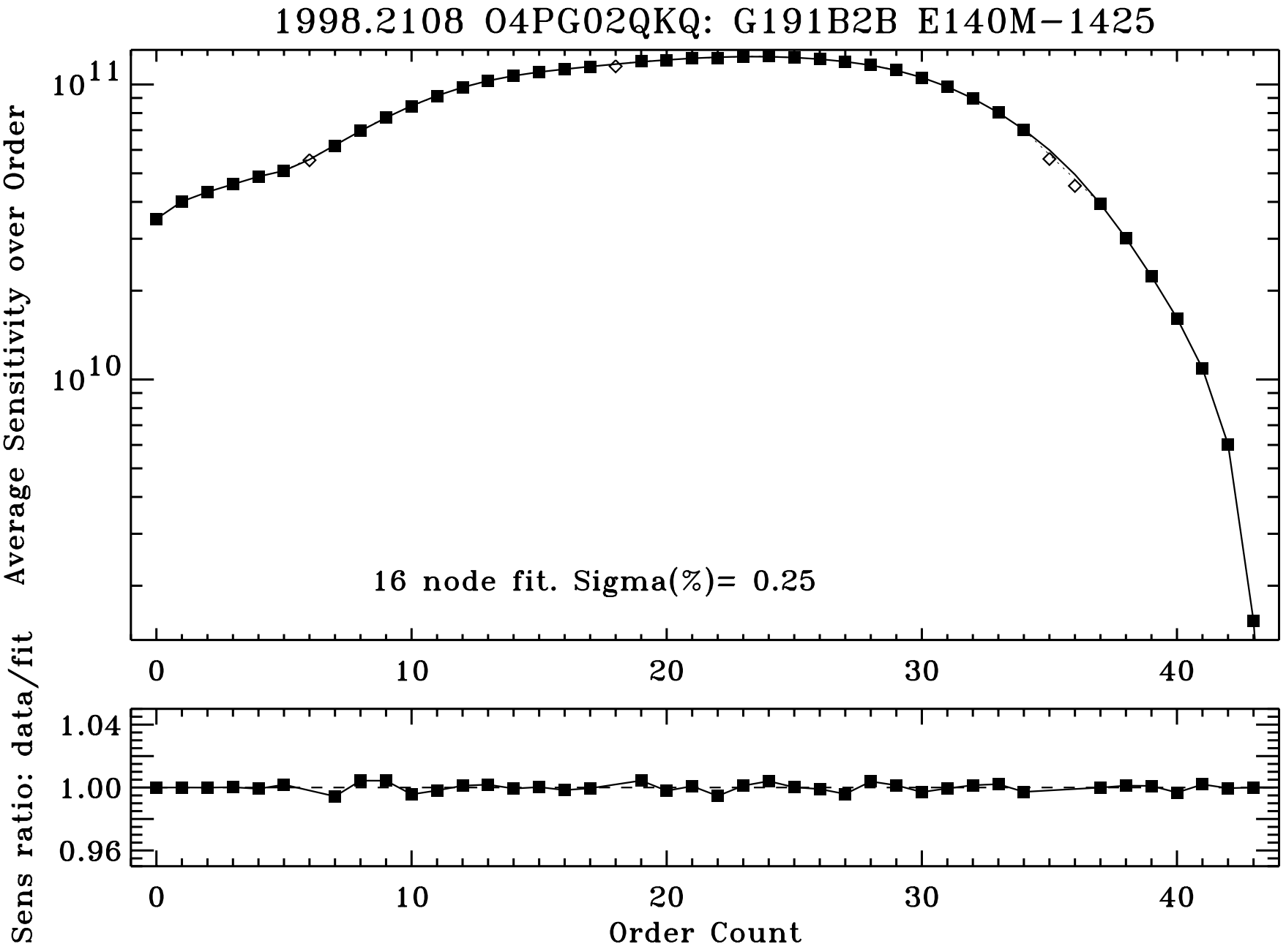

Fig. 3 (cont.)

BOHLIN: echsens 3-Jun-1998 15:27

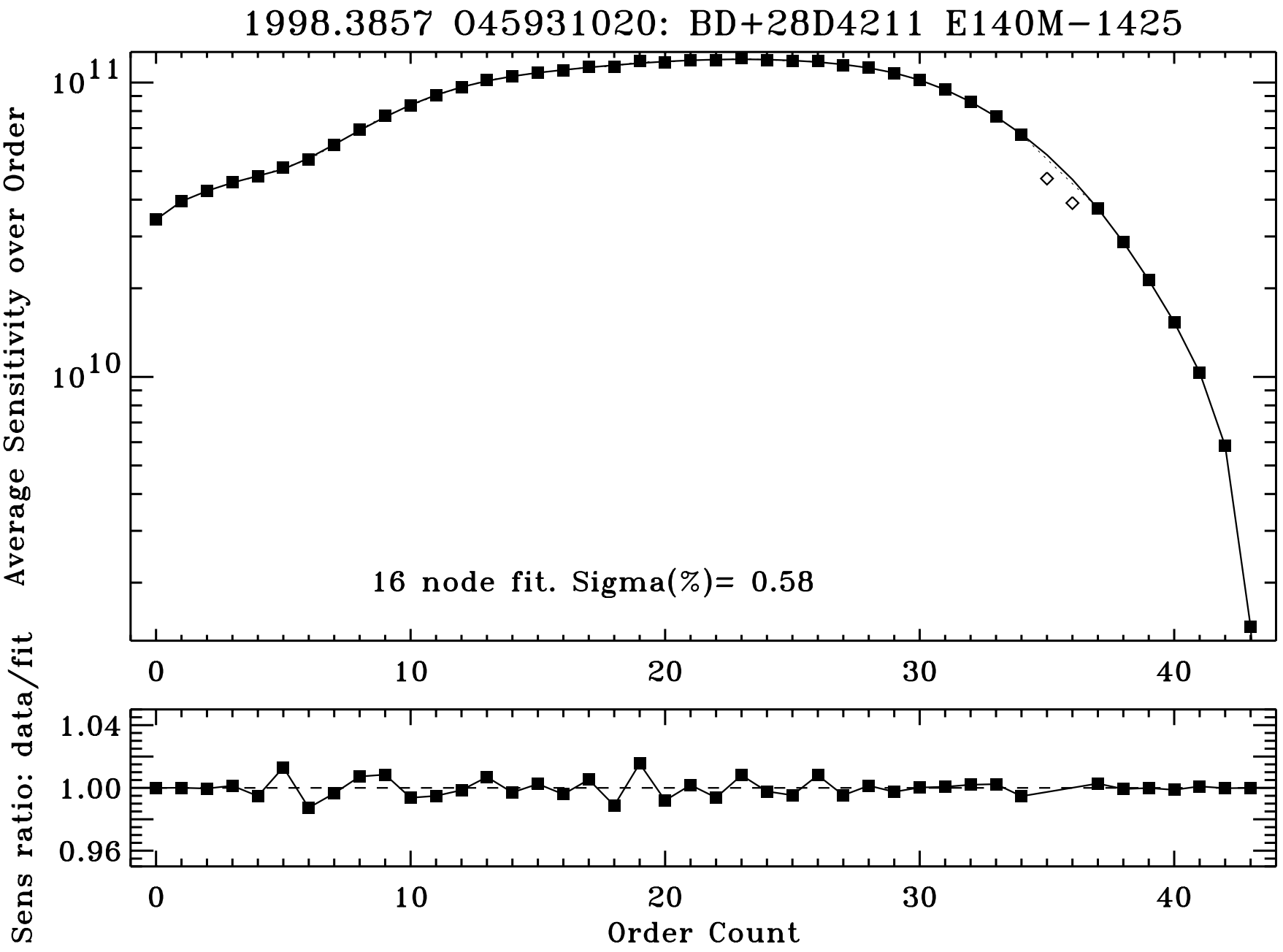
1998.3857 045931020: BD+28D4211 E140M−1425
Average Sensitivity over Order
10^{11}
10^{10}
16 node fit. Sigma(%)= 0.58
0
10
20
30
40
Sens ratio: data/fit
1.04
1.00
0.96
0
10
20
30
40
Order Count
BOHLIN: echsens 3-Jun-1998 15:27

Fig. 3 (cont.)

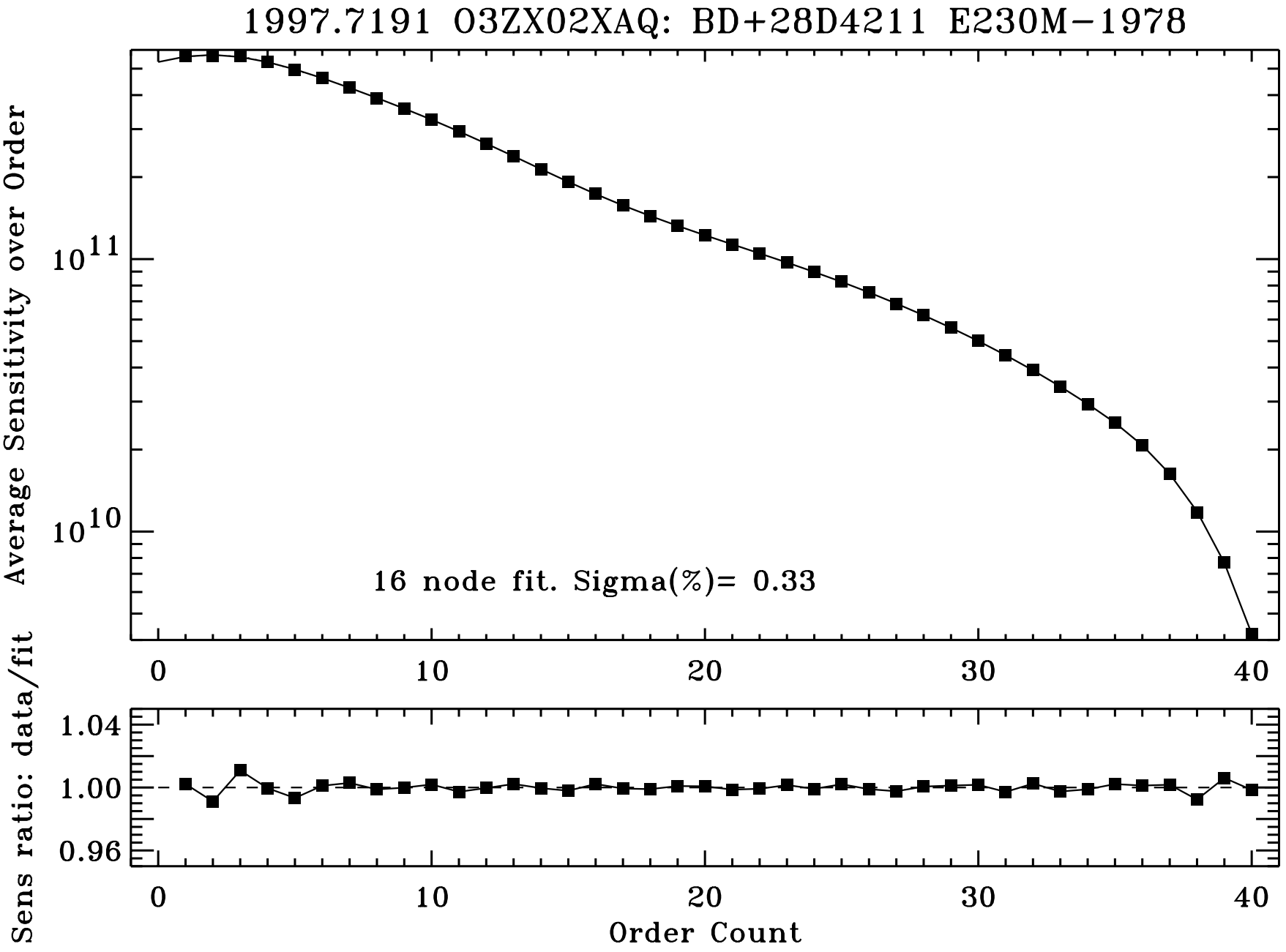

Fig. 3 (cont.)

BOHLIN: echsens 3-Jun-1998 15:27

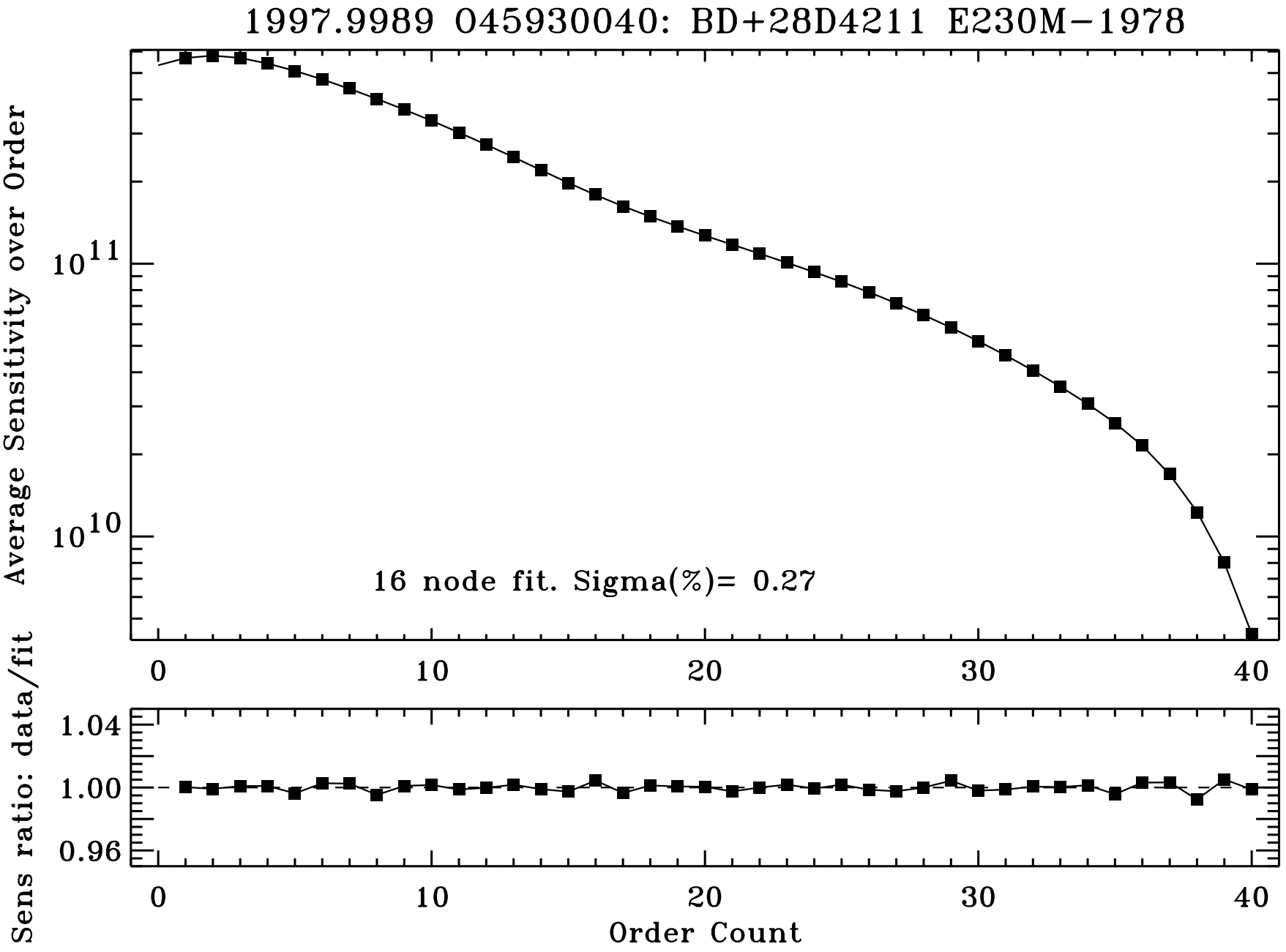
1997.9989 045930040: BD+28D4211 E230M-1978
Average Sensitivity over Order
10^{11}
10^{10}
16 node fit. Sigma(%)= 0.27
0
10
20
30
40
Sens ratio: data/fit
1.04
1.00
0.96
0
10
20
30
40
Order Count
BOHLIN: echsens 3-Jun-1998 15:27

Fig. 3 (cont.)

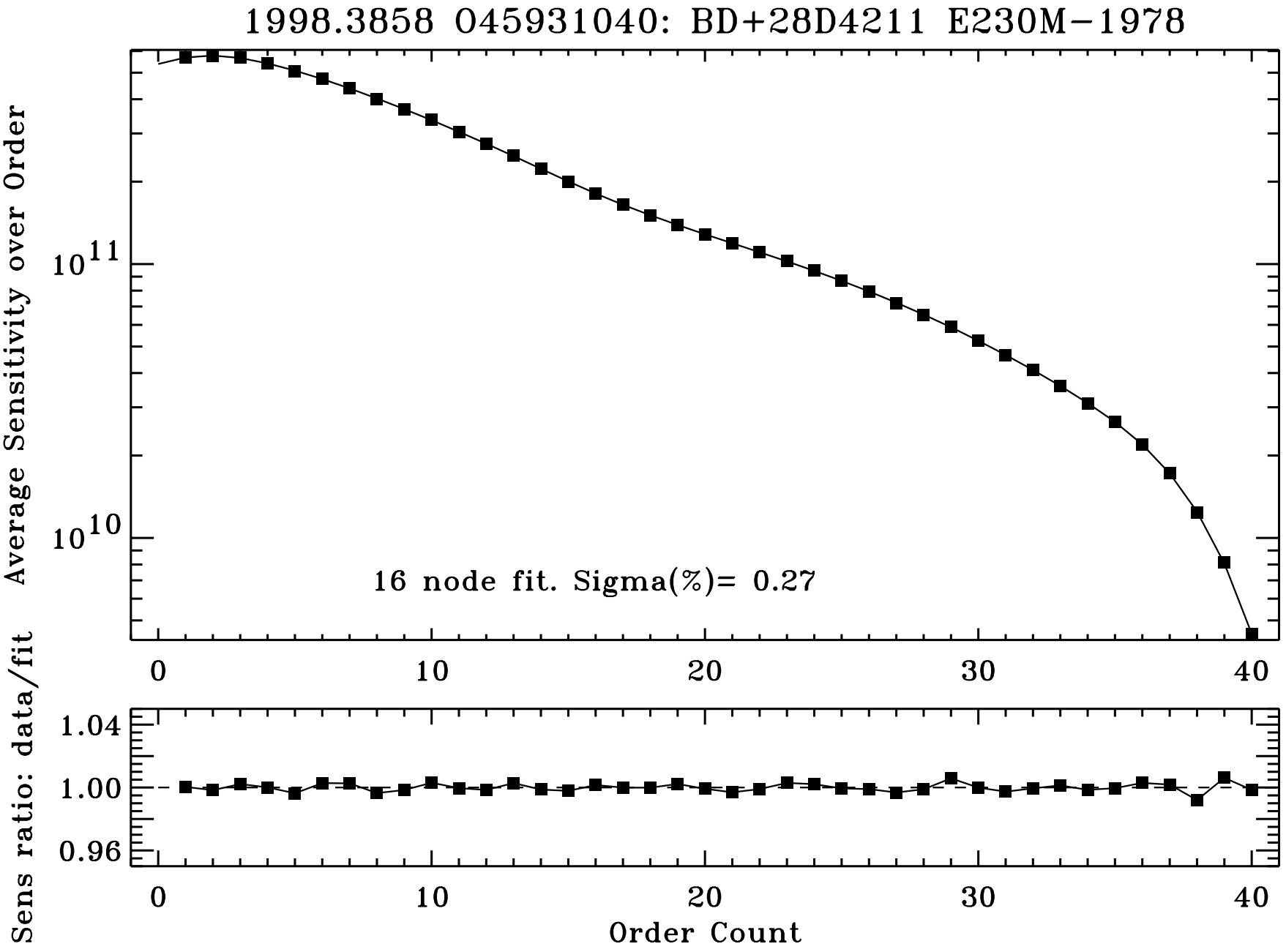
1998.3858 045931040: BD+28D4211 E230M-1978
Average Sensitivity over Order
10^{11}
10^{10}
16 node fit. Sigma(%)= 0.27
0
10
20
30
40
Sens ratio: data/fit
1.04
1.00
0.96
0
10
20
30
40
Order Count
BOHLIN: echsens 3-Jun-1998 15:27

Fig. 3 (cont.)

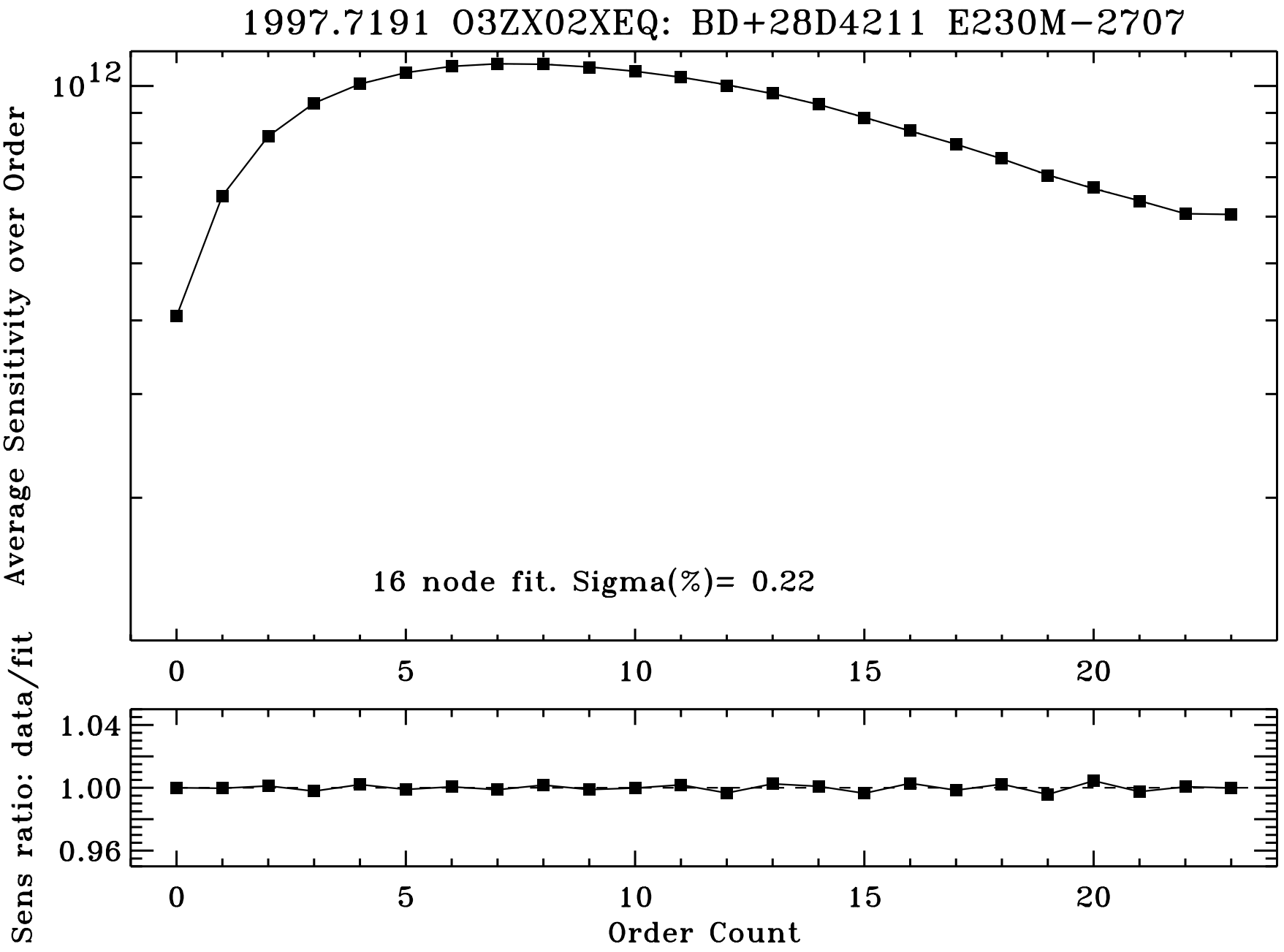
1997.7191 O3ZX02XEQ: BD+28D4211 E230M-2707
Average Sensitivity over Order
10^{12}
16 node fit. Sigma(%)= 0.22
Sens ratio: data/fit
1.04
1.00
0.96
0
5
10
15
20
Order Count
BOHLIN: echsens 3-Jun-1998 15:27

Fig. 3 (cont.)

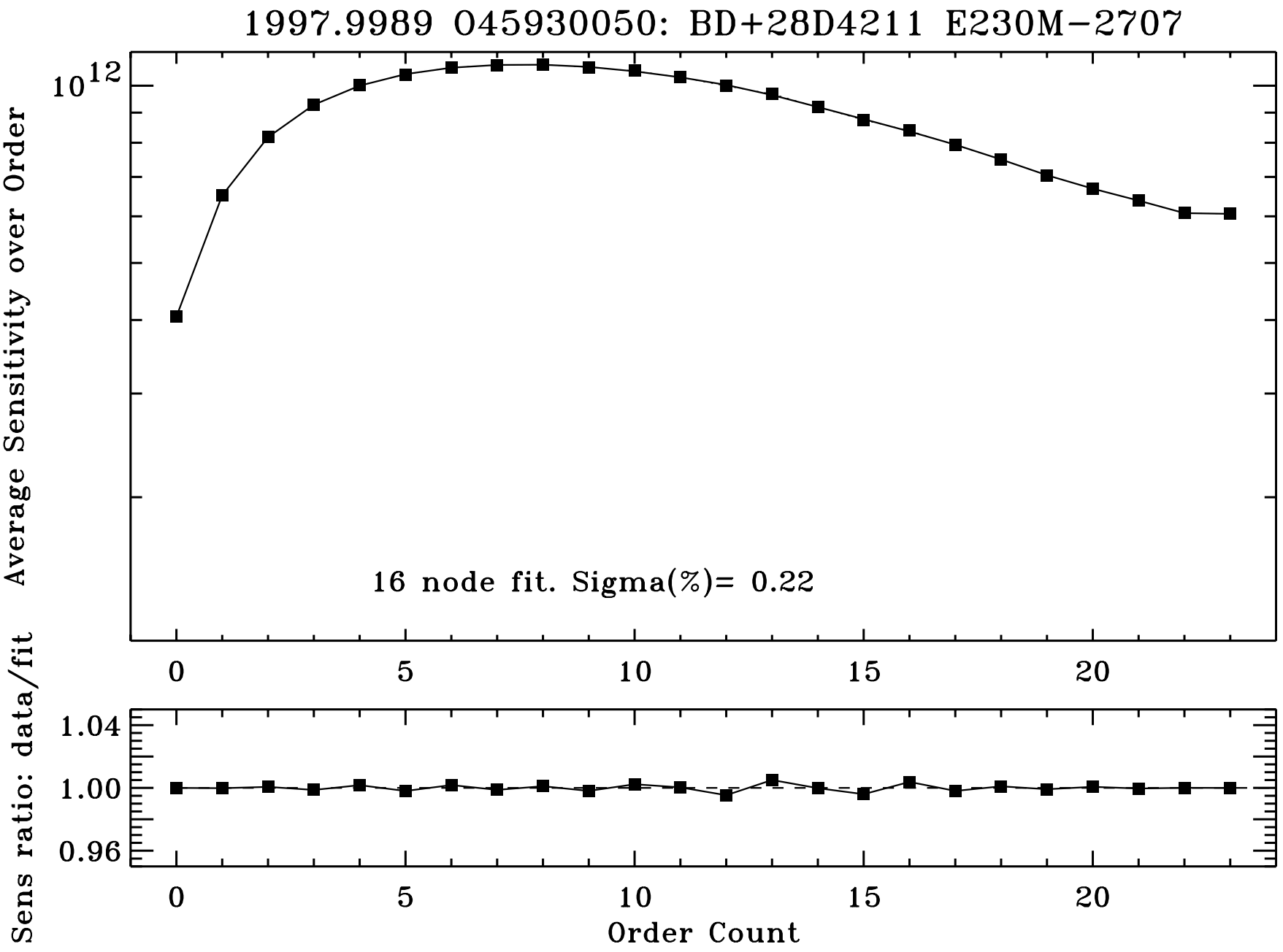
1997.9989 045930050: BD+28D4211 E230M-2707
Average Sensitivity over Order
10^{12}
16 node fit. Sigma(%)= 0.22
Sens ratio: data/fit
1.04
1.00
0.96
0
5
10
15
20
Order Count
BOHLIN: echsens 3-Jun-1998 15:27

Fig. 3 (cont.)

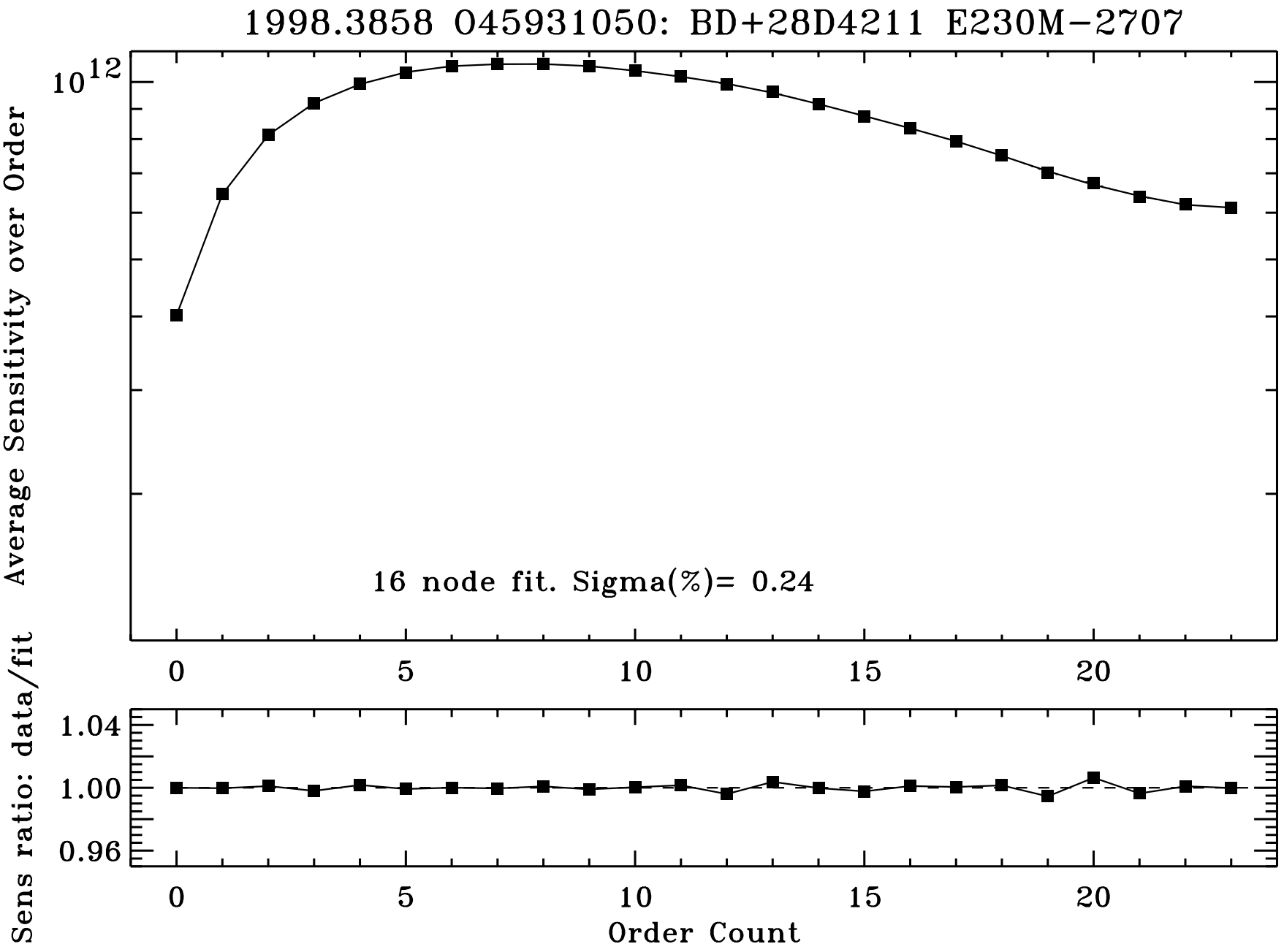
1998.3858 045931050: BD+28D4211 E230M-2707
Average Sensitivity over Order
10^{12}
16 node fit. Sigma(%)= 0.24
0
5
10
15
20
Sens ratio: data/fit
1.04
1.00
0.96
0
5
10
15
20
Order Count
BOHLIN: echsens 3-Jun-1998 15:27

Fig. 3 (cont.)

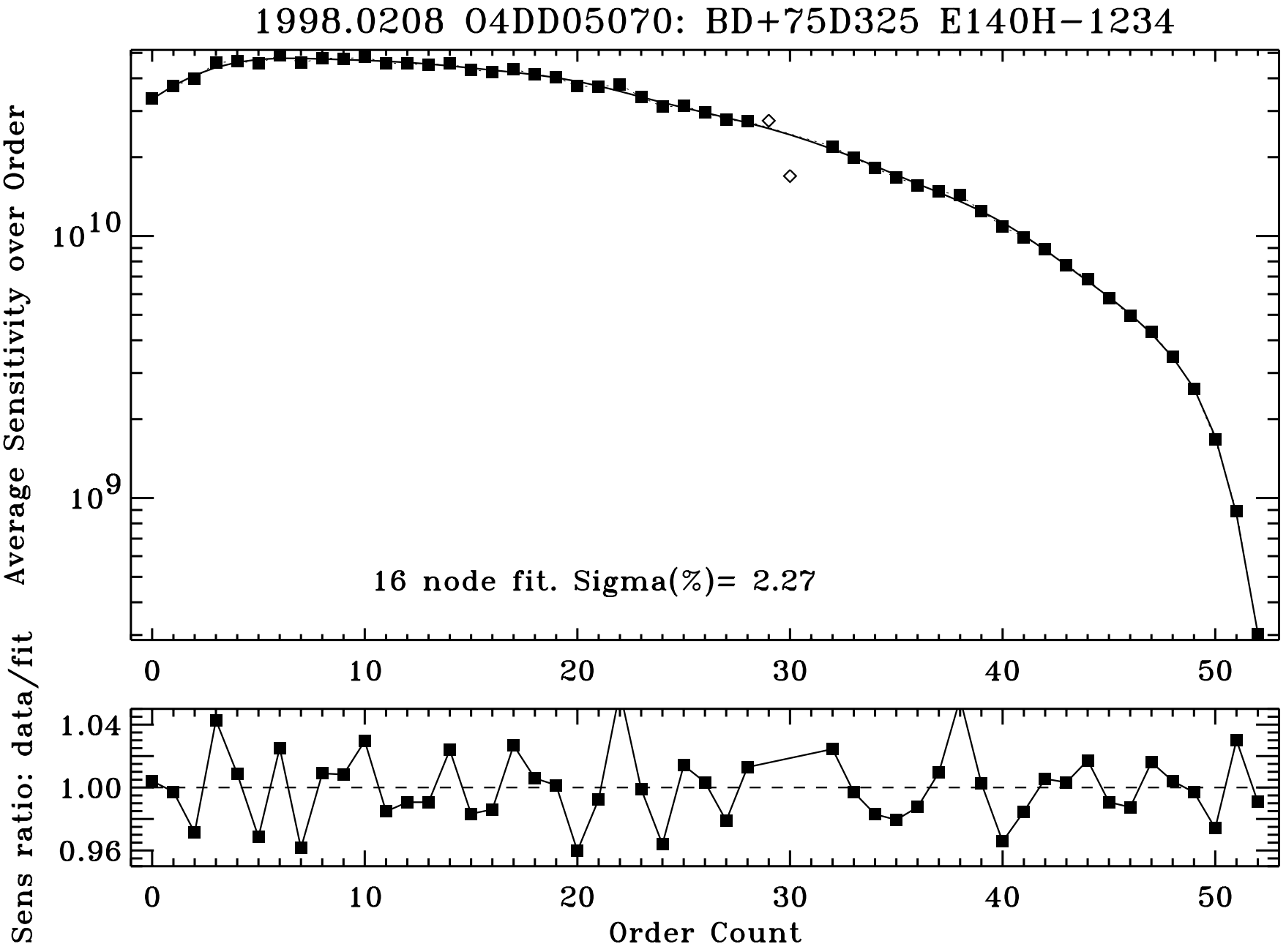
1998.0208 04DD05070: BD+75D325 E140H-1234
Average Sensitivity over Order
10^{10}
10^{9}
16 node fit. Sigma(%)= 2.27
0
10
20
30
40
50
Sens ratio: data/fit
1.04
1.00
0.96
0
10
20
30
40
50
Order Count
BOHLIN: echsens 3-Jun-1998 15:27

Fig. 3 (cont.)

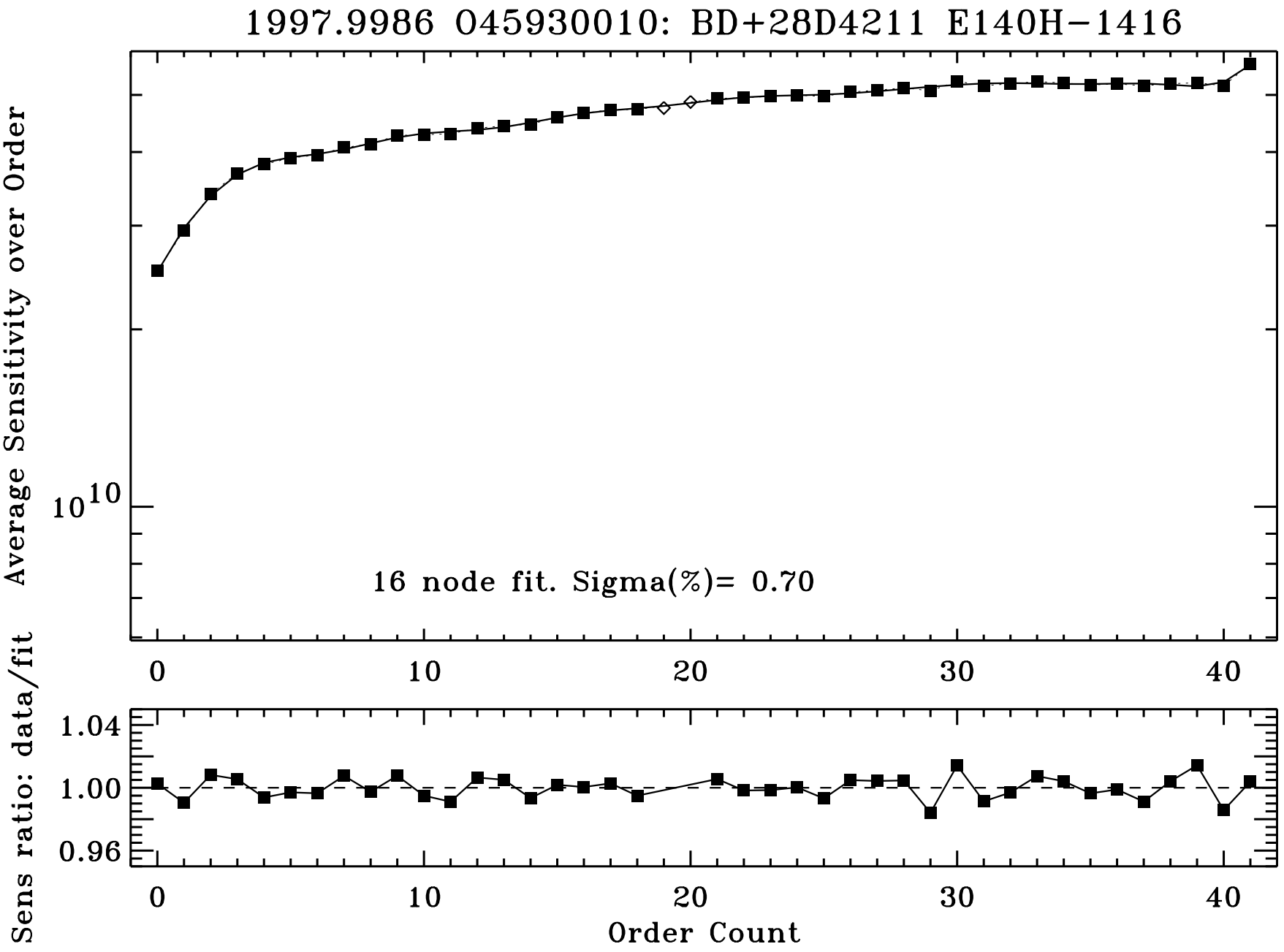

Fig. 3 (cont.)

BOHLIN: echsens 3-Jun-1998 15:27

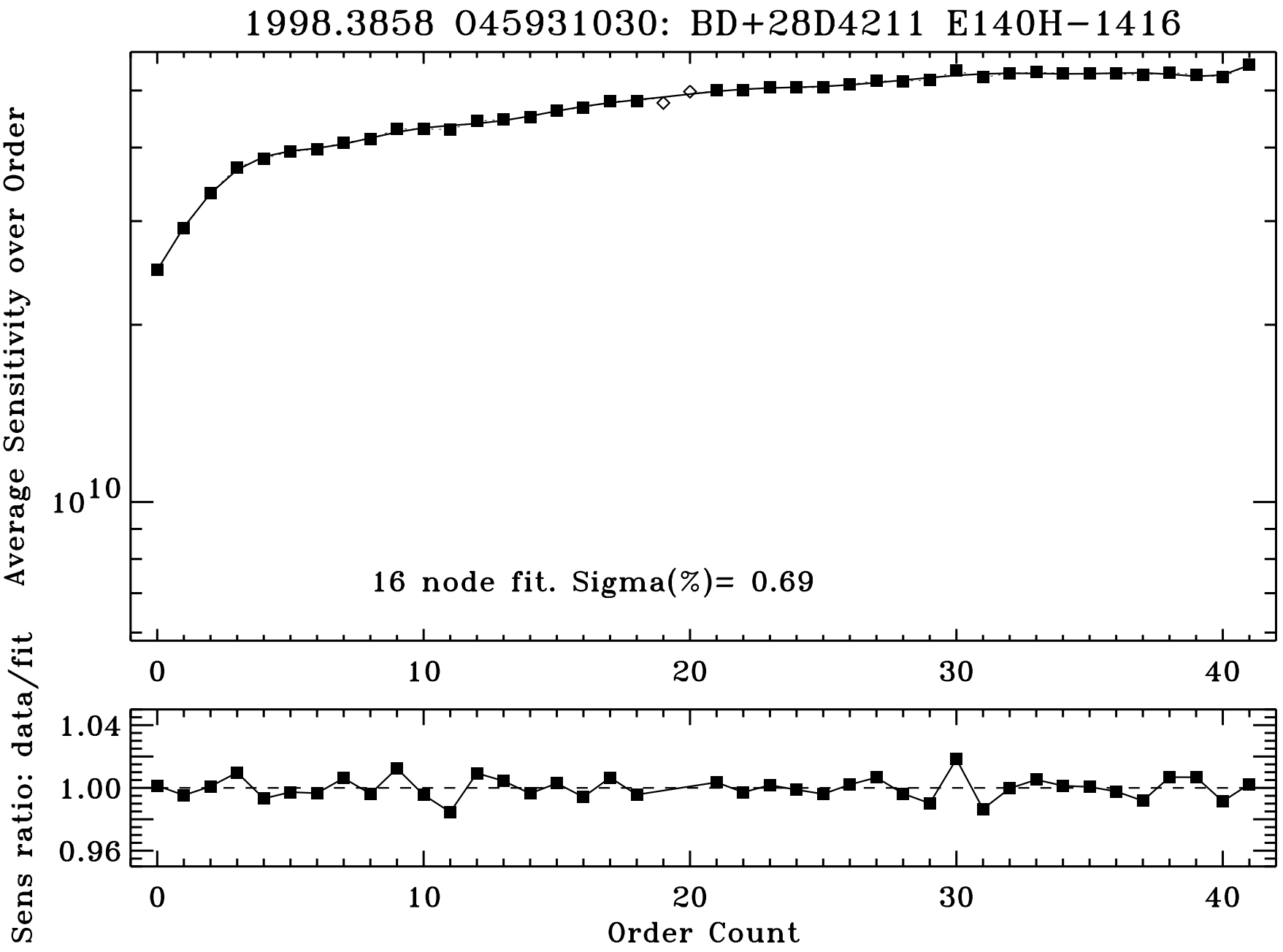
1998.3858 045931030: BD+28D4211 E140H-1416
Average Sensitivity over Order
10^{10}
16 node fit. Sigma(%)= 0.69
0
10
20
30
40
Sens ratio: data/fit
1.04
1.00
0.96
0
10
20
30
40
Order Count
BOHLIN: echsens 3-Jun-1998 15:27

Fig. 3 (cont.)

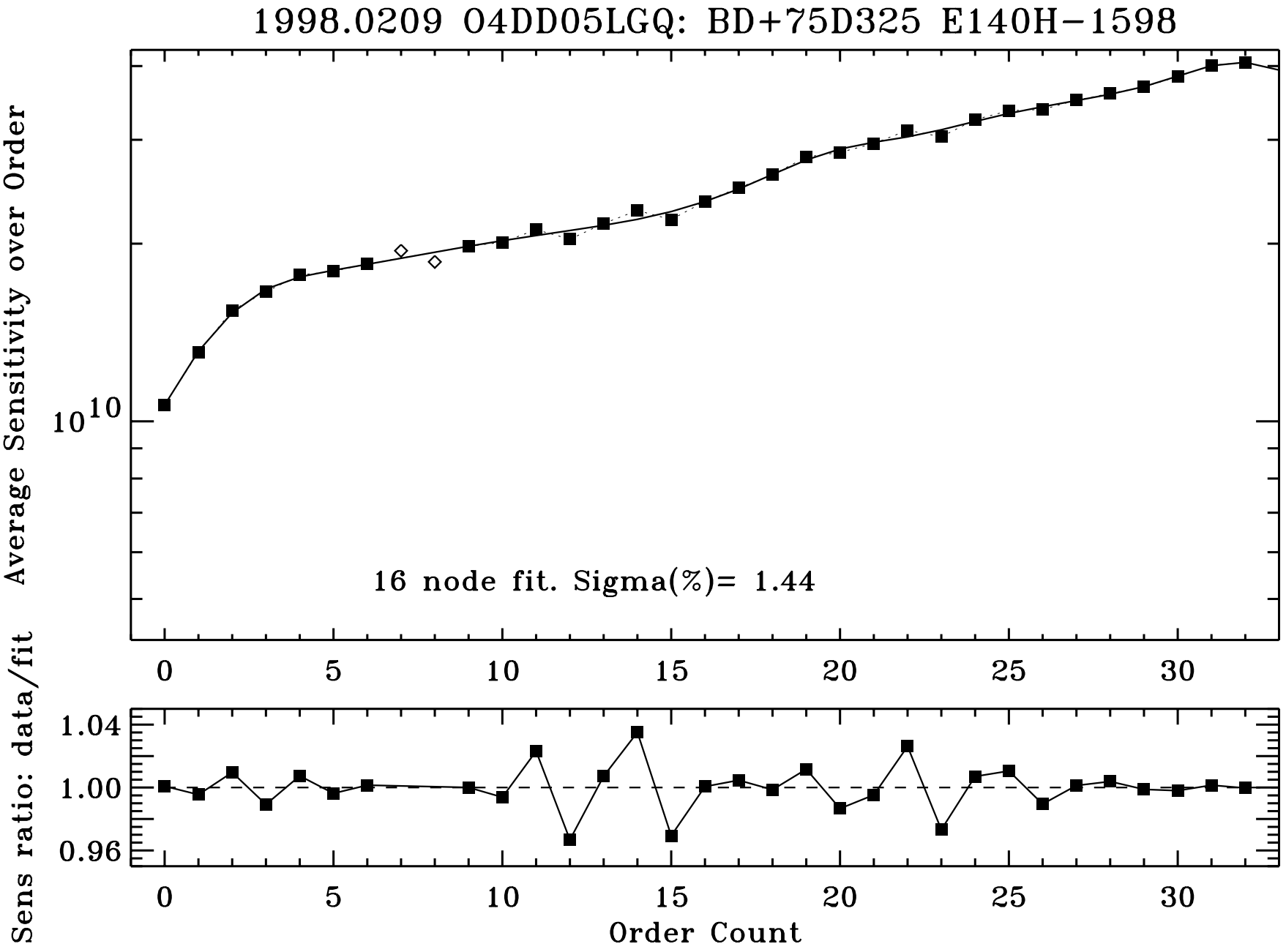
1998.0209 O4DD05LGQ: BD+75D325 E140H-1598
Average Sensitivity over Order
10^{10}
16 node fit. Sigma(%)= 1.44
0
5
10
15
20
25
30
Sens ratio: data/fit
1.04
1.00
0.96
Order Count
BOHLIN: echsens 3-Jun-1998 15:28

Fig. 3 (cont.)

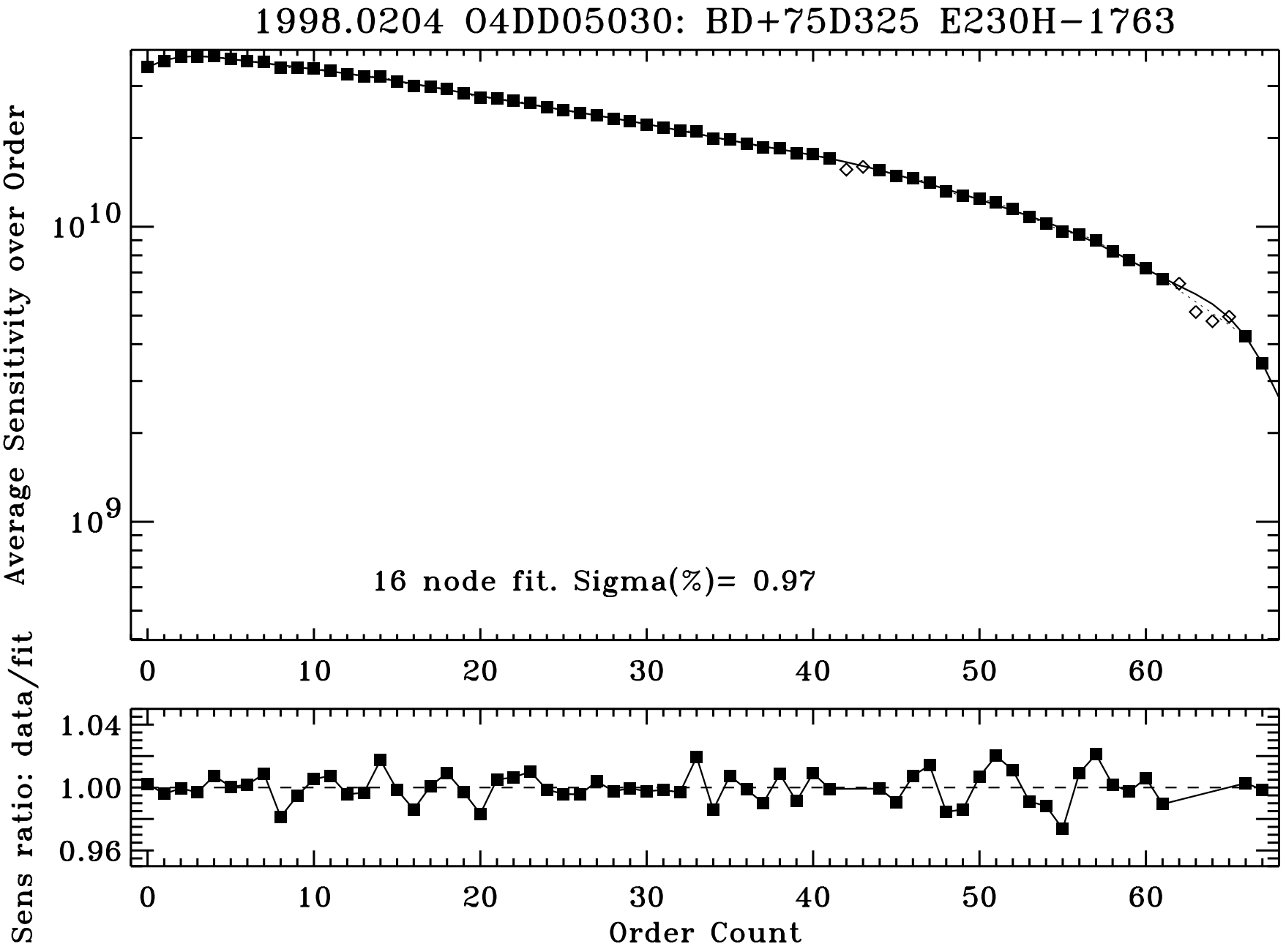
1998.0204 04DD05030: BD+75D325 E230H-1763
Average Sensitivity over Order
10^{10}
10^{9}
16 node fit. Sigma(%)= 0.97
0
10
20
30
40
50
60
Sens ratio: data/fit
1.04
1.00
0.96
Order Count
BOHLIN: echsens 3-Jun-1998 15:28

Fig. 3 (cont.)

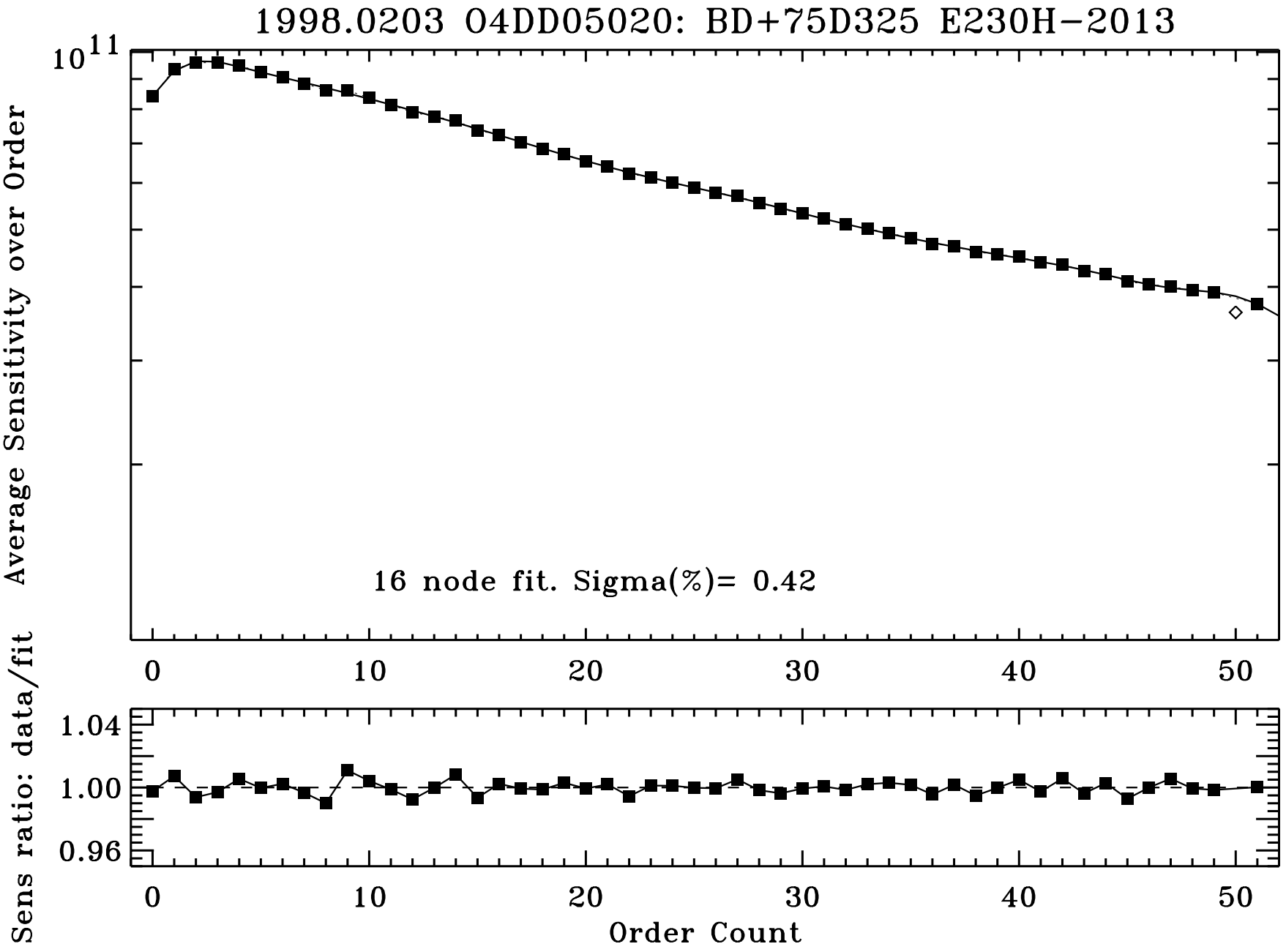
1998.0203 O4DD05020: BD+75D325 E230H-2013
10^{11}
Average Sensitivity over Order
16 node fit. Sigma(%)= 0.42
0
10
20
30
40
50
1.04
1.00
0.96
Sens ratio: data/fit
Order Count
BOHLIN: echsens 3-Jun-1998 15:28

Fig. 3 (cont.)

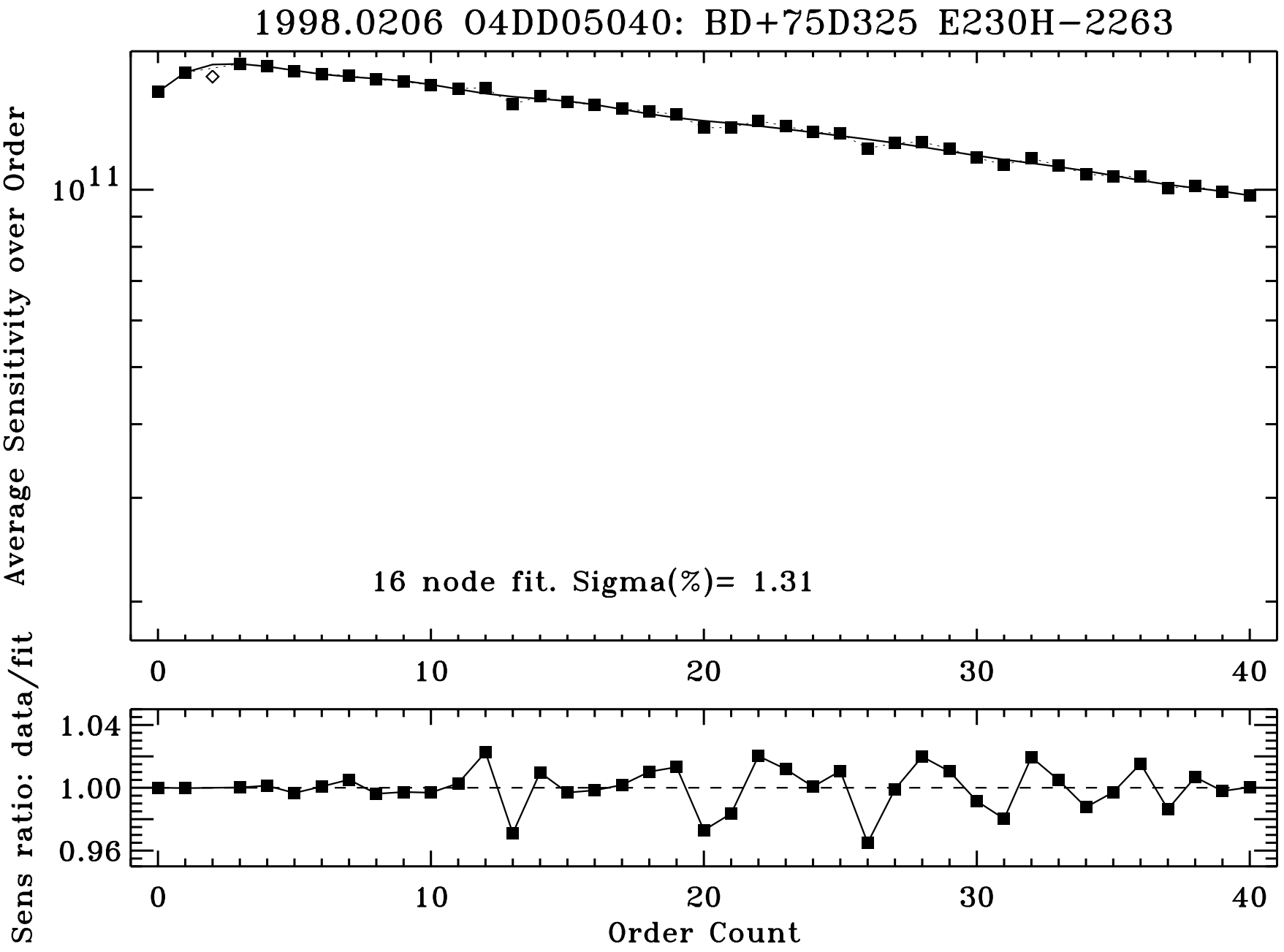
1998.0206 04DD05040: BD+75D325 E230H-2263
Average Sensitivity over Order
10^{11}
16 node fit. Sigma(%)= 1.31
0
10
20
30
40
Sens ratio: data/fit
1.04
1.00
0.96
0
10
20
30
40
Order Count
BOHLIN: echsens 3-Jun-1998 15:28

Fig. 3 (cont.)

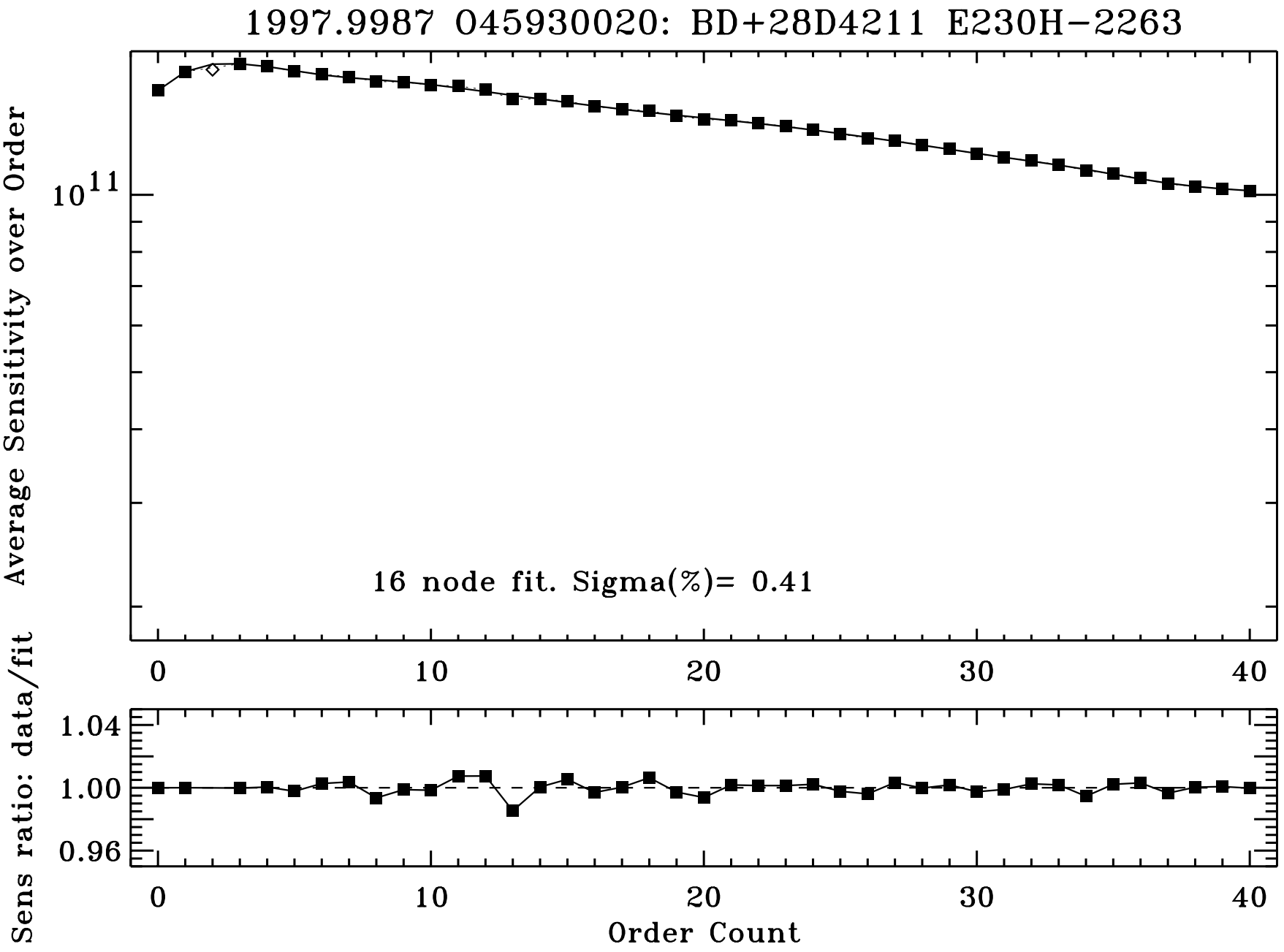
1997.9987 045930020: BD+28D4211 E230H-2263
Average Sensitivity over Order
10^{11}
16 node fit. Sigma(%)= 0.41
0
10
20
30
40
Sens ratio: data/fit
1.04
1.00
0.96
0
10
20
30
40
Order Count
BOHLIN: echsens 3-Jun-1998 15:28

Fig. 3 (cont.)

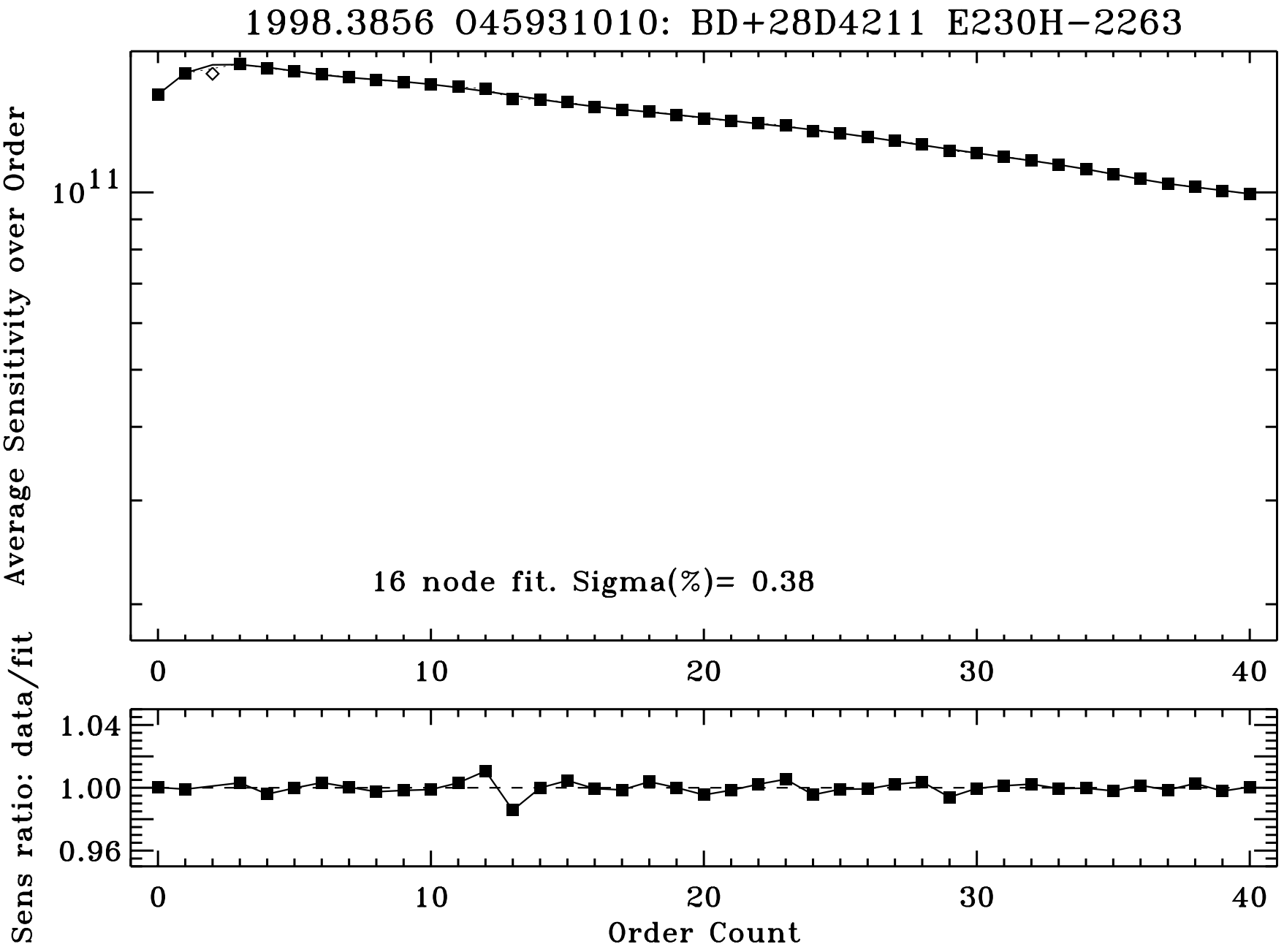
1998.3856 045931010: BD+28D4211 E230H-2263
Average Sensitivity over Order
10^{11}
16 node fit. Sigma(%)= 0.38
0
10
20
30
40
Sens ratio: data/fit
1.04
1.00
0.96
0
10
20
30
40
Order Count
BOHLIN: echsens 3-Jun-1998 15:28

Fig. 3 (cont.)

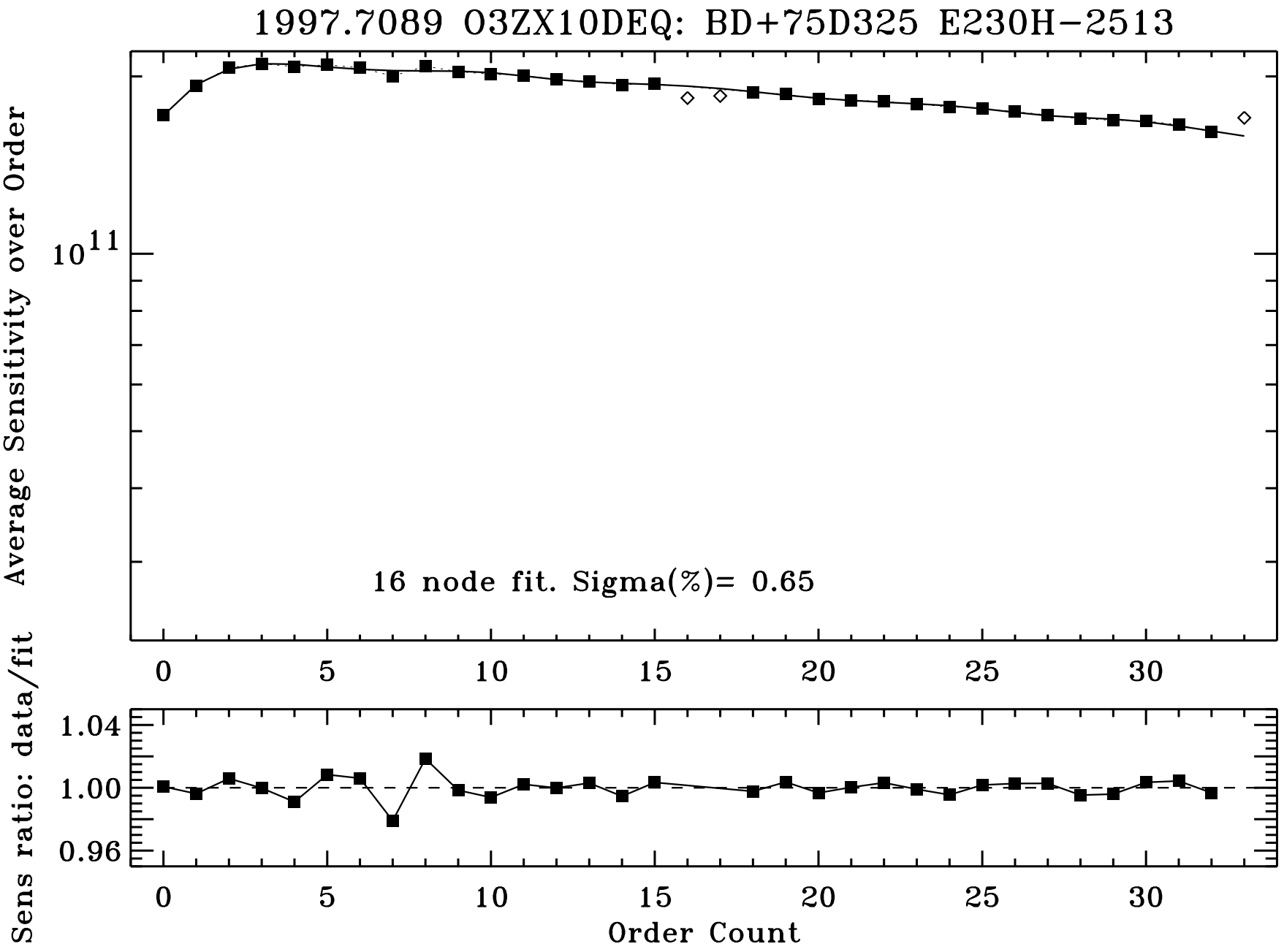
1997.7089 O3ZX10DEQ: BD+75D325 E230H-2513
Average Sensitivity over Order
10^{11}
16 node fit. Sigma(%)= 0.65
Sens ratio: data/fit
1.04
1.00
0.96
0
5
10
15
20
25
30
Order Count
BOHLIN: echsens 3-Jun-1998 15:28

Fig. 3 (cont.)

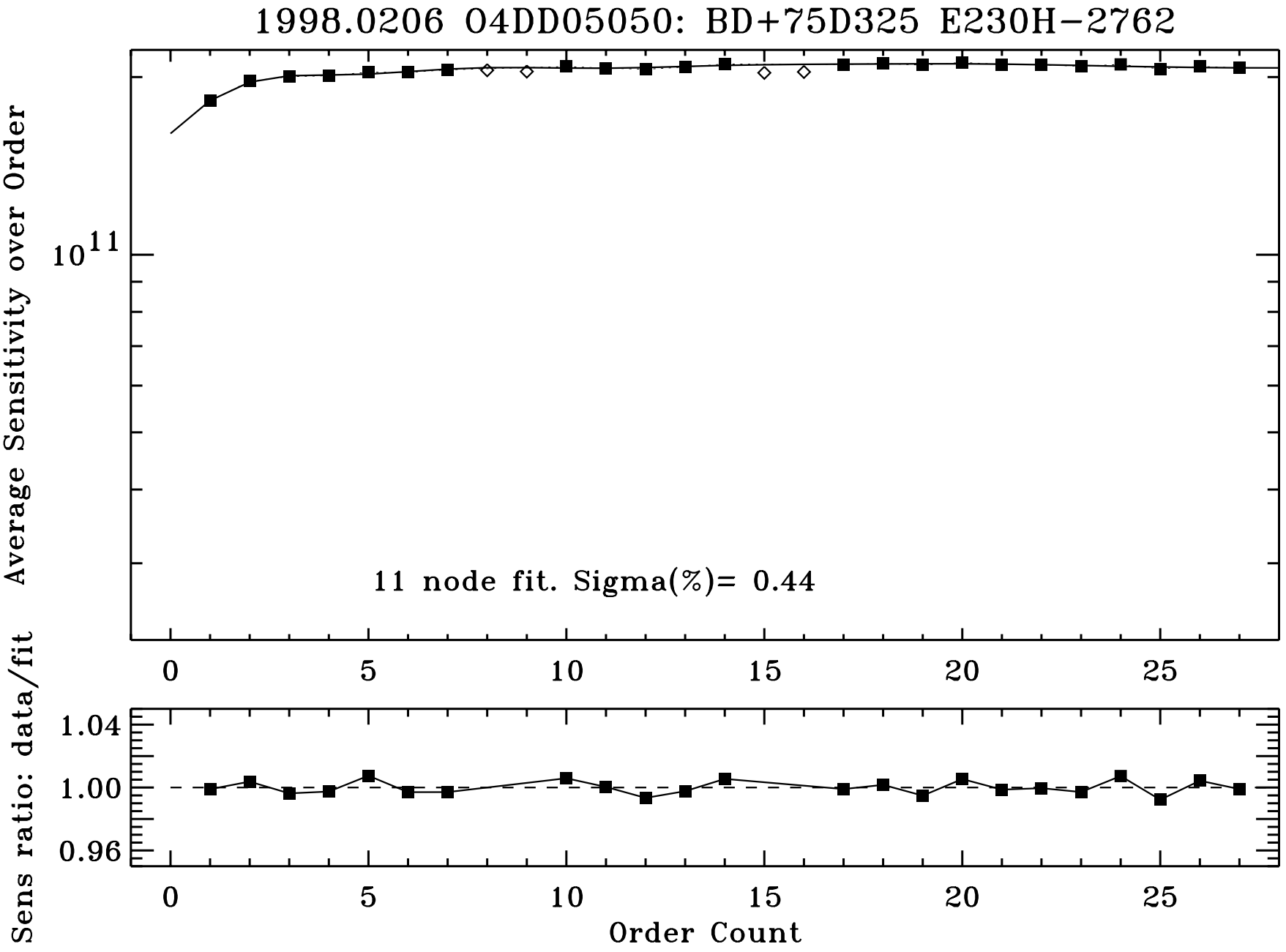

Fig. 3 (cont.)

BOHLIN: echsens 3-Jun-1998 15:28

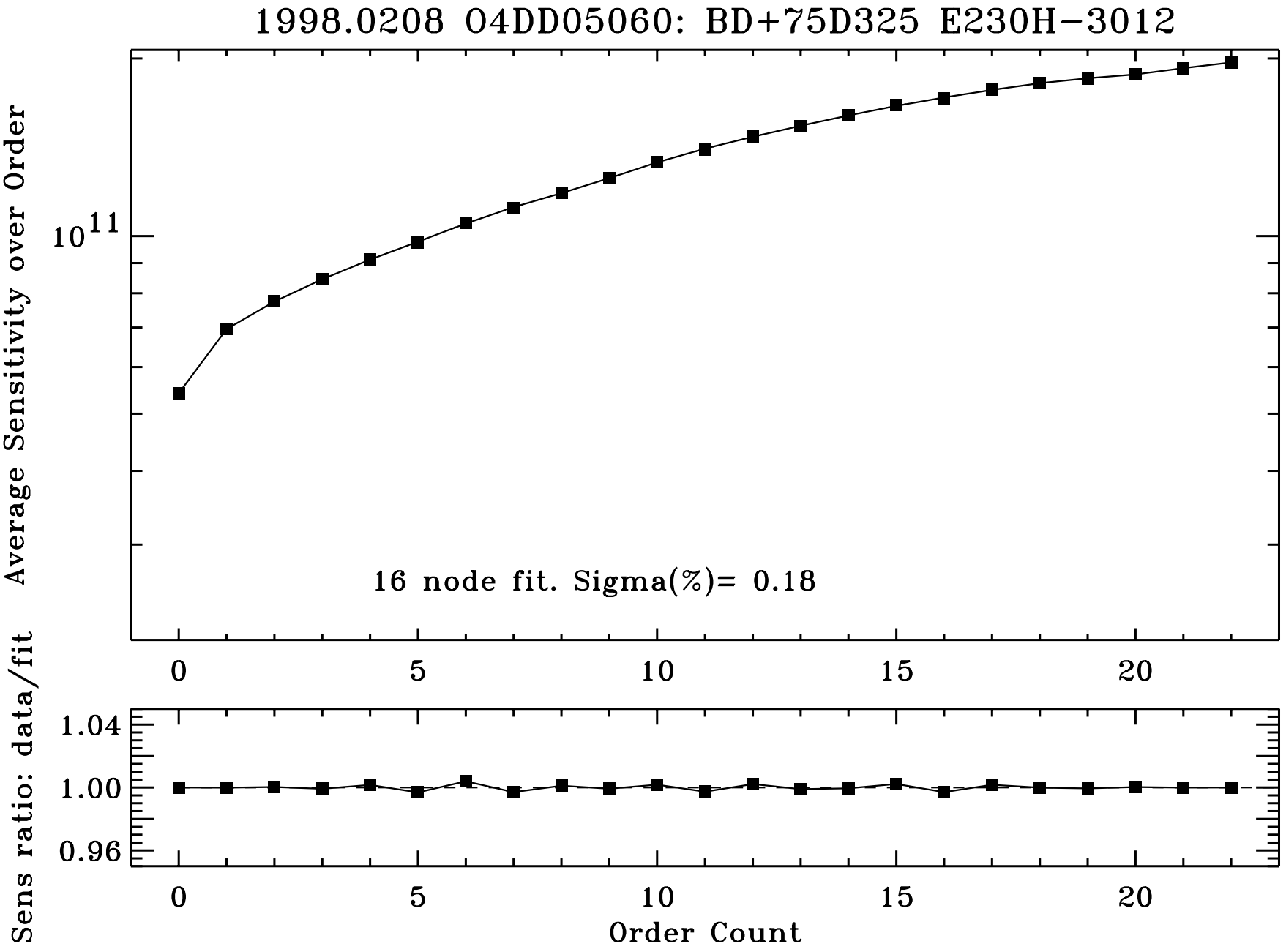

Fig. 3 (cont.)

BOHLIN: echsens 3-Jun-1998 15:28

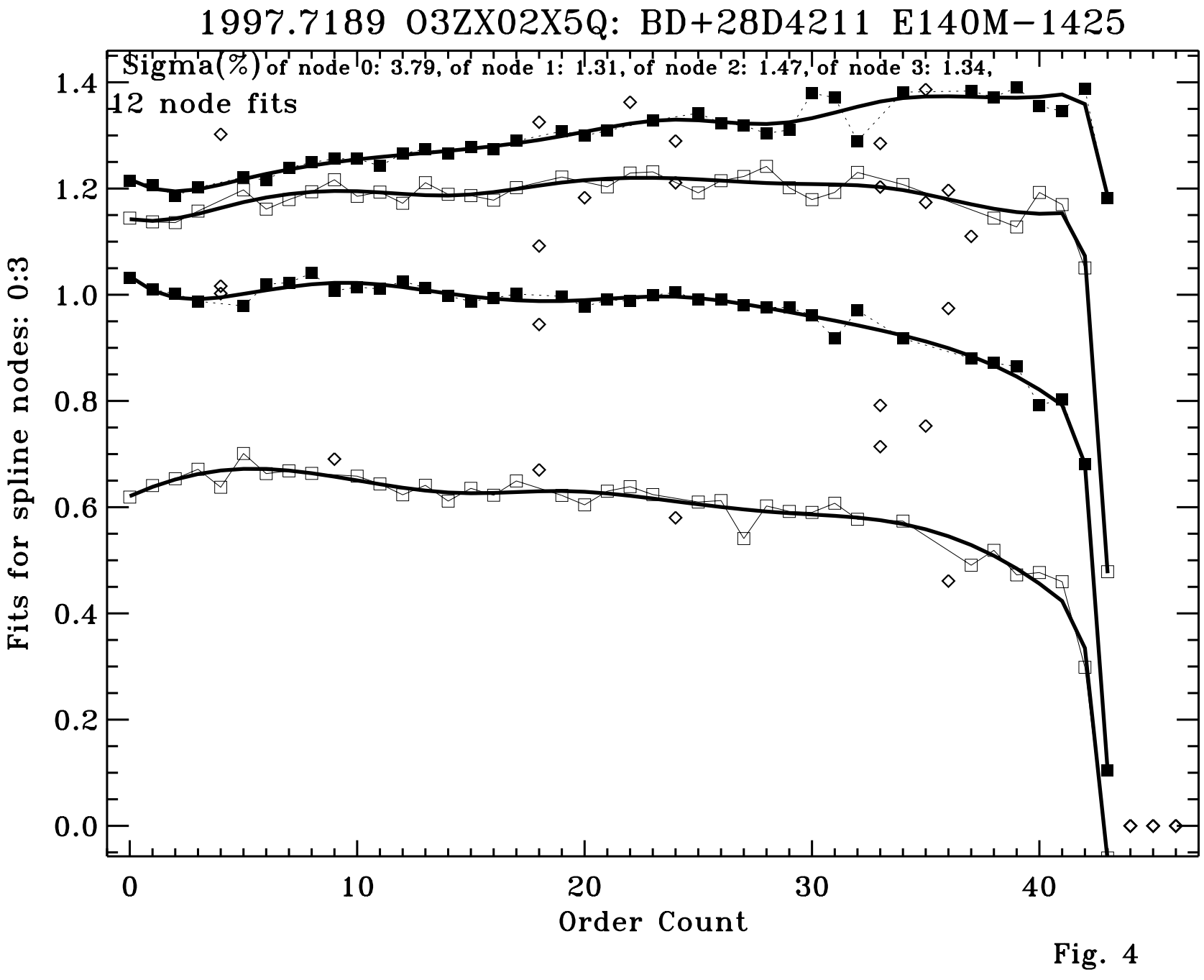
1997.7189 03ZX02X5Q: BD+28D4211 E140M-1425
Sigma(%) of node 0: 3.79, of node 1: 1.31, of node 2: 1.47, of node 3: 1.34,
12 node fits
Fits for spline nodes: 0:3
1.4
1.2
1.0
0.8
0.6
0.4
0.2
0.0
0
10
20
30
40
Order Count
BOHLIN: echsens 3-Jun-1998 14:59

Fig. 4

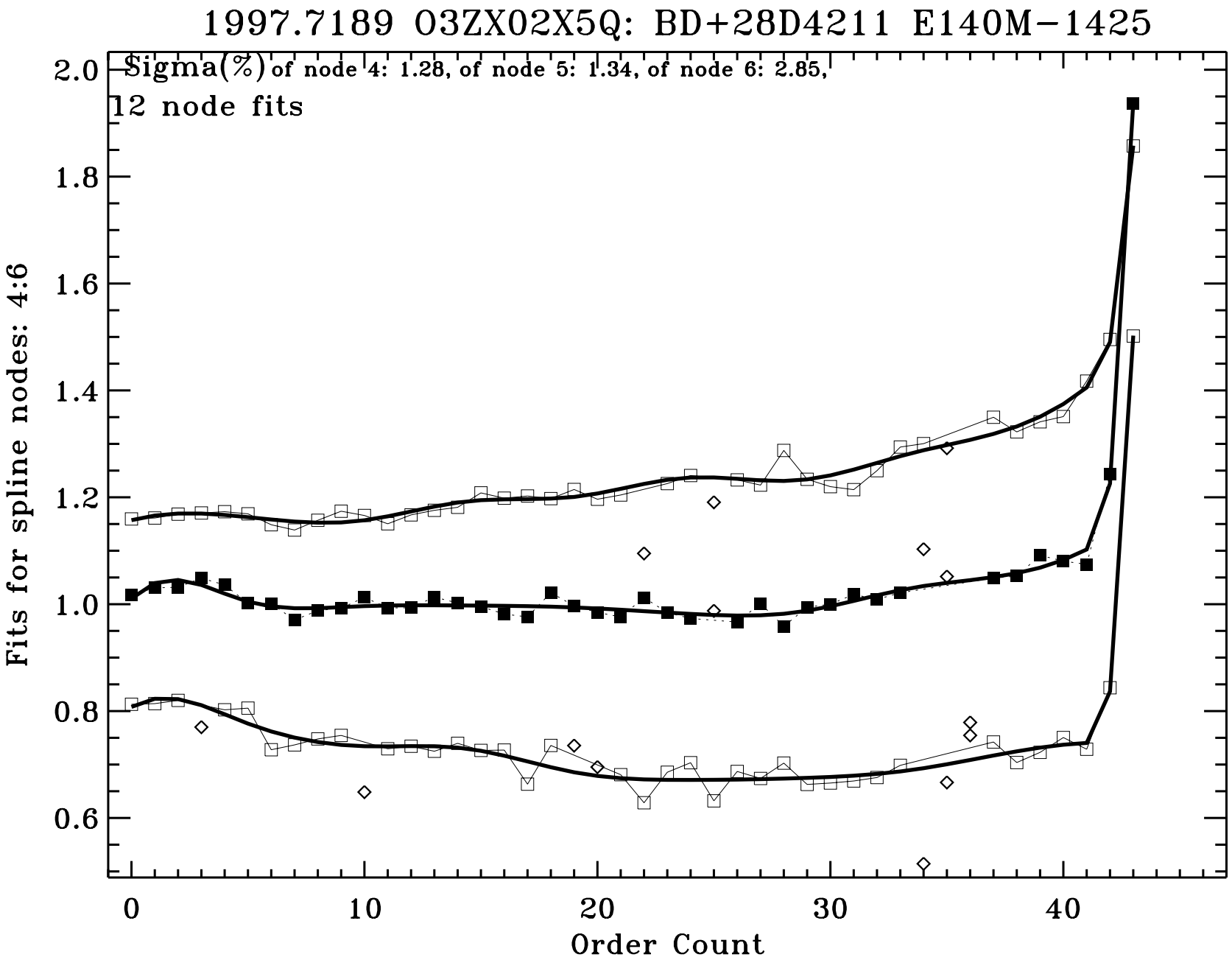
1997.7189 03ZX02X5Q: BD+28D4211 E140M-1425
Sigma(%) of node 4: 1.28, of node 5: 1.34, of node 6: 2.85,
12 node fits
Fits for spline nodes: 4:6
Order Count
2.0
1.8
1.6
1.4
1.2
1.0
0.8
0.6
0
10
20
30
40
BOHLIN: echsens 3-Jun-1998 14:59

Fig. 4 (cont.)

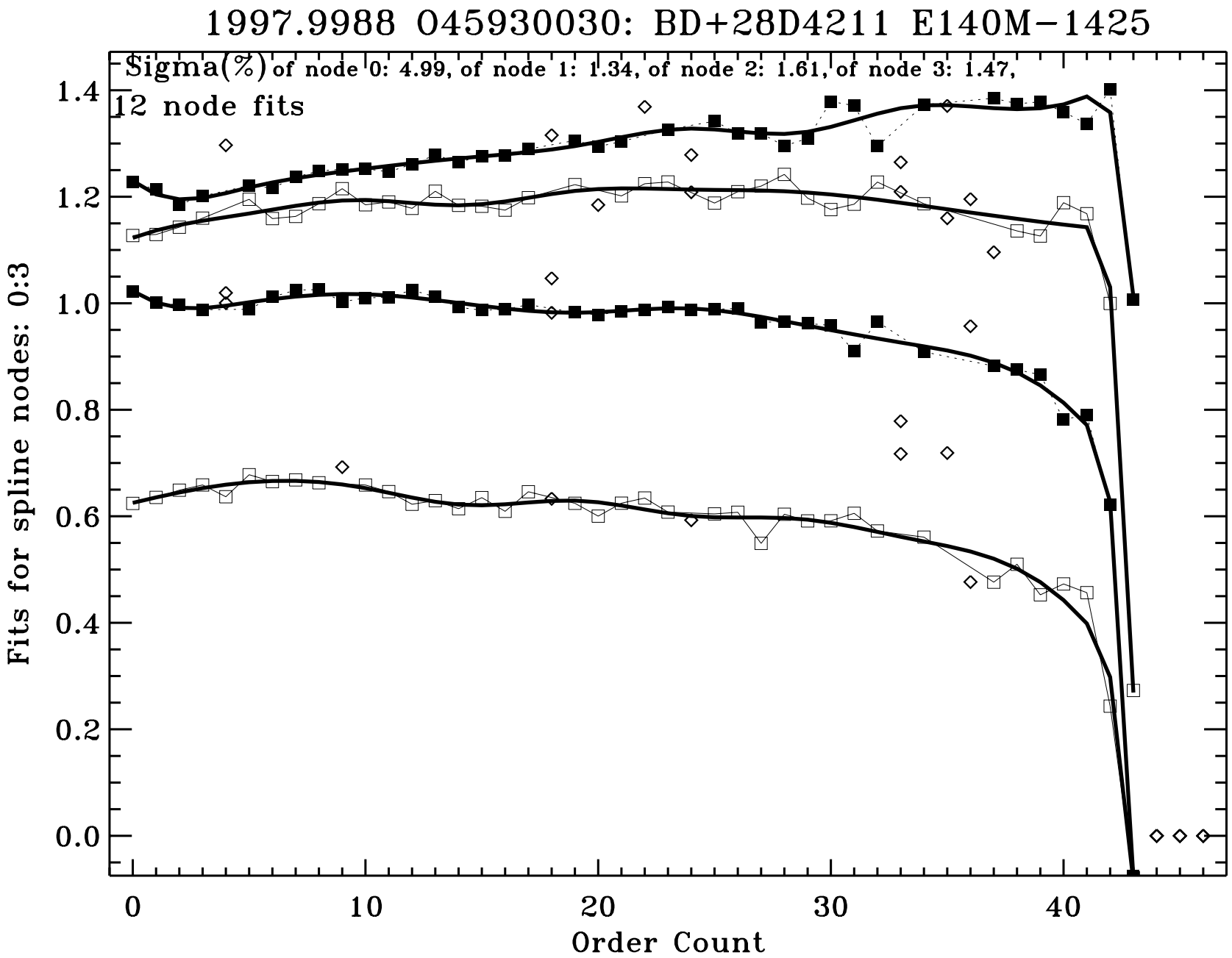
1997.9988 045930030: BD+28D4211 E140M-1425
Sigma(%) of node 0: 4.99, of node 1: 1.34, of node 2: 1.61, of node 3: 1.47,
12 node fits
Fits for spline nodes: 0:3
Order Count
0.0
0.2
0.4
0.6
0.8
1.0
1.2
1.4
0
10
20
30
40
BOHLIN: echsens 3-Jun-1998 14:59

Fig. 4 (cont.)

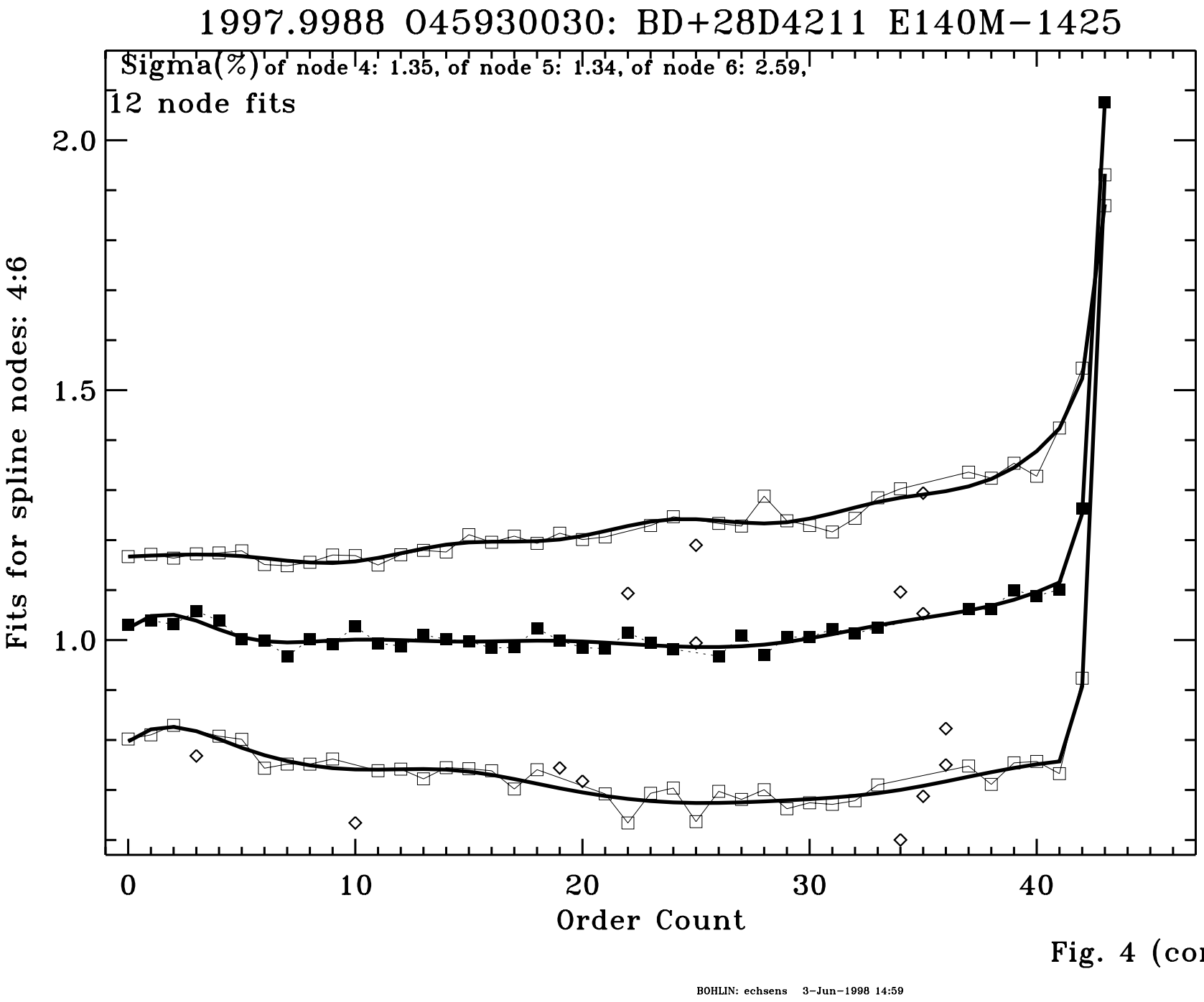
1997.9988 045930030: BD+28D4211 E140M−1425
Sigma(%) of node 4: 1.35, of node 5: 1.34, of node 6: 2.59,
12 node fits
Fits for spline nodes: 4:6
2.0
1.5
1.0
0
10
20
30
40
Order Count
BOHLIN: echsens 3-Jun-1998 14:59

Fig. 4 (cont.)

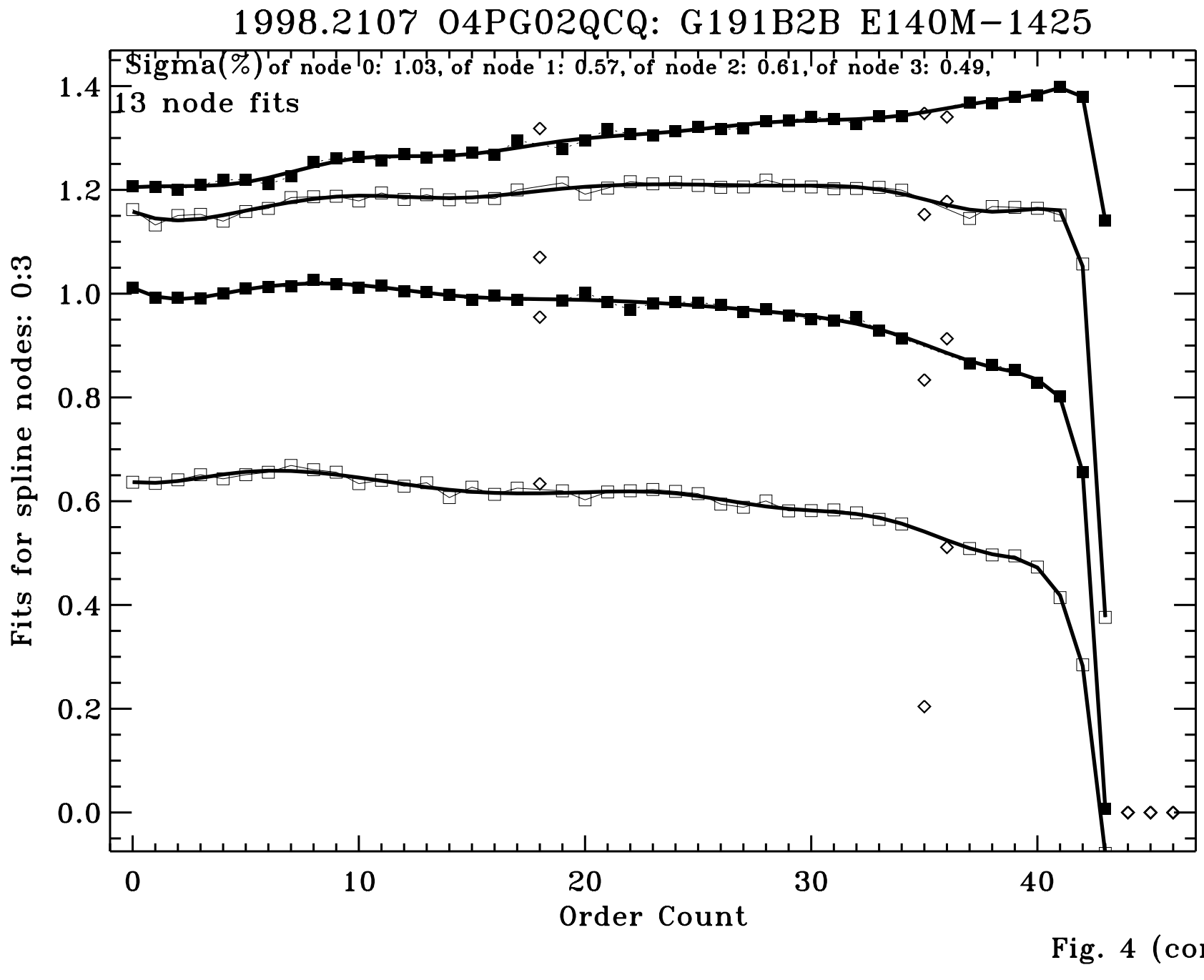
1998.2107 04PG02QCQ: G191B2B E140M-1425
Sigma(%) of node 0: 1.03, of node 1: 0.57, of node 2: 0.61, of node 3: 0.49,
13 node fits
Fits for spline nodes: 0:3
Order Count
0.0
0.2
0.4
0.6
0.8
1.0
1.2
1.4
0
10
20
30
40
BOHLIN: echsens 3-Jun-1998 14:59

Fig. 4 (cont.)

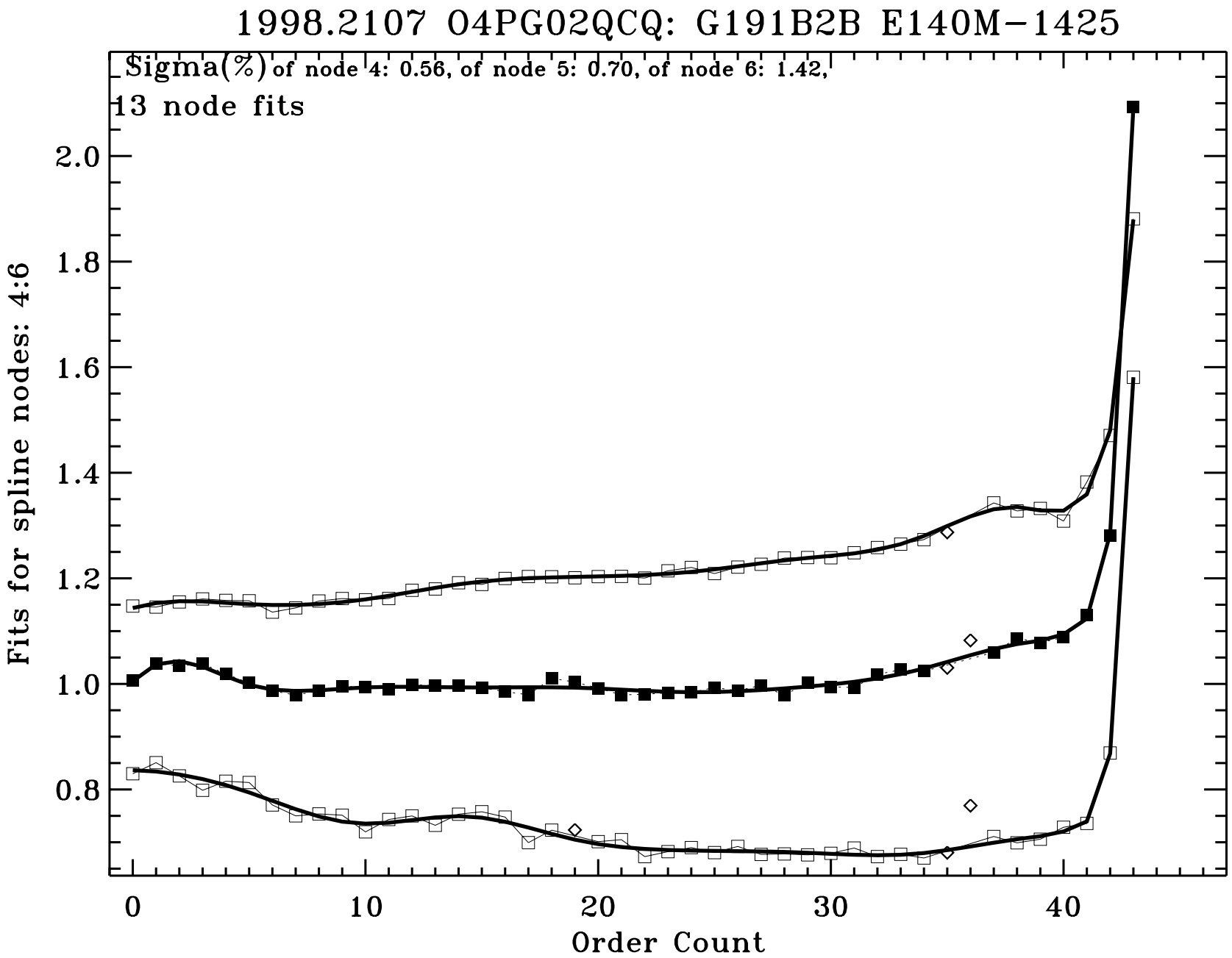
1998.2107 04PG02QCQ: G191B2B E140M-1425
Sigma(%) of node 4: 0.56, of node 5: 0.70, of node 6: 1.42,
13 node fits
Fits for spline nodes: 4:6
2.0
1.8
1.6
1.4
1.2
1.0
0.8
0
10
20
30
40
Order Count
BOHLIN: echsens 3-Jun-1998 14:59

Fig. 4 (cont.)

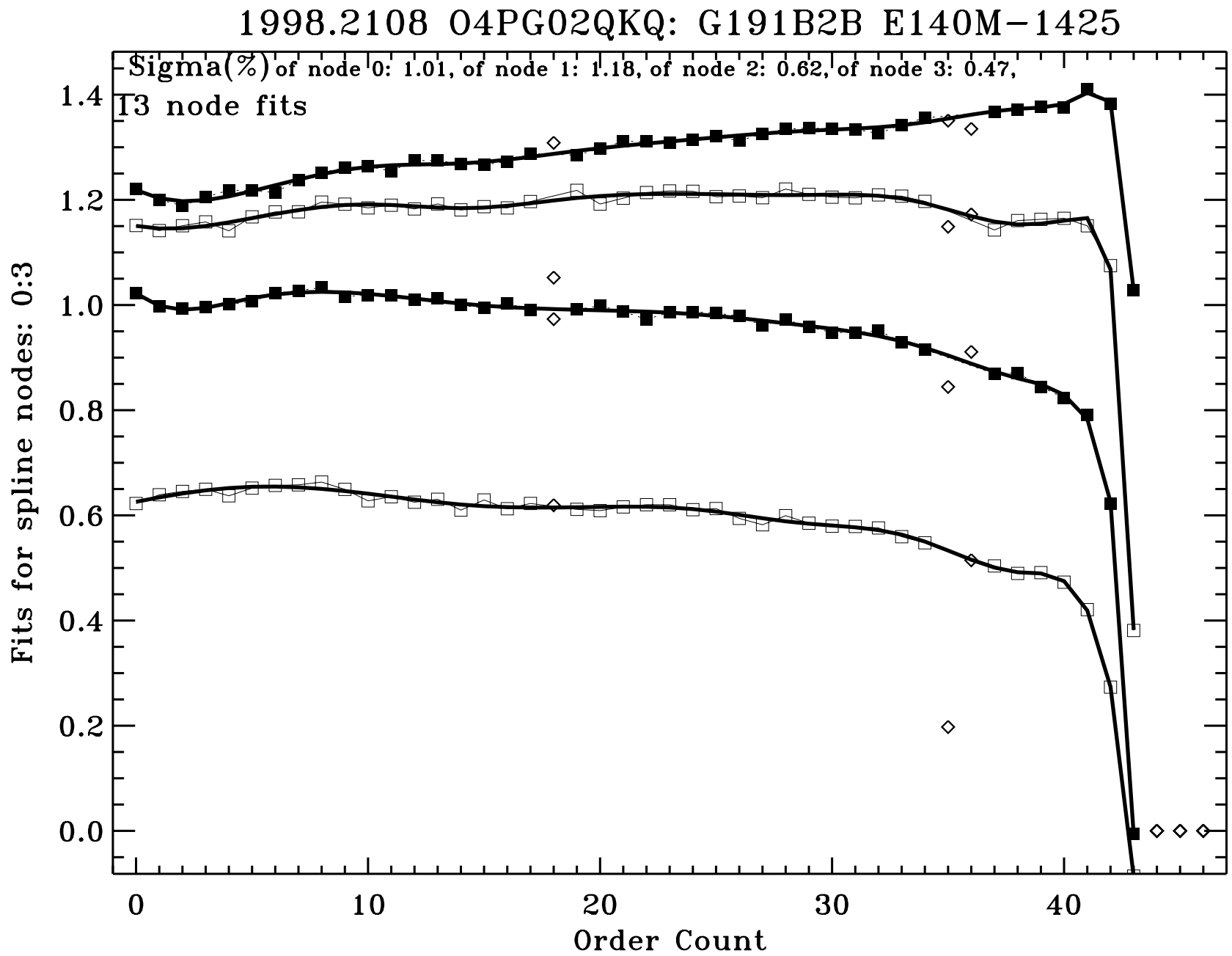
1998.2108 04PG02QKQ: G191B2B E140M−1425
Sigma(%) of node 0: 1.01, of node 1: 1.18, of node 2: 0.62, of node 3: 0.47,
T3 node fits
Fits for spline nodes: 0:3
Order Count
0.0
0.2
0.4
0.6
0.8
1.0
1.2
1.4
0
10
20
30
40
BOHLIN: echsens 3-Jun-1998 14:59

Fig. 4 (cont.)

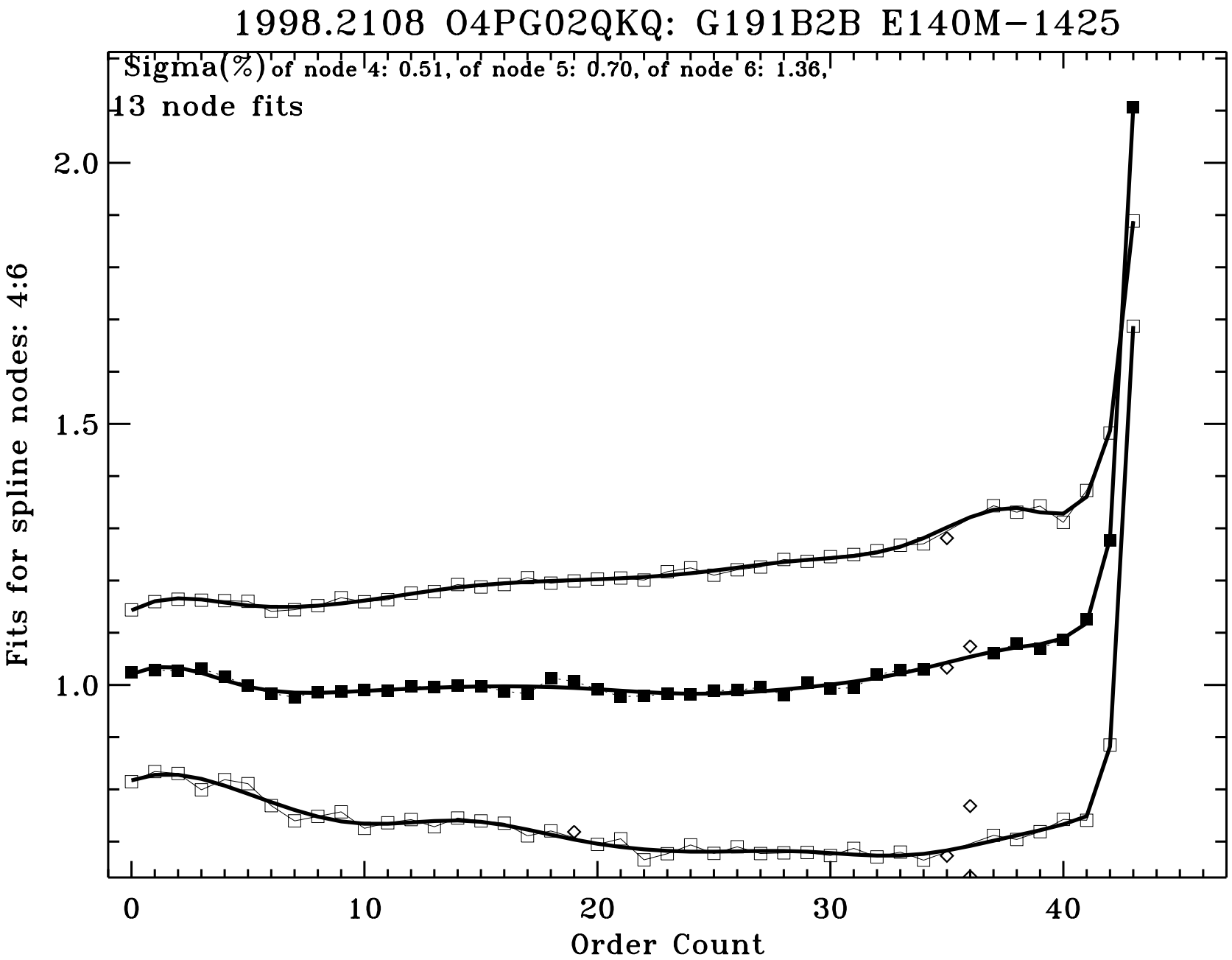
1998.2108 04PG02QKQ: G191B2B E140M-1425
Sigma(%) of node 4: 0.51, of node 5: 0.70, of node 6: 1.36,
13 node fits
Fits for spline nodes: 4:6
2.0
1.5
1.0
0
10
20
30
40
Order Count
BOHLIN: echsens 3-Jun-1998 14:59

Fig. 4 (cont.)

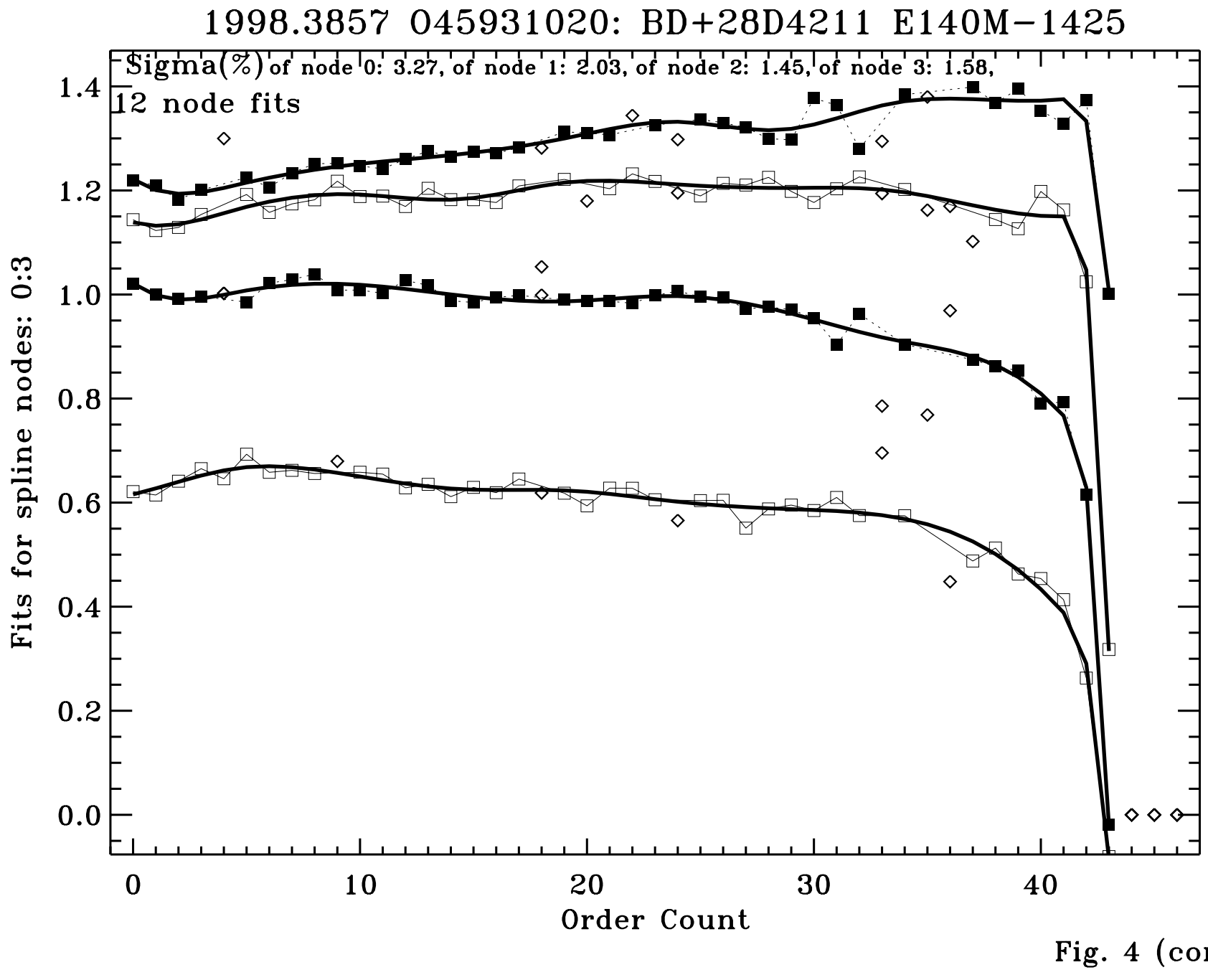
1998.3857 045931020: BD+28D4211 E140M-1425
Sigma(%) of node 0: 3.27, of node 1: 2.03, of node 2: 1.45, of node 3: 1.58,
12 node fits
Fits for spline nodes: 0:3
1.4
1.2
1.0
0.8
0.6
0.4
0.2
0.0
0
10
20
30
40
Order Count
BOHLIN: echsens 3-Jun-1998 14:59

Fig. 4 (cont.)

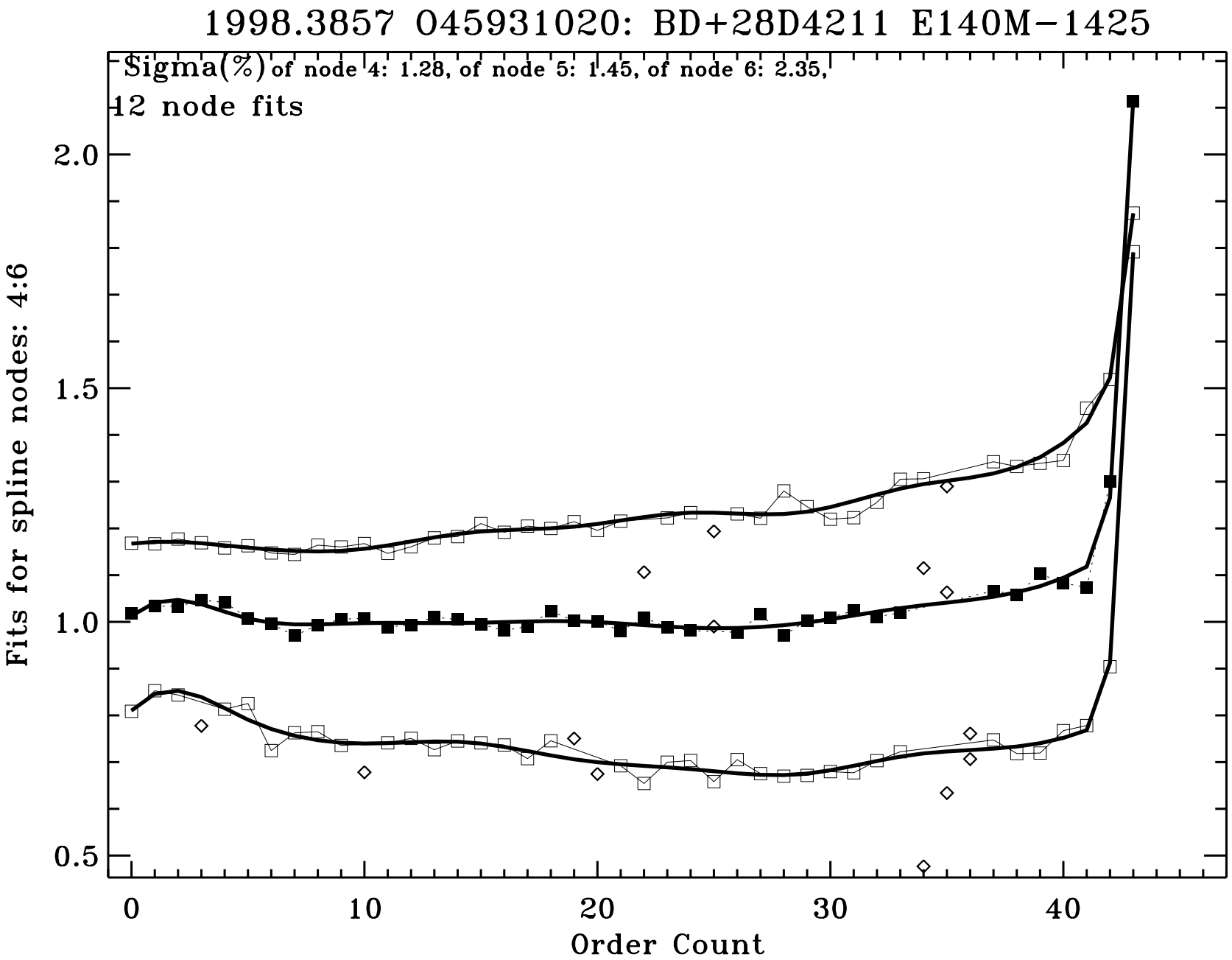
1998.3857 045931020: BD+28D4211 E140M-1425
Sigma(%) of node 4: 1.28, of node 5: 1.45, of node 6: 2.35,
12 node fits
Fits for spline nodes: 4:6
2.0
1.5
1.0
0.5
0
10
20
30
40
Order Count
BOHLIN: echsens 3-Jun-1998 14:59

Fig. 4 (cont.)

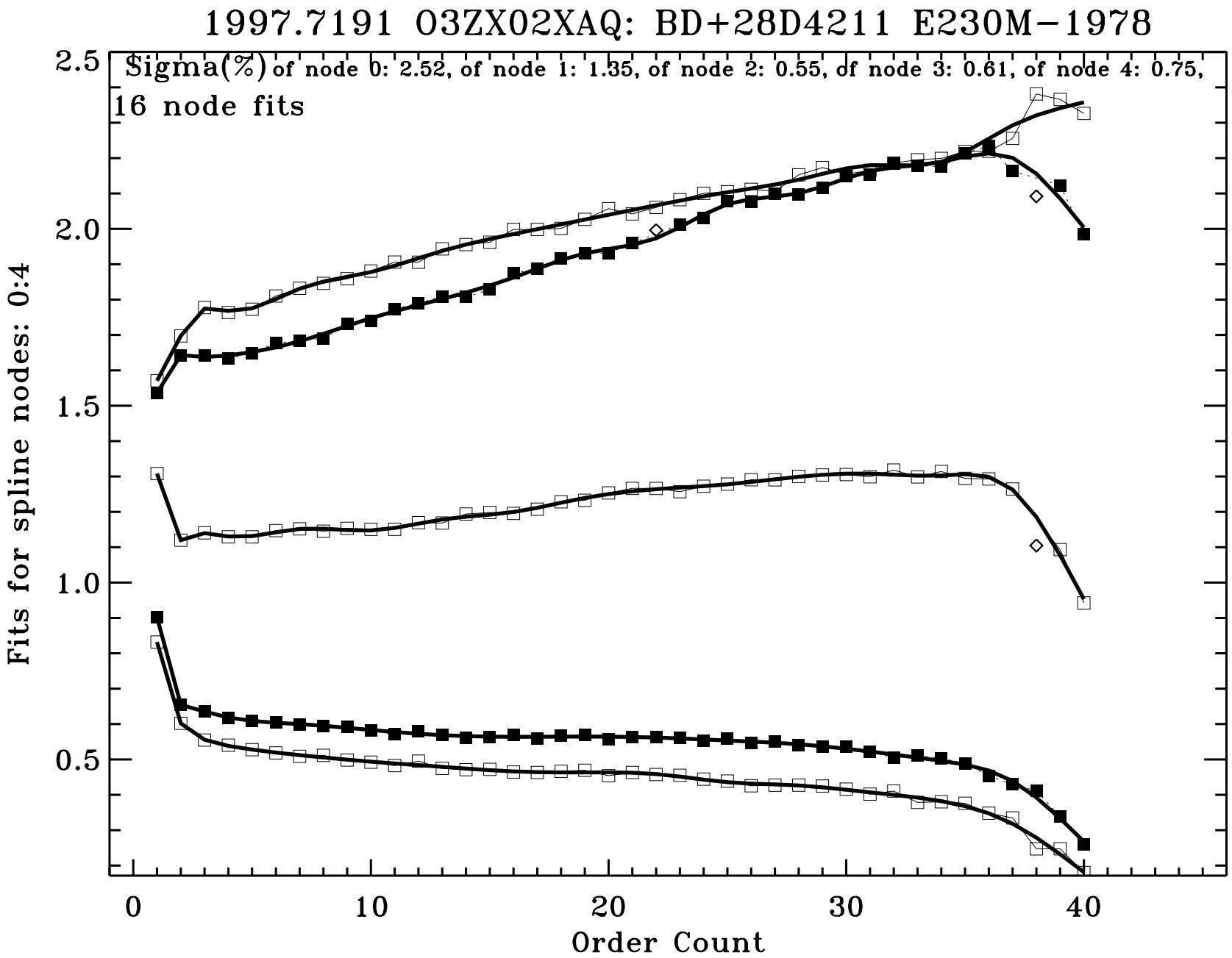
1997.7191 03ZX02XAQ: BD+28D4211 E230M-1978
Sigma(%) of node 0: 2.52, of node 1: 1.35, of node 2: 0.55, of node 3: 0.61, of node 4: 0.75,
16 node fits
Fits for spline nodes: 0:4
2.5
2.0
1.5
1.0
0.5
0
10
20
30
40
Order Count
BOHLIN: echsens 3-Jun-1998 14:59

Fig. 4 (cont.)

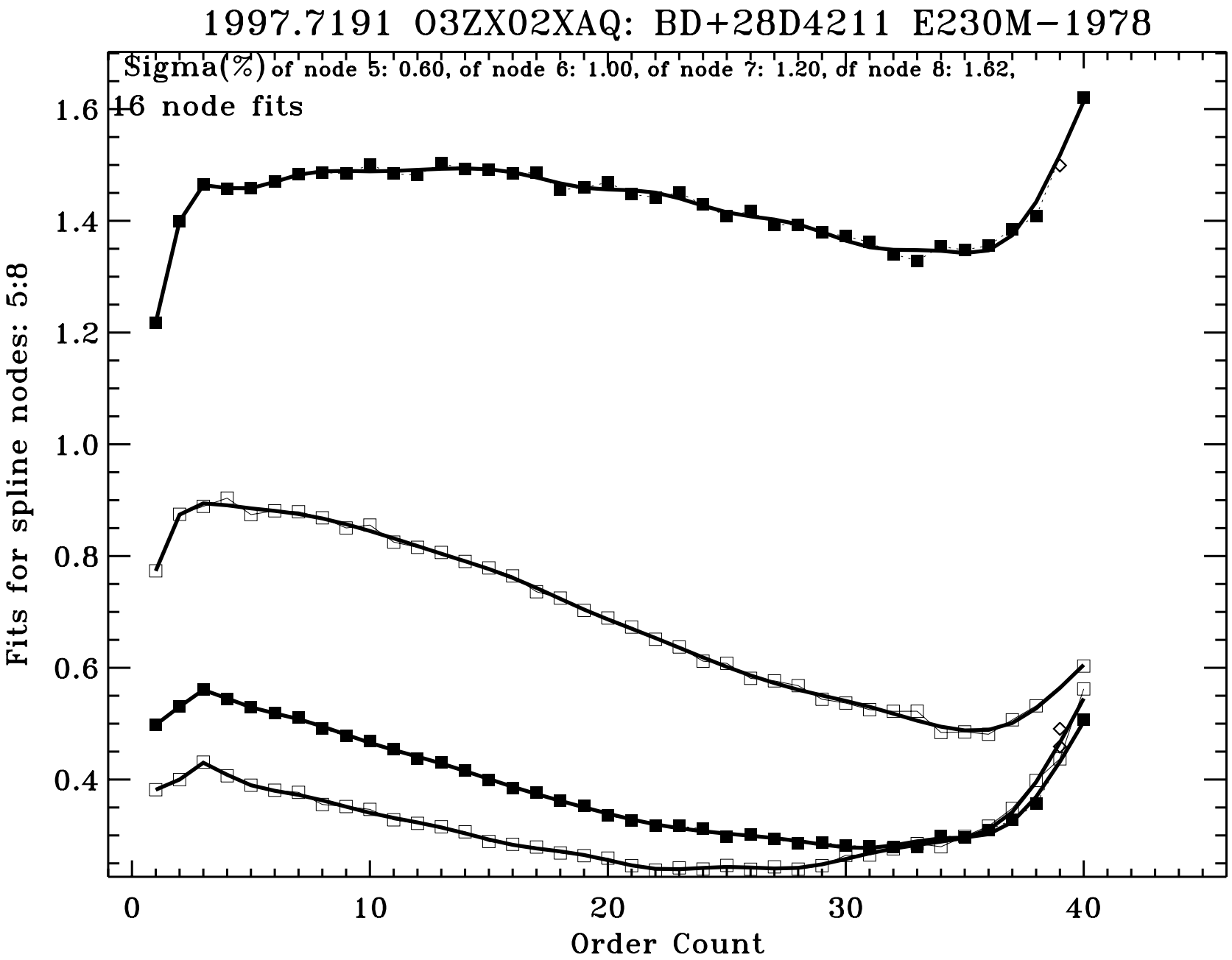
1997.7191 03ZX02XAQ: BD+28D4211 E230M-1978
Sigma(%) of node 5: 0.60, of node 6: 1.00, of node 7: 1.20, of node 8: 1.62,
16 node fits
Fits for spline nodes: 5:8
1.6
1.4
1.2
1.0
0.8
0.6
0.4
0
10
20
30
40
Order Count
BOHLIN: echsens 3-Jun-1998 14:59

Fig. 4 (cont.)

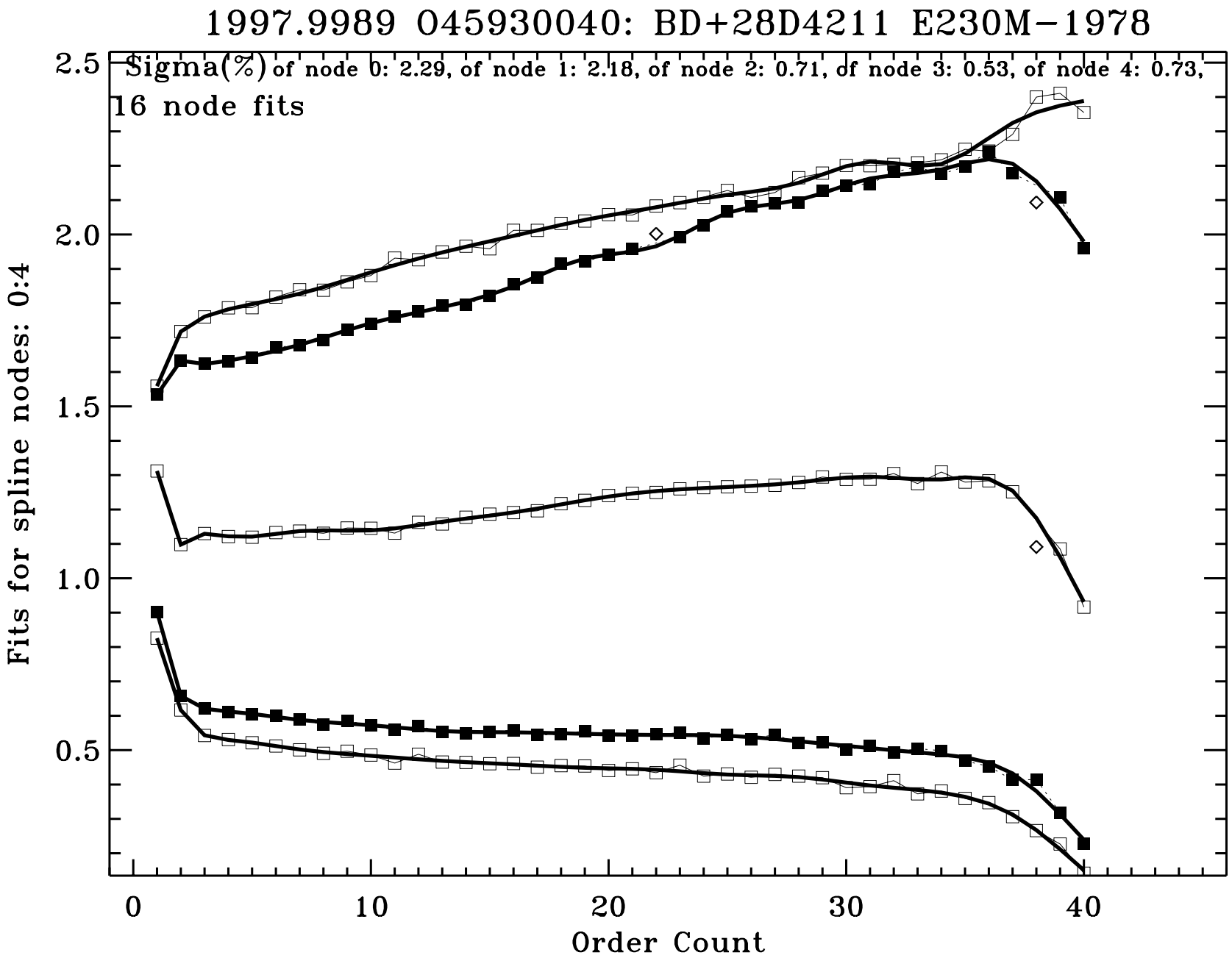
1997.9989 045930040: BD+28D4211 E230M-1978
Sigma(%) of node 0: 2.29, of node 1: 2.18, of node 2: 0.71, of node 3: 0.53, of node 4: 0.73,
16 node fits
Fits for spline nodes: 0:4
2.5
2.0
1.5
1.0
0.5
0
10
20
30
40
Order Count
BOHLIN: echsens 3-Jun-1998 15:00

Fig. 4 (cont.)

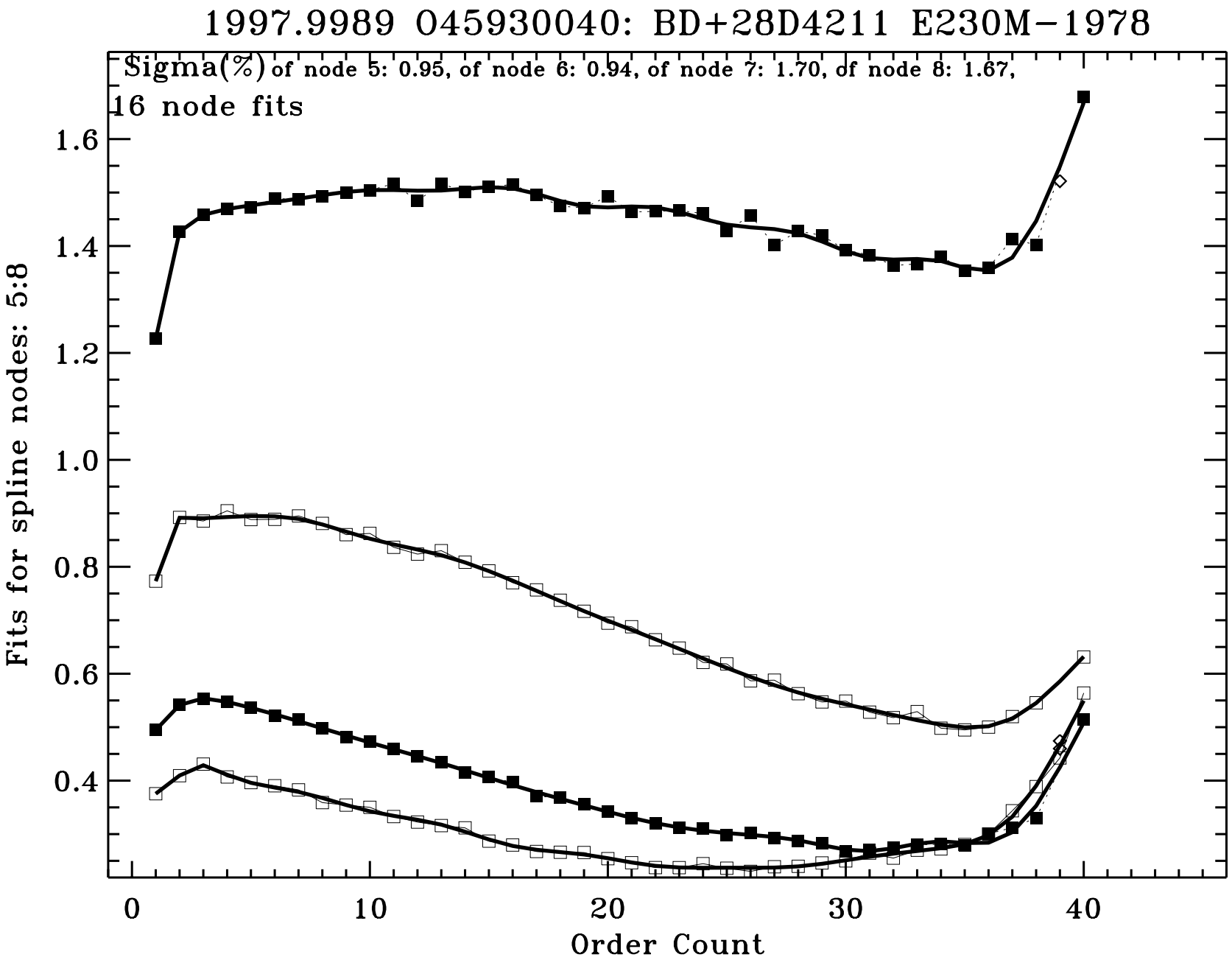
1997.9989 045930040: BD+28D4211 E230M-1978
Sigma(%) of node 5: 0.95, of node 6: 0.94, of node 7: 1.70, of node 8: 1.67,
16 node fits
Fits for spline nodes: 5:8
1.6
1.4
1.2
1.0
0.8
0.6
0.4
0
10
20
30
40
Order Count
BOHLIN: echsens 3-Jun-1998 15:00

Fig. 4 (cont.)

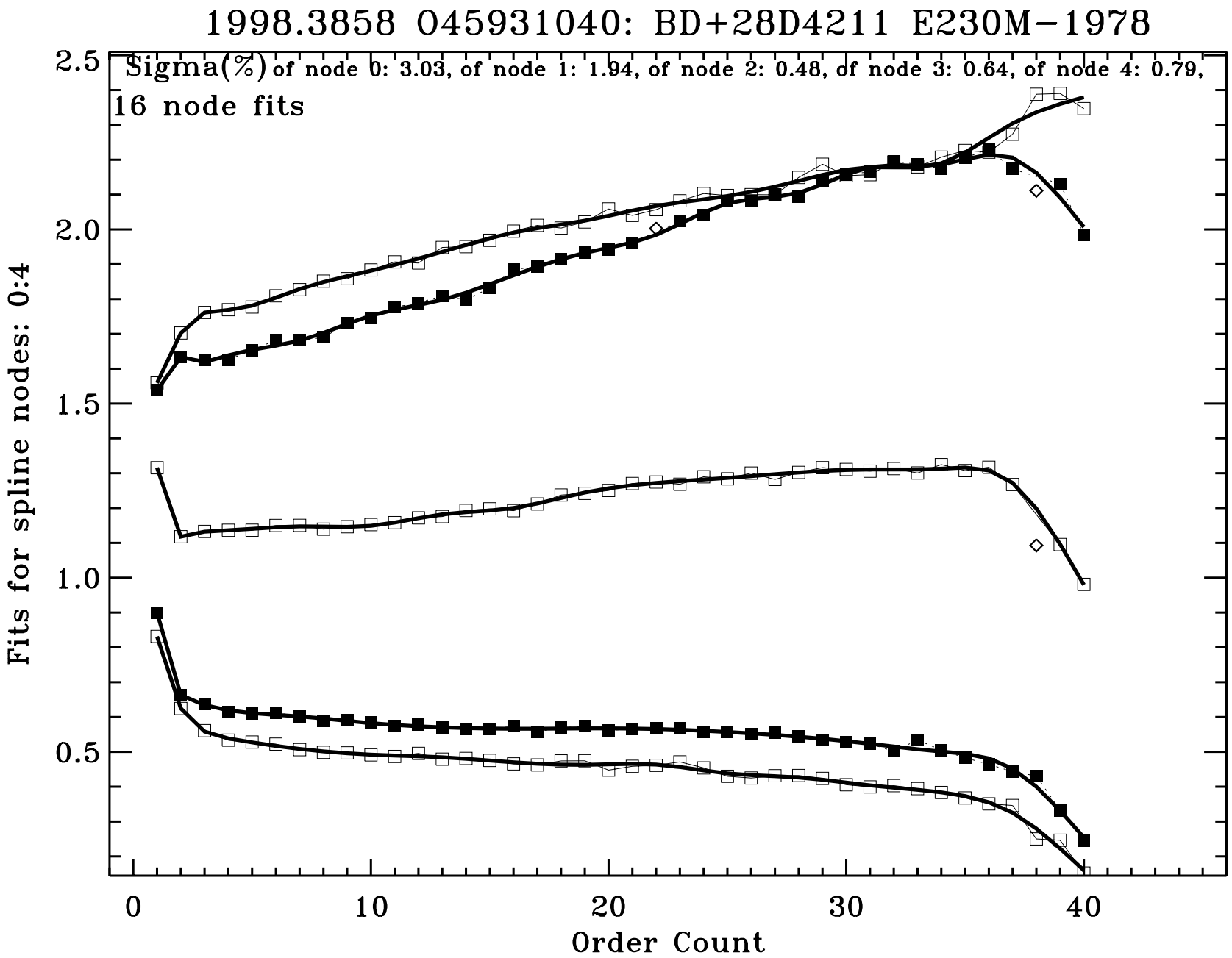
1998.3858 045931040: BD+28D4211 E230M-1978
Sigma(%) of node 0: 3.03, of node 1: 1.94, of node 2: 0.48, of node 3: 0.64, of node 4: 0.79,
16 node fits
Fits for spline nodes: 0:4
2.5
2.0
1.5
1.0
0.5
0
10
20
30
40
Order Count
BOHLIN: echsens 3-Jun-1998 15:00

Fig. 4 (cont.)

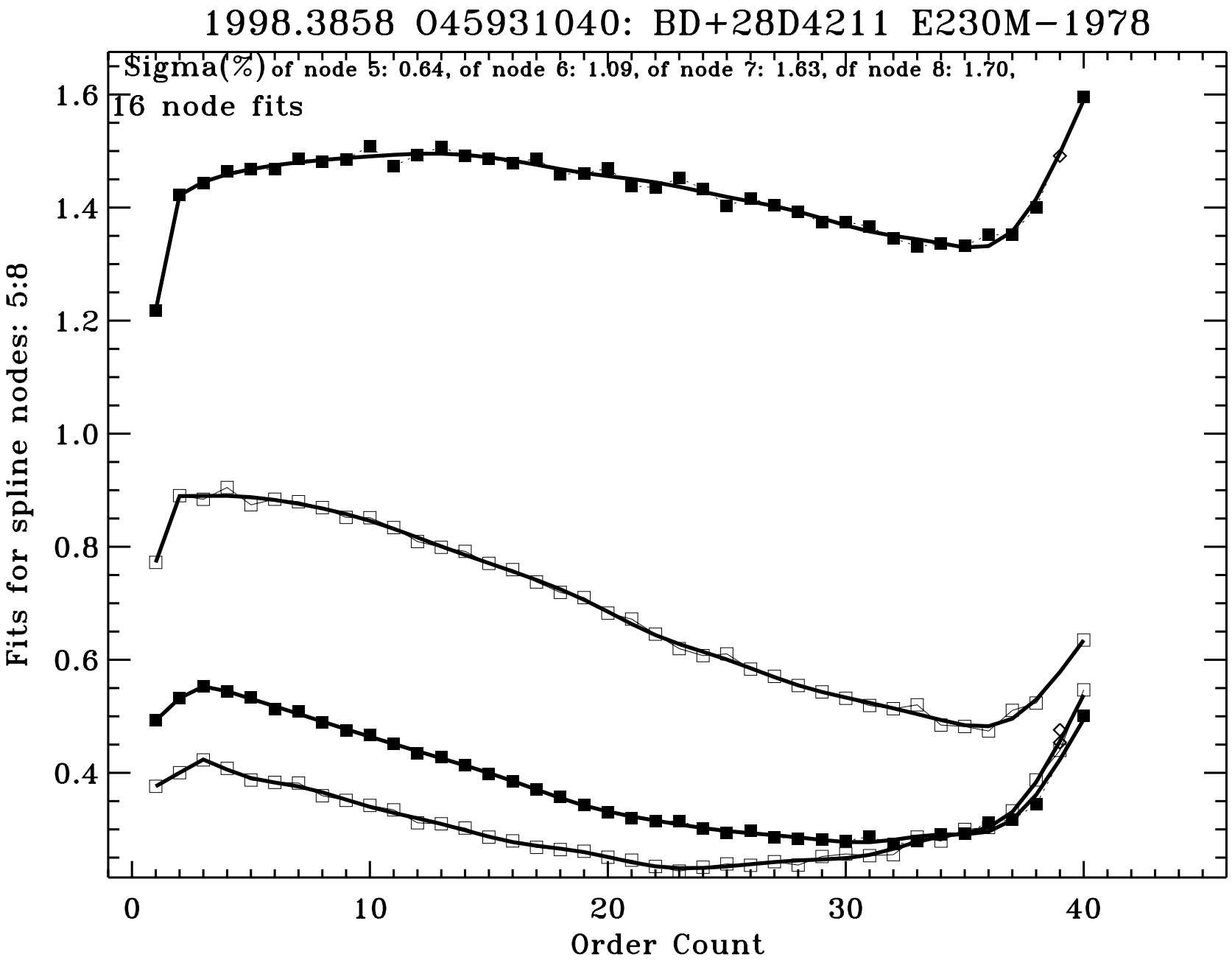
1998.3858 045931040: BD+28D4211 E230M-1978
Sigma(%) of node 5: 0.64, of node 6: 1.09, of node 7: 1.63, of node 8: 1.70,
16 node fits
Fits for spline nodes: 5:8
1.6
1.4
1.2
1.0
0.8
0.6
0.4
0
10
20
30
40
Order Count
BOHLIN: echsens 3-Jun-1998 15:00

Fig. 4 (cont.)

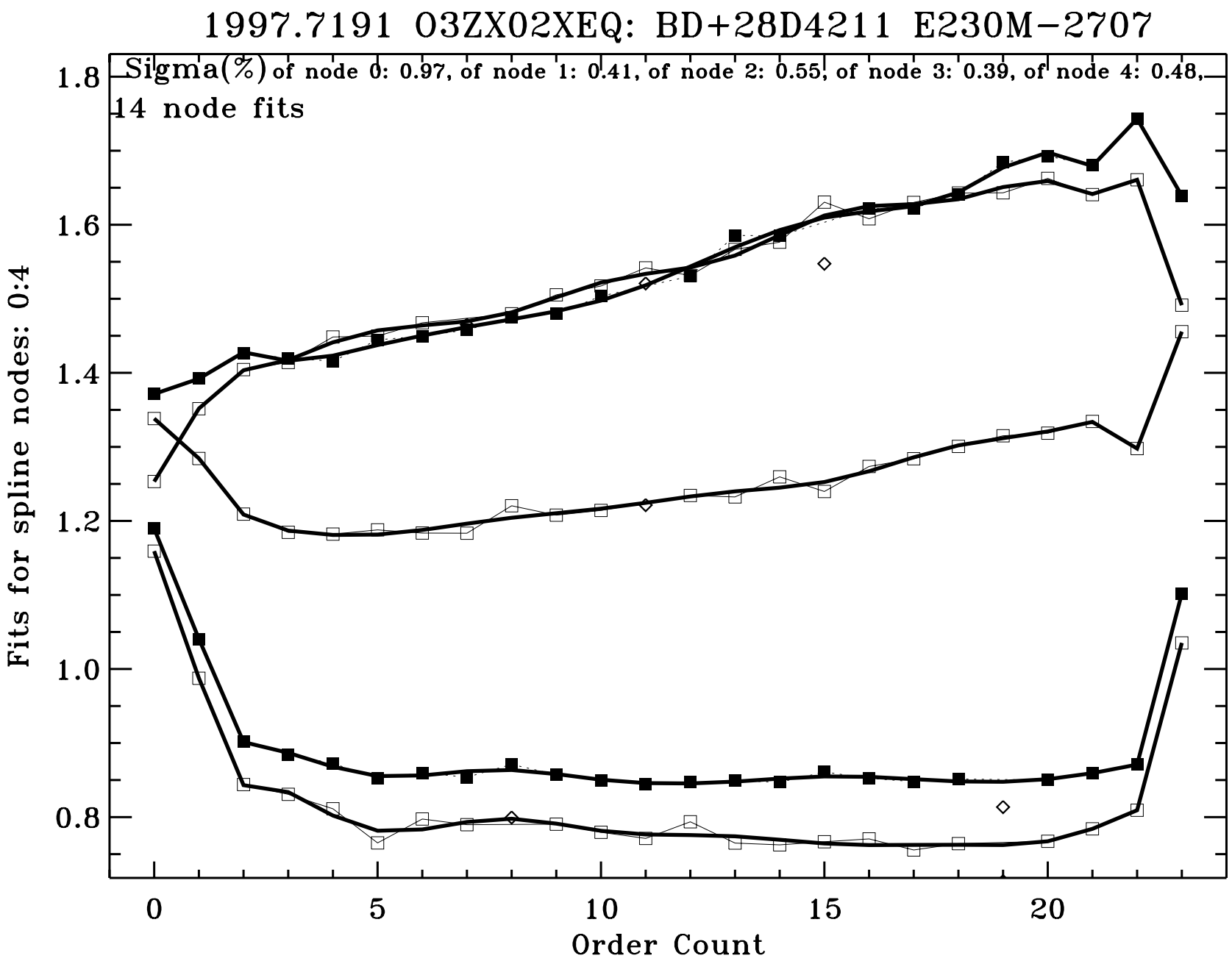
1997.7191 03ZX02XEQ: BD+28D4211 E230M-2707
Sigma(%) of node 0: 0.97, of node 1: 0.41, of node 2: 0.55, of node 3: 0.39, of node 4: 0.48,
14 node fits
Fits for spline nodes: 0:4
1.8
1.6
1.4
1.2
1.0
0.8
0
5
10
15
20
Order Count
BOHLIN: echsens 3-Jun-1998 15:00

Fig. 4 (cont.)

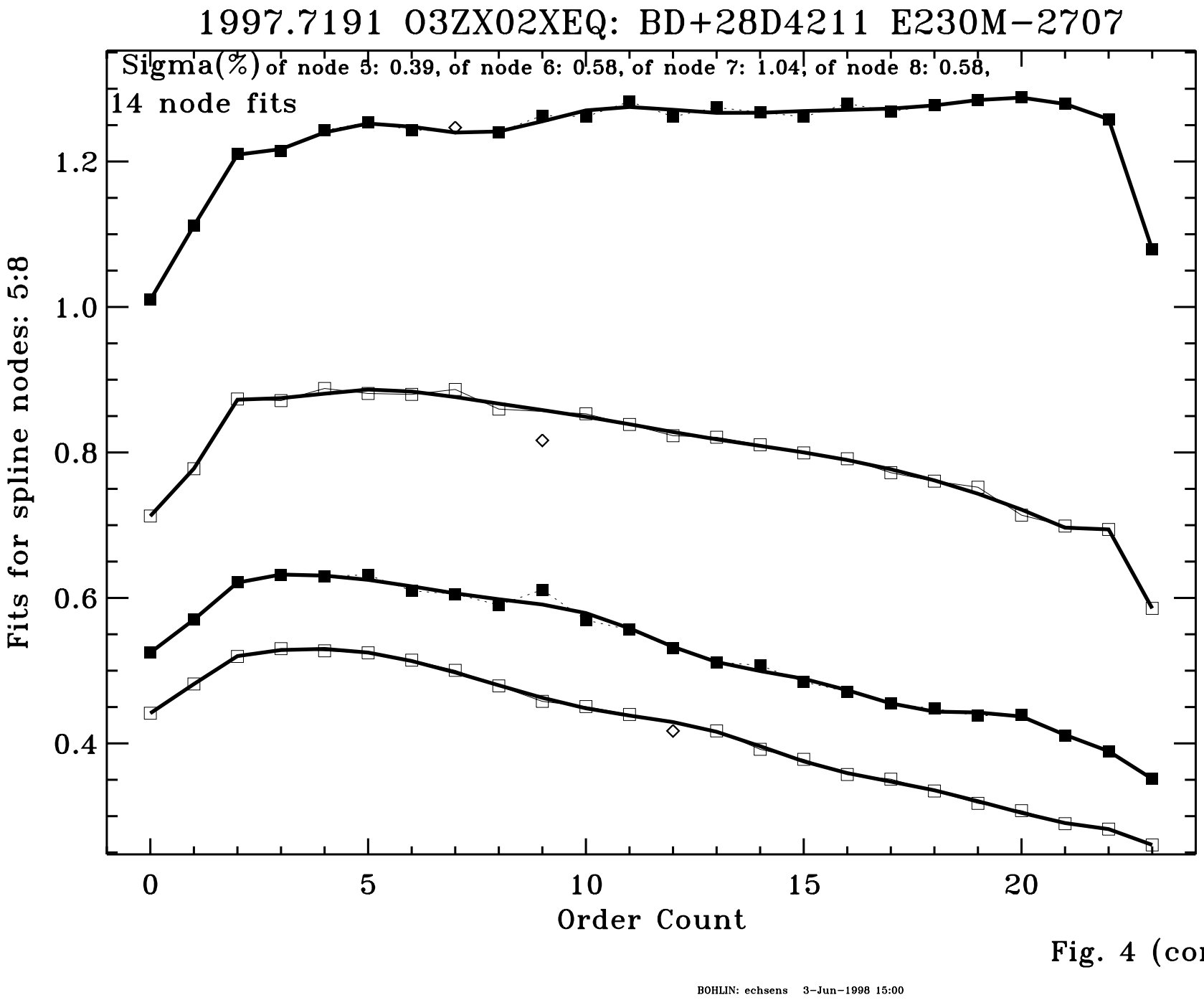
1997.7191 03ZX02XEQ: BD+28D4211 E230M-2707
Sigma(%) of node 5: 0.39, of node 6: 0.58, of node 7: 1.04, of node 8: 0.58,
14 node fits
Fits for spline nodes: 5:8
1.2
1.0
0.8
0.6
0.4
0
5
10
15
20
Order Count
BOHLIN: echsens 3-Jun-1998 15:00

Fig. 4 (cont.)

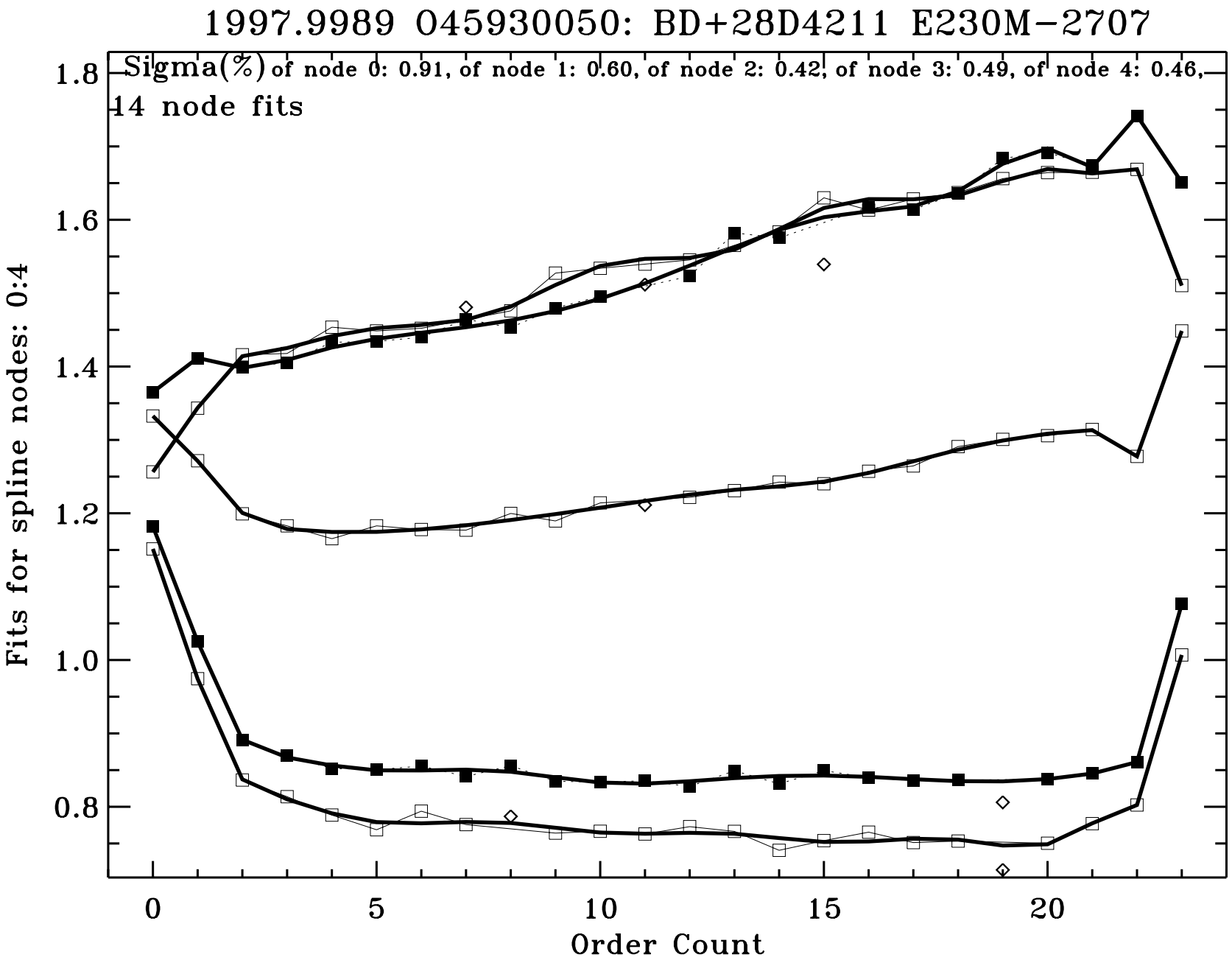
1997.9989 045930050: BD+28D4211 E230M-2707
Sigma(%) of node 0: 0.91, of node 1: 0.60, of node 2: 0.42, of node 3: 0.49, of node 4: 0.46,
14 node fits
Fits for spline nodes: 0:4
1.8
1.6
1.4
1.2
1.0
0.8
0
5
10
15
20
Order Count
BOHLIN: echsens 3-Jun-1998 15:00

Fig. 4 (cont.)

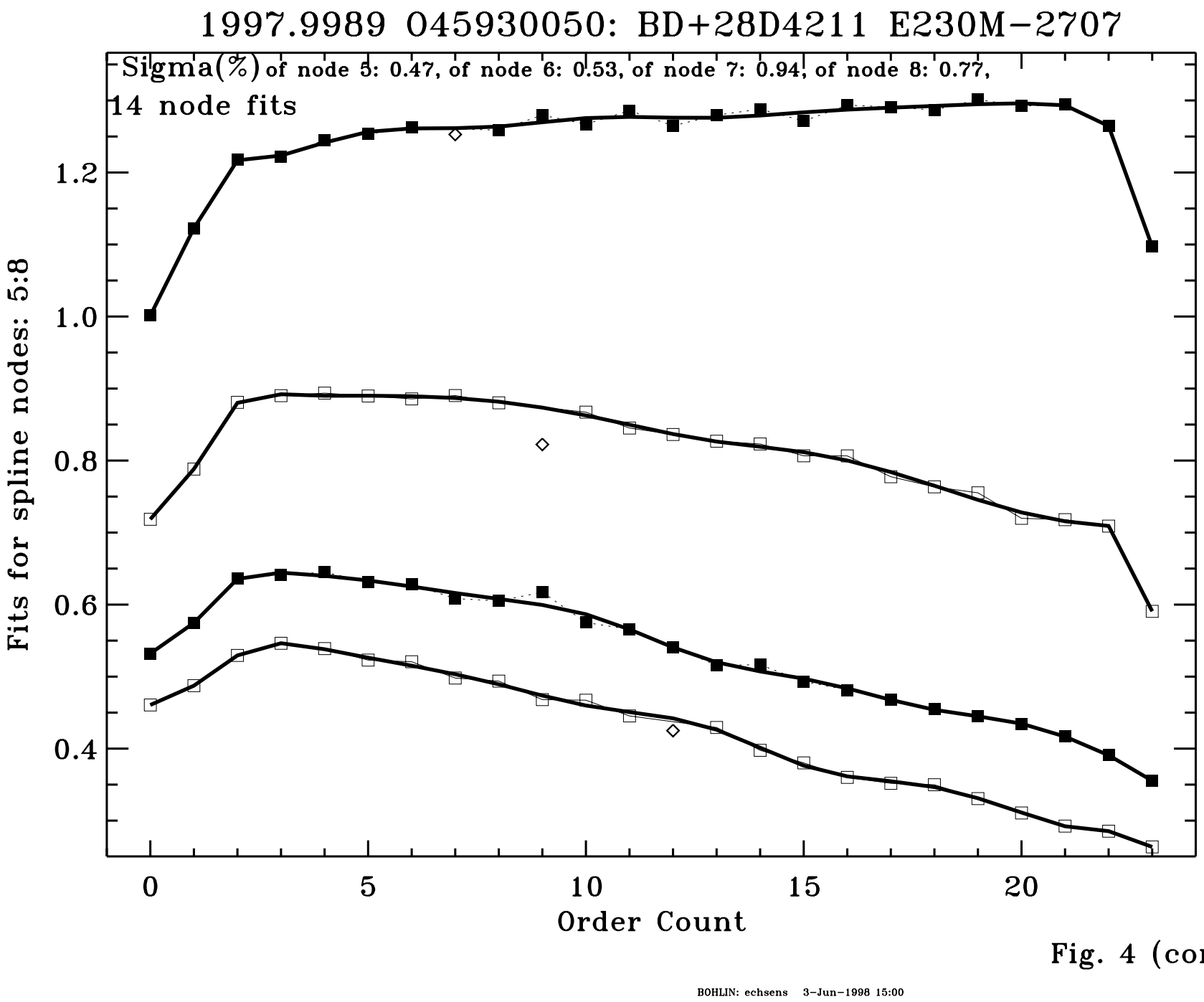
1997.9989 045930050: BD+28D4211 E230M-2707
Sigma(%) of node 5: 0.47, of node 6: 0.53, of node 7: 0.94, of node 8: 0.77,
14 node fits
Fits for spline nodes: 5:8
1.2
1.0
0.8
0.6
0.4
0
5
10
15
20
Order Count
BOHLIN: echsens 3-Jun-1998 15:00

Fig. 4 (cont.)

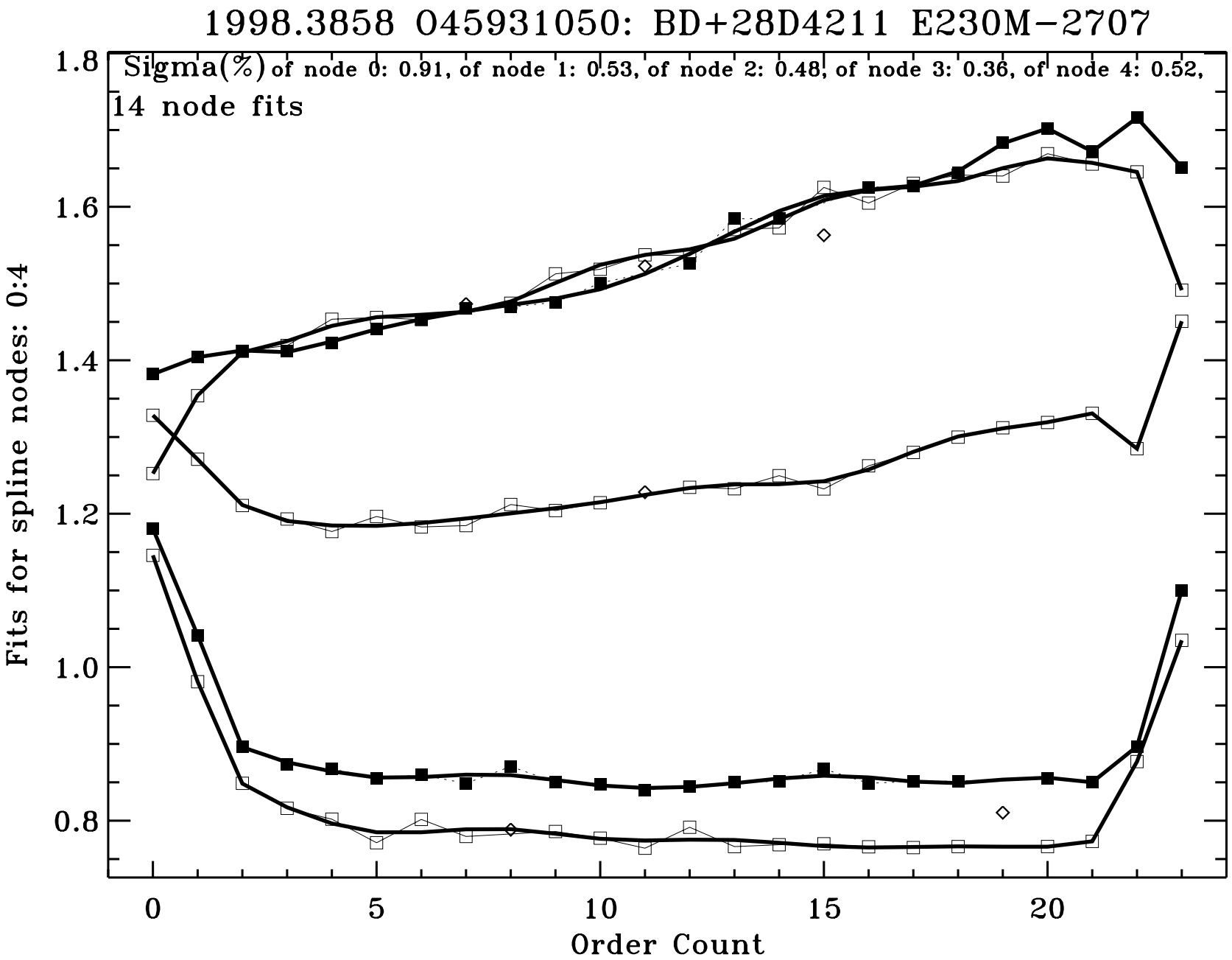
1998.3858 045931050: BD+28D4211 E230M-2707
Sigma(%) of node 0: 0.91, of node 1: 0.53, of node 2: 0.48, of node 3: 0.36, of node 4: 0.52,
14 node fits
Fits for spline nodes: 0:4
1.8
1.6
1.4
1.2
1.0
0.8
0
5
10
15
20
Order Count
BOHLIN: echsens 3-Jun-1998 15:00

Fig. 4 (cont.)

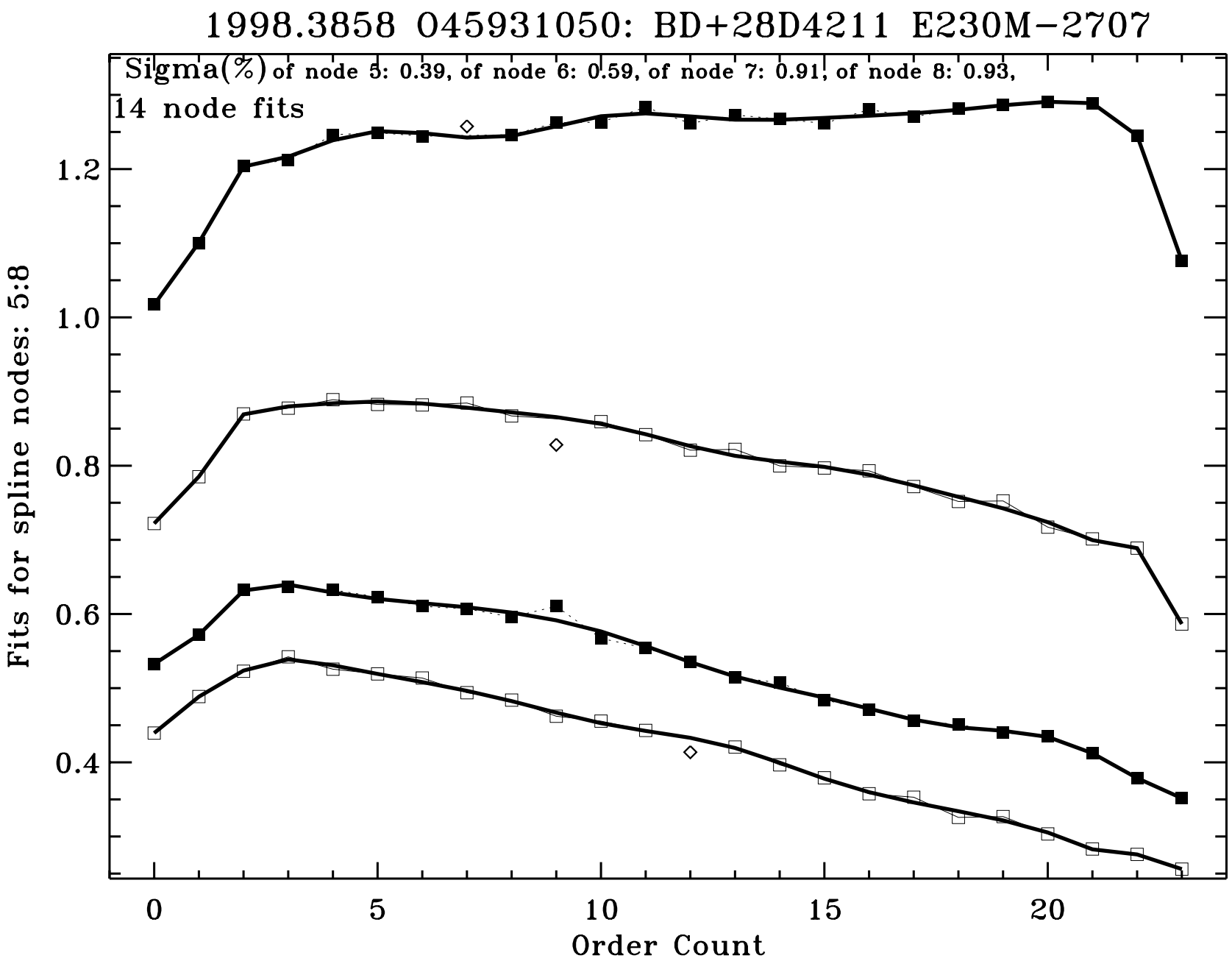
1998.3858 045931050: BD+28D4211 E230M-2707
Sigma(%) of node 5: 0.39, of node 6: 0.59, of node 7: 0.91, of node 8: 0.93,
14 node fits
Fits for spline nodes: 5:8
1.2
1.0
0.8
0.6
0.4
0
5
10
15
20
Order Count
BOHLIN: echsens 3-Jun-1998 15:00

Fig. 4 (cont.)

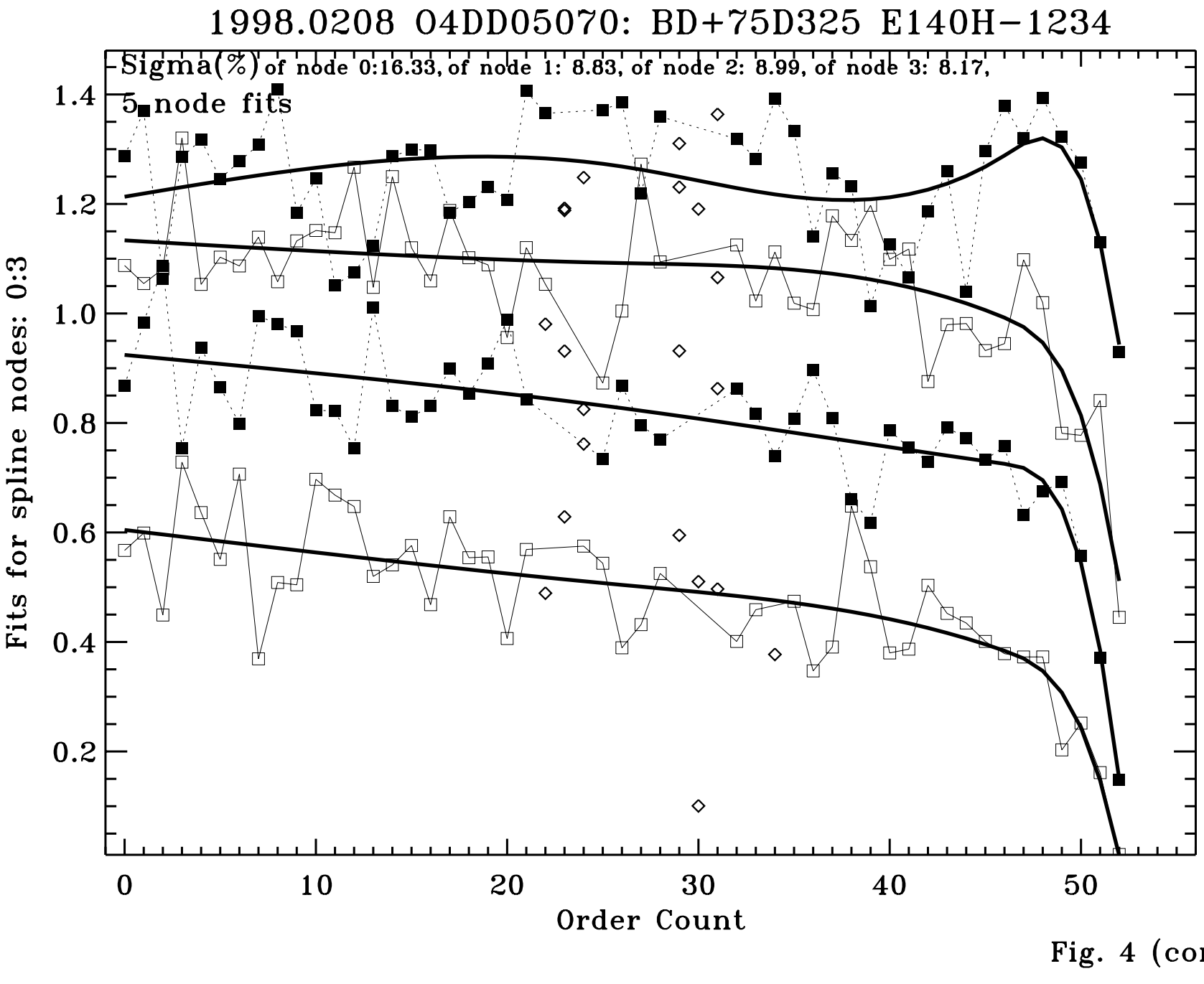
1998.0208 04DD05070: BD+75D325 E140H-1234
Sigma(%) of node 0:16.33, of node 1: 8.83, of node 2: 8.99, of node 3: 8.17,
5 node fits
Fits for spline nodes: 0:3
1.4
1.2
1.0
0.8
0.6
0.4
0.2
0
10
20
30
40
50
Order Count
BOHLIN: echsens 3-Jun-1998 15:00

Fig. 4 (cont.)

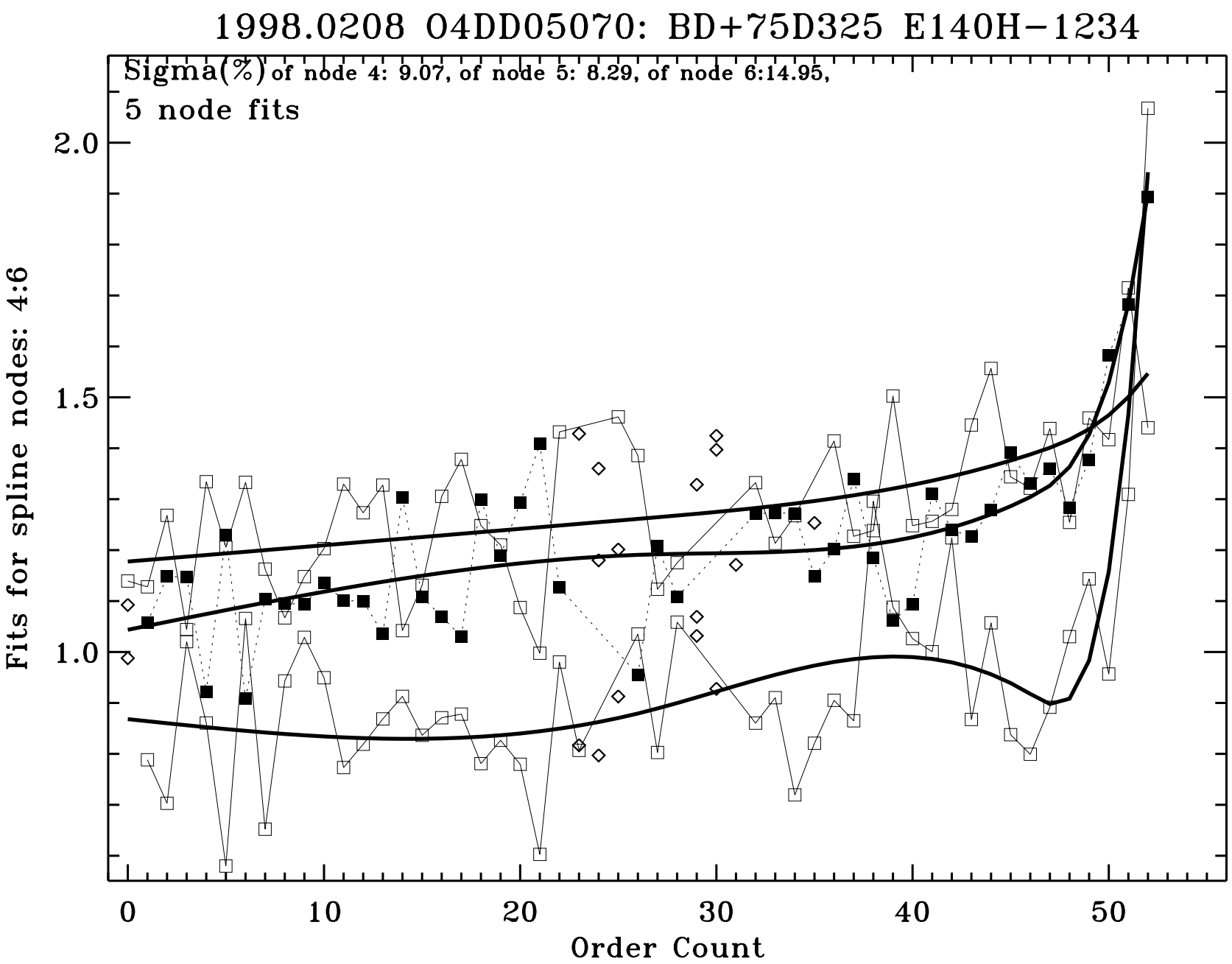
1998.0208 04DD05070: BD+75D325 E140H-1234
Sigma(%) of node 4: 9.07, of node 5: 8.29, of node 6:14.95,
5 node fits
Fits for spline nodes: 4:6
2.0
1.5
1.0
0
10
20
30
40
50
Order Count
BOHLIN: echsens 3-Jun-1998 15:00

Fig. 4 (cont.)

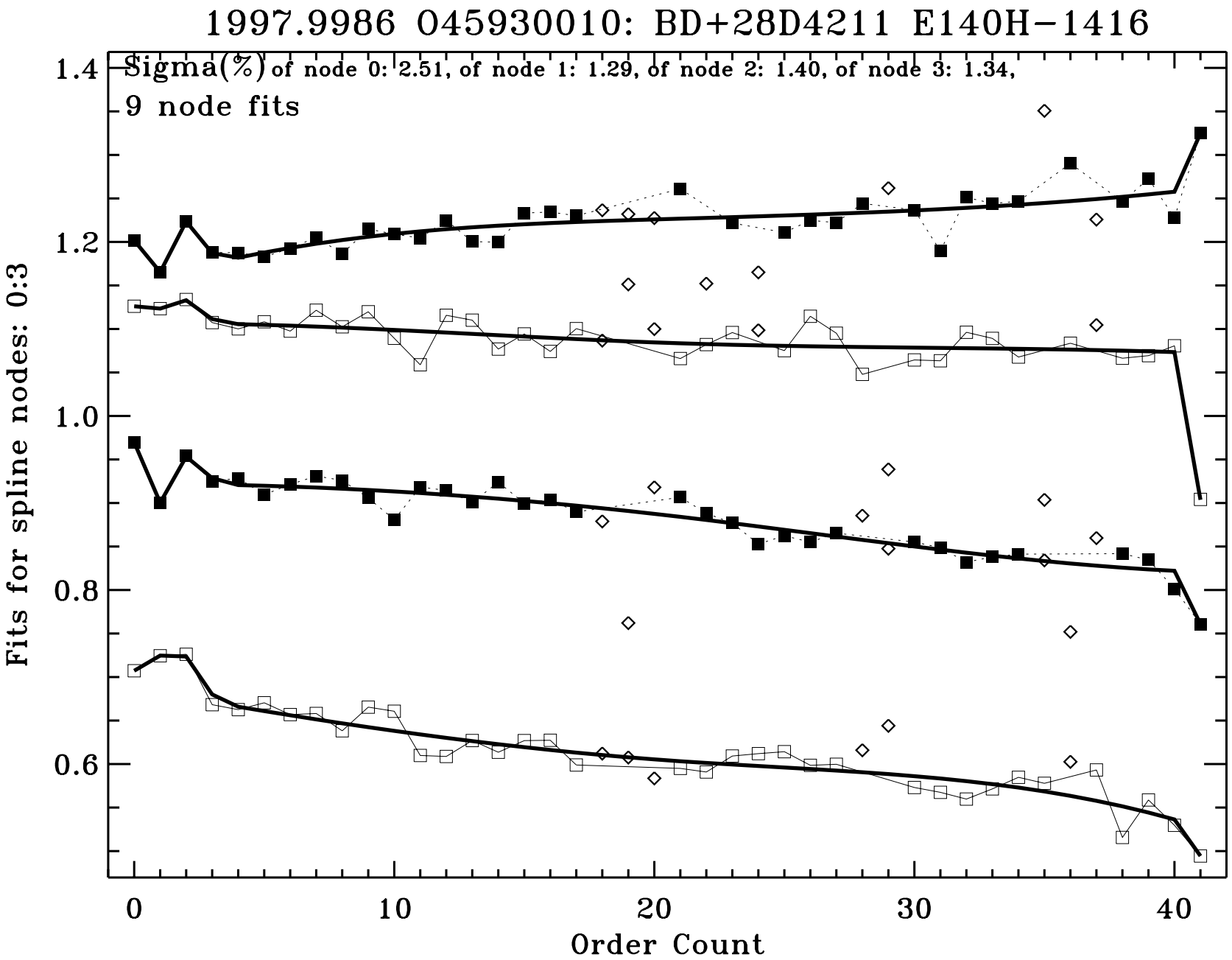
1997.9986 045930010: BD+28D4211 E140H-1416
Sigma(%) of node 0: 2.51, of node 1: 1.29, of node 2: 1.40, of node 3: 1.34,
9 node fits
Fits for spline nodes: 0:3
1.4
1.2
1.0
0.8
0.6
0
10
20
30
40
Order Count
BOHLIN: echsens 3-Jun-1998 15:00

Fig. 4 (cont.)

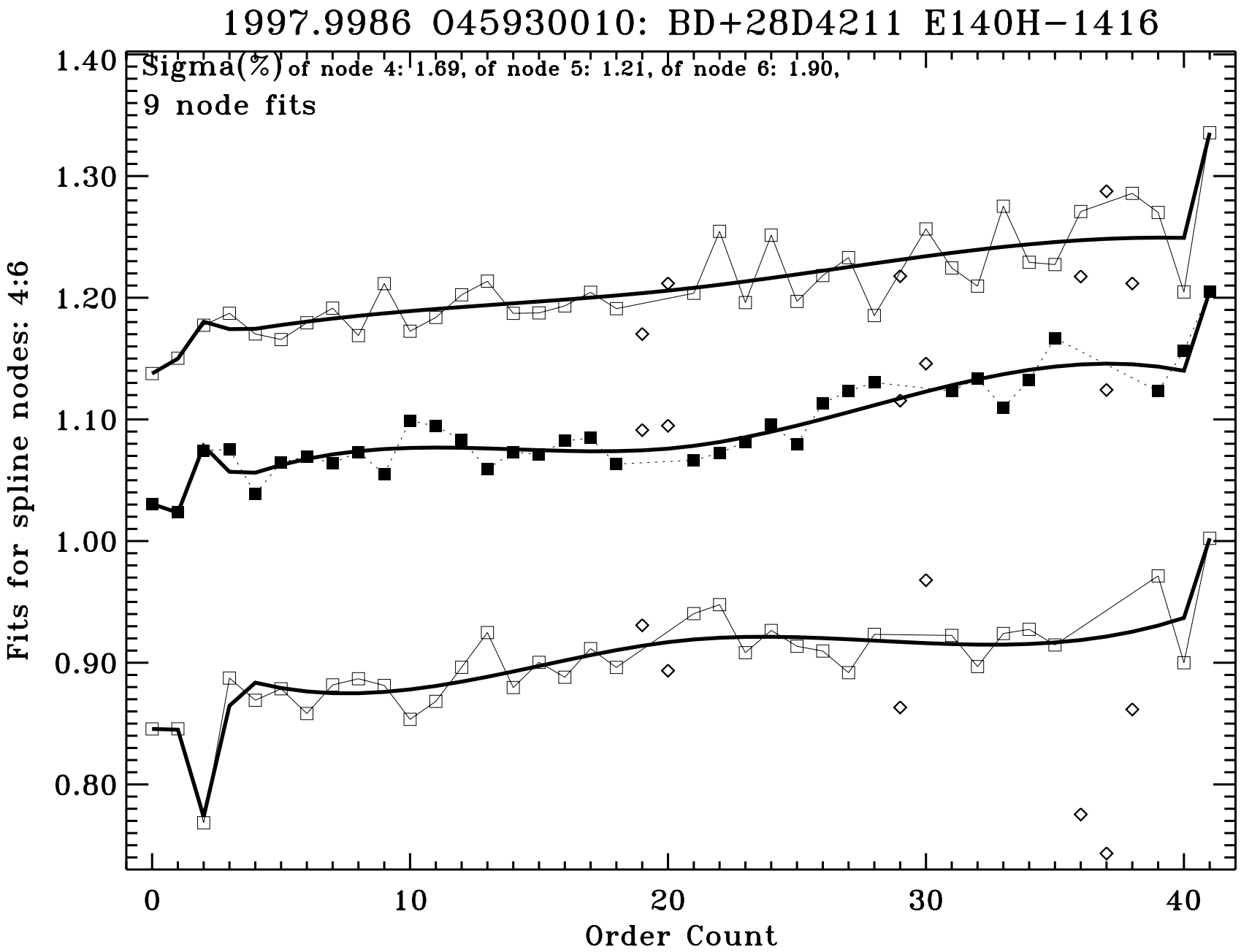
1997.9986 045930010: BD+28D4211 E140H-1416
Sigma(%) of node 4: 1.69, of node 5: 1.21, of node 6: 1.90,
9 node fits
Fits for spline nodes: 4:6
1.40
1.30
1.20
1.10
1.00
0.90
0.80
0
10
20
30
40
Order Count
BOHLIN: echsens 3-Jun-1998 15:00

Fig. 4 (cont.)

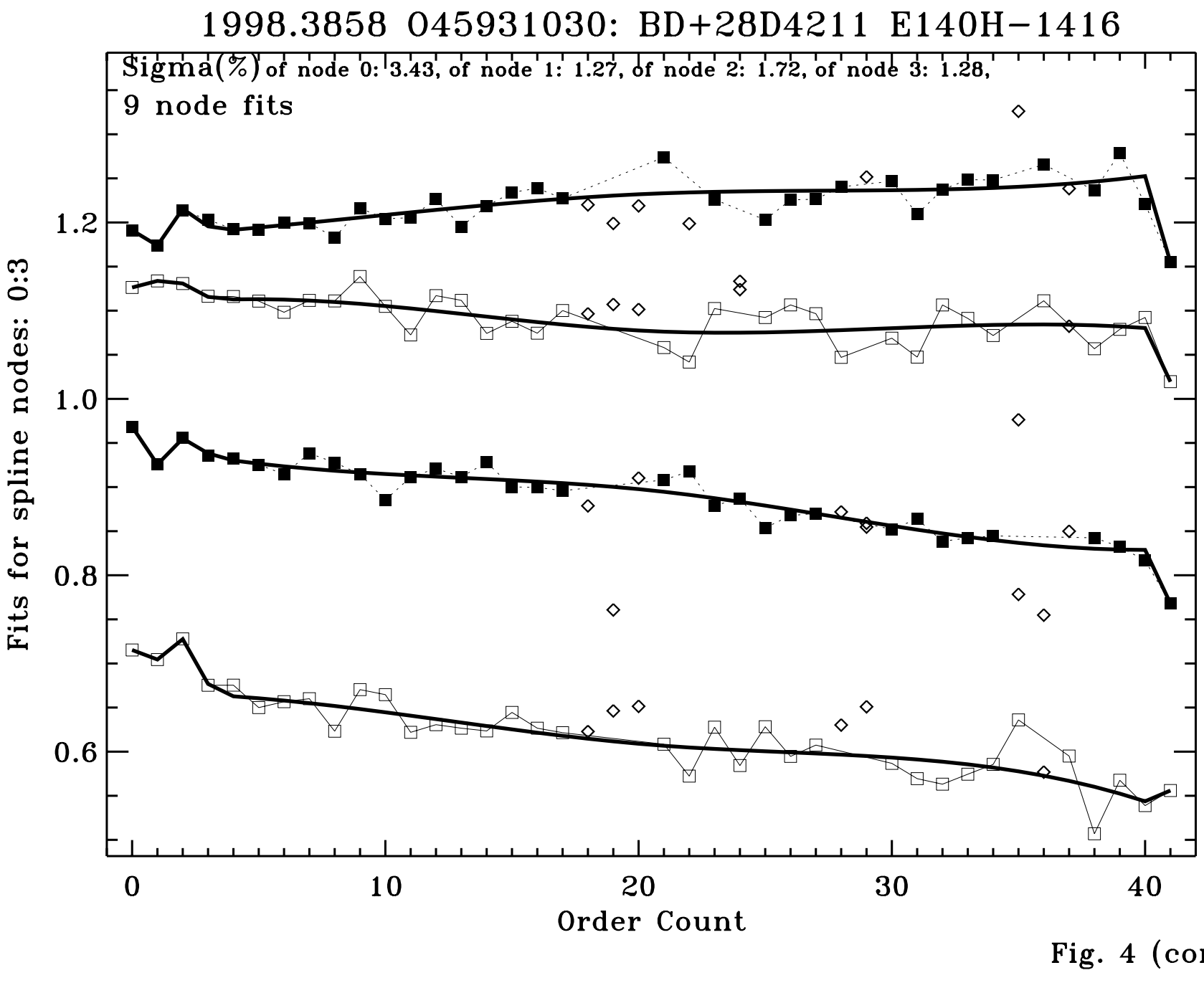
1998.3858 045931030: BD+28D4211 E140H-1416
Sigma(%) of node 0: 3.43, of node 1: 1.27, of node 2: 1.72, of node 3: 1.28,
9 node fits
Fits for spline nodes: 0:3
1.2
1.0
0.8
0.6
0
10
20
30
40
Order Count
BOHLIN: echsens 3-Jun-1998 15:00

Fig. 4 (cont.)

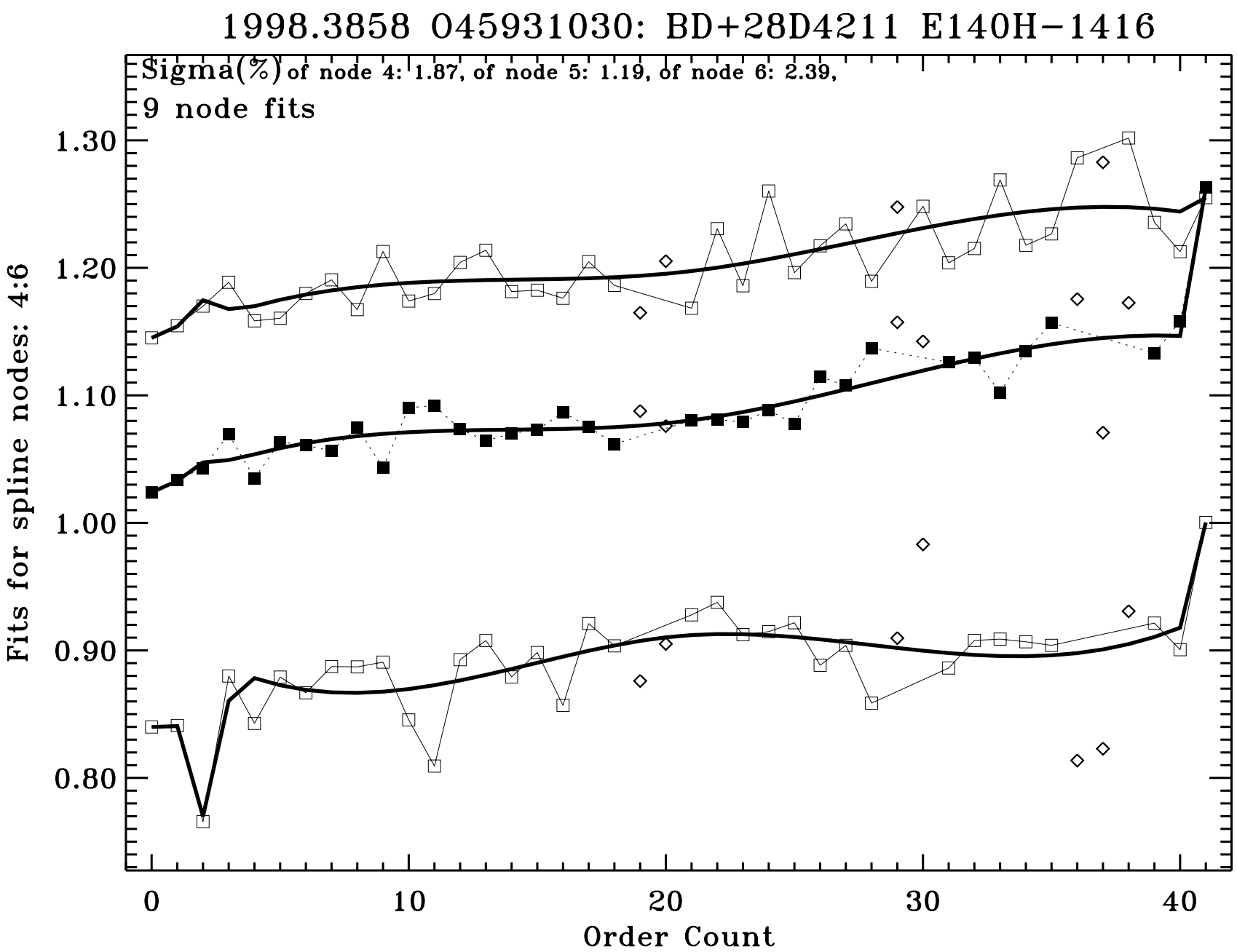
1998.3858 045931030: BD+28D4211 E140H-1416
Sigma(%) of node 4: 1.87, of node 5: 1.19, of node 6: 2.39,
9 node fits
Fits for spline nodes: 4:6
1.30
1.20
1.10
1.00
0.90
0.80
0
10
20
30
40
Order Count
BOHLIN: echsens 3-Jun-1998 15:00

Fig. 4 (cont.)

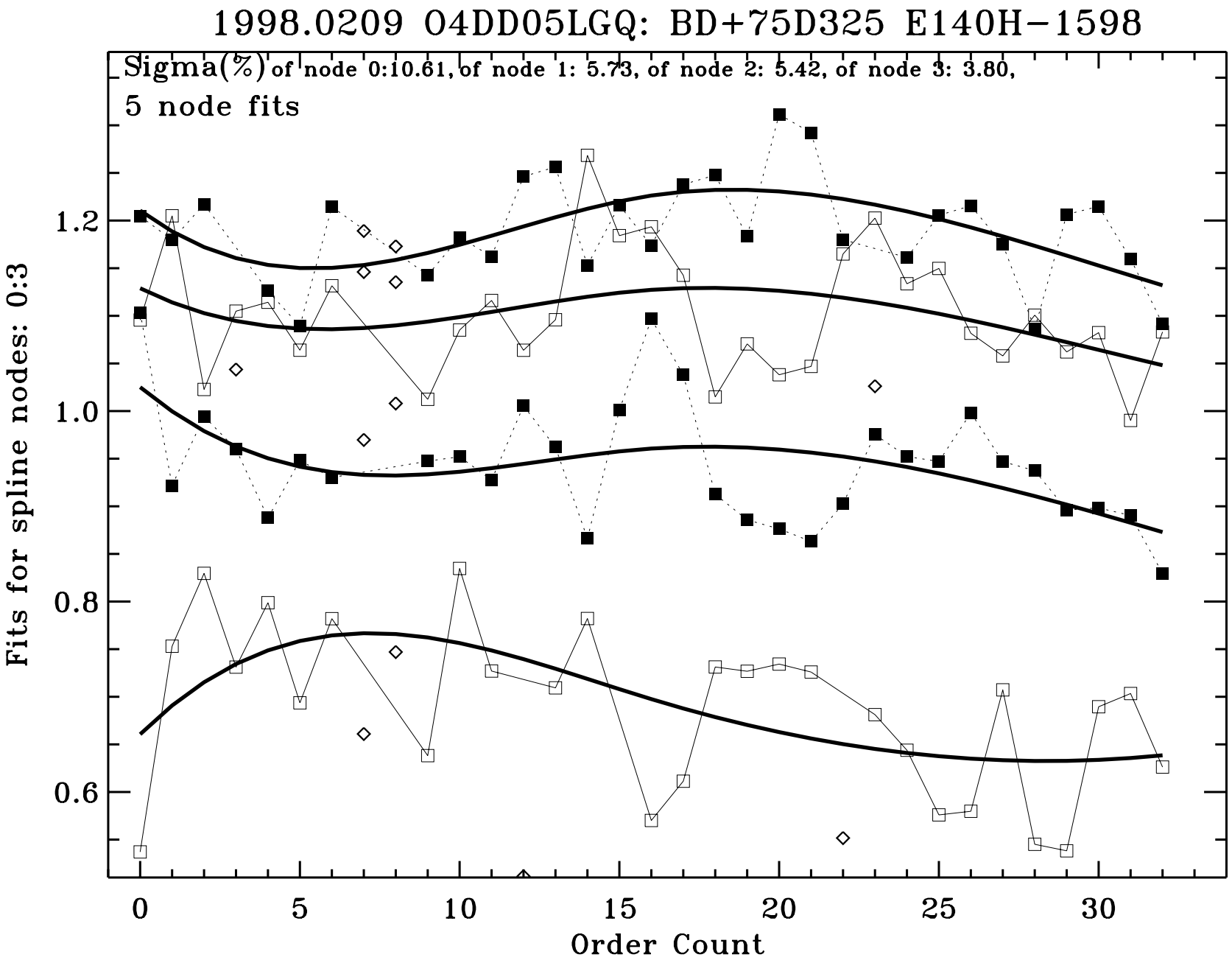
1998.0209 04DD05LGQ: BD+75D325 E140H-1598
Sigma(%) of node 0:10.61, of node 1: 5.73, of node 2: 5.42, of node 3: 3.80,
5 node fits
Fits for spline nodes: 0:3
1.2
1.0
0.8
0.6
0
5
10
15
20
25
30
Order Count
BOHLIN: echsens 3-Jun-1998 15:00

Fig. 4 (cont.)

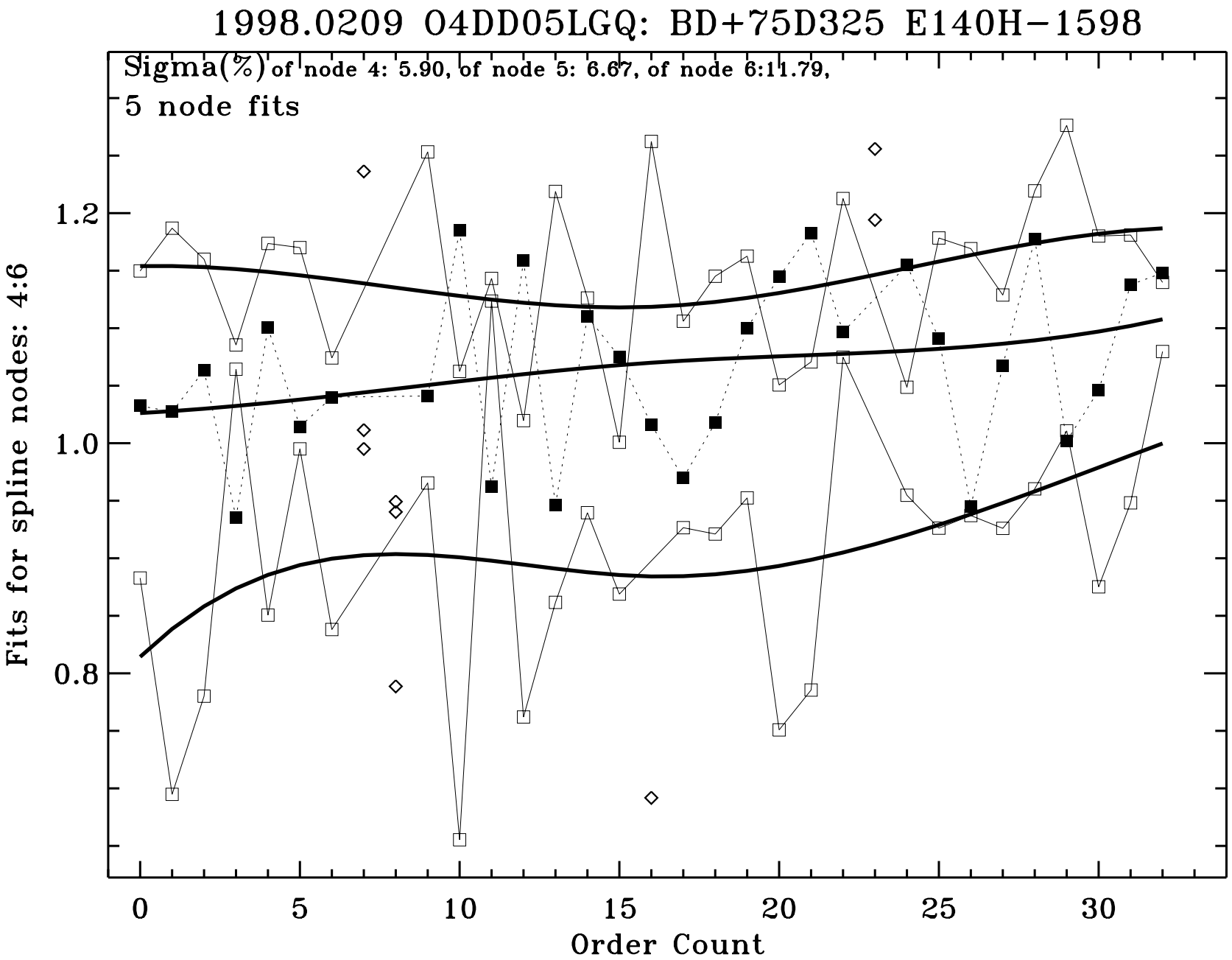
1998.0209 04DD05LGQ: BD+75D325 E140H-1598
Sigma(%) of node 4: 5.90, of node 5: 6.67, of node 6:11.79,
5 node fits
Fits for spline nodes: 4:6
1.2
1.0
0.8
0
5
10
15
20
25
30
Order Count
BOHLIN: echsens 3-Jun-1998 15:00

Fig. 4 (cont.)

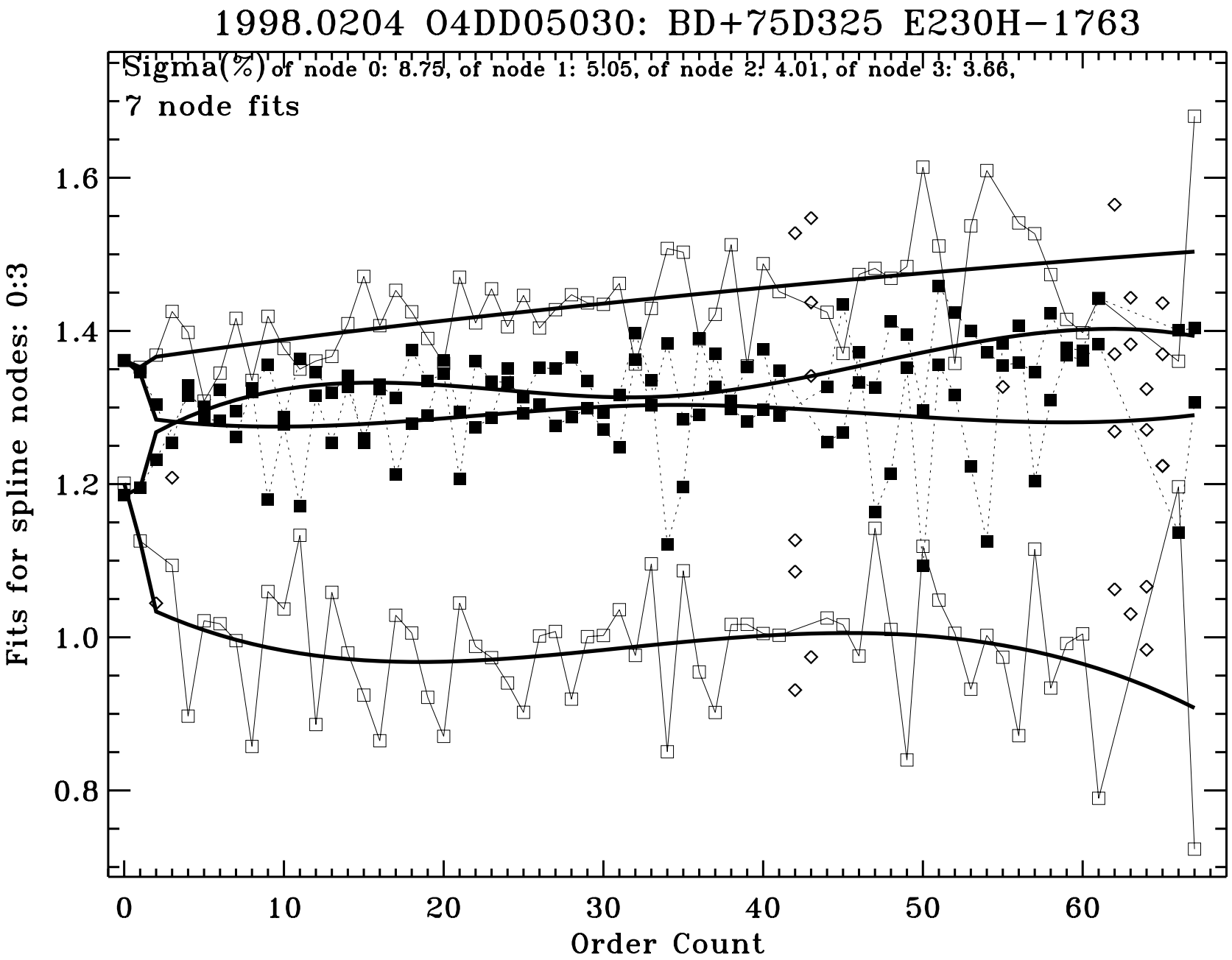
1998.0204 04DD05030: BD+75D325 E230H-1763
Sigma(%) of node 0: 8.75, of node 1: 5.05, of node 2: 4.01, of node 3: 3.66,
7 node fits
Fits for spline nodes: 0:3
1.6
1.4
1.2
1.0
0.8
0
10
20
30
40
50
60
Order Count
BOHLIN: echsens 3-Jun-1998 15:00

Fig. 4 (cont.)

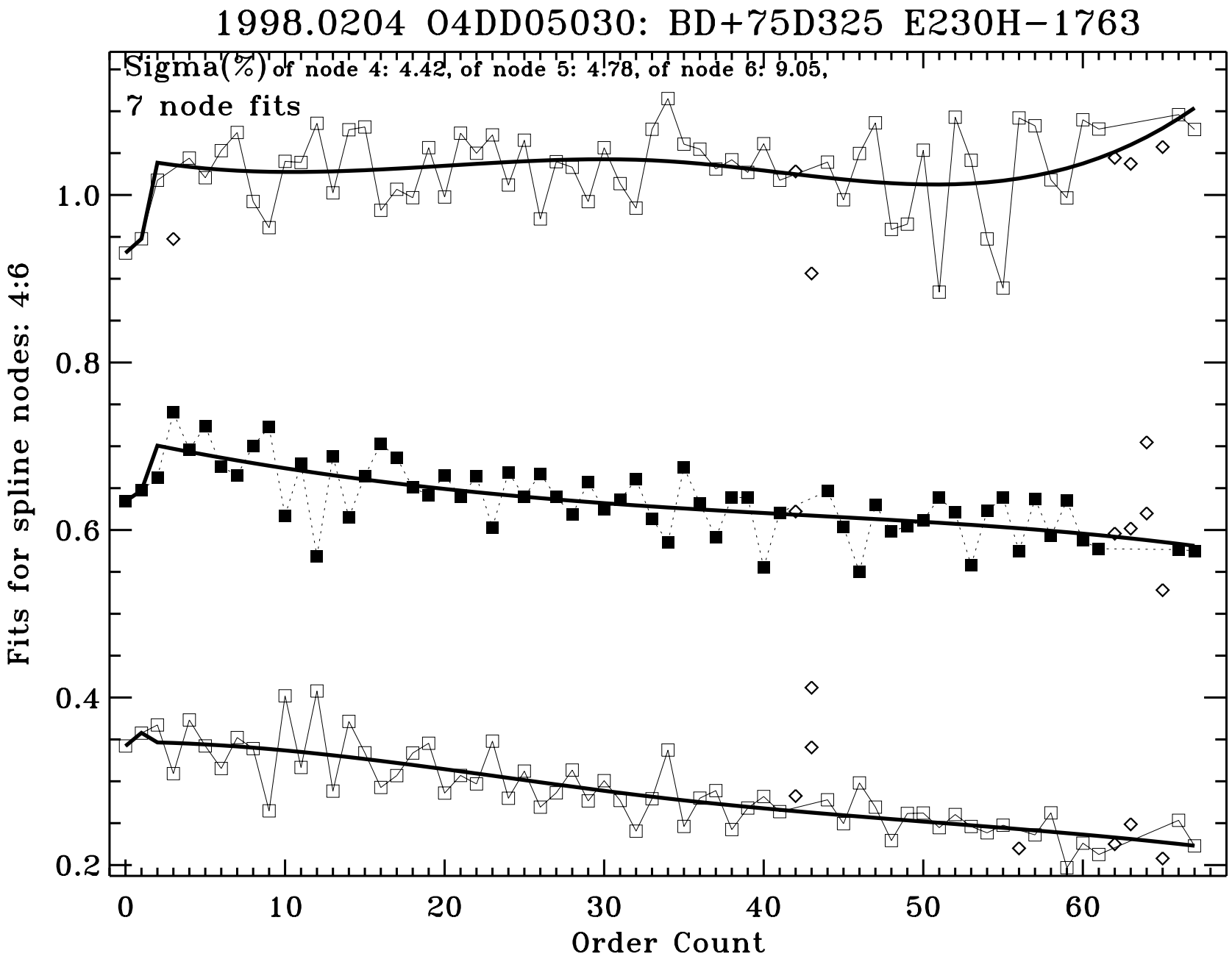
1998.0204 04DD05030: BD+75D325 E230H-1763
Sigma(%) of node 4: 4.42, of node 5: 4.78, of node 6: 9.05,
7 node fits
Fits for spline nodes: 4:6
1.0
0.8
0.6
0.4
0.2
0
10
20
30
40
50
60
Order Count
BOHLIN: echsens 3-Jun-1998 15:00

Fig. 4 (cont.)

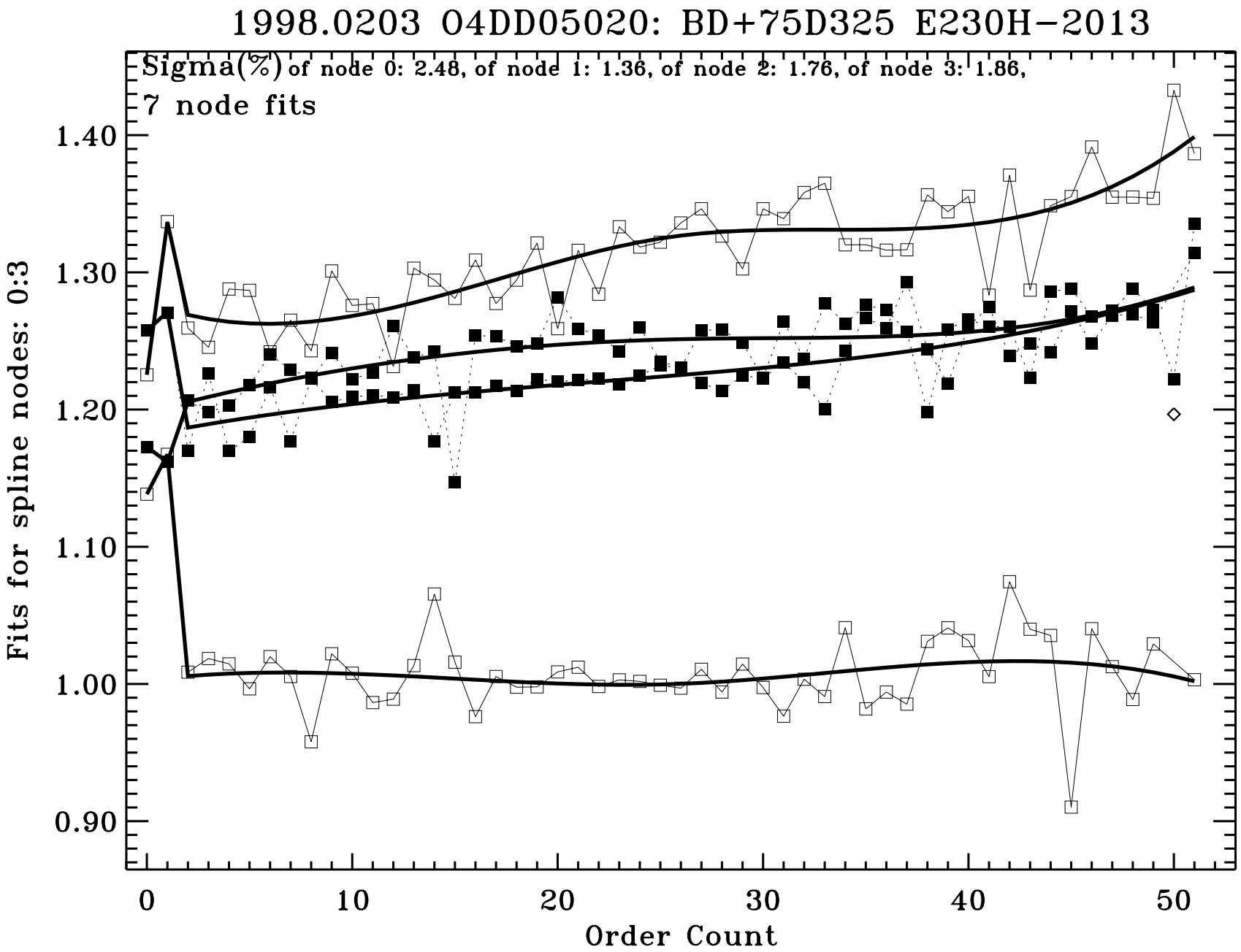
1998.0203 04DD05020: BD+75D325 E230H-2013
Sigma(%) of node 0: 2.48, of node 1: 1.36, of node 2: 1.76, of node 3: 1.86,
7 node fits
Fits for spline nodes: 0:3
1.40
1.30
1.20
1.10
1.00
0.90
0
10
20
30
40
50
Order Count
BOHLIN: echsens 3-Jun-1998 15:00

Fig. 4 (cont.)

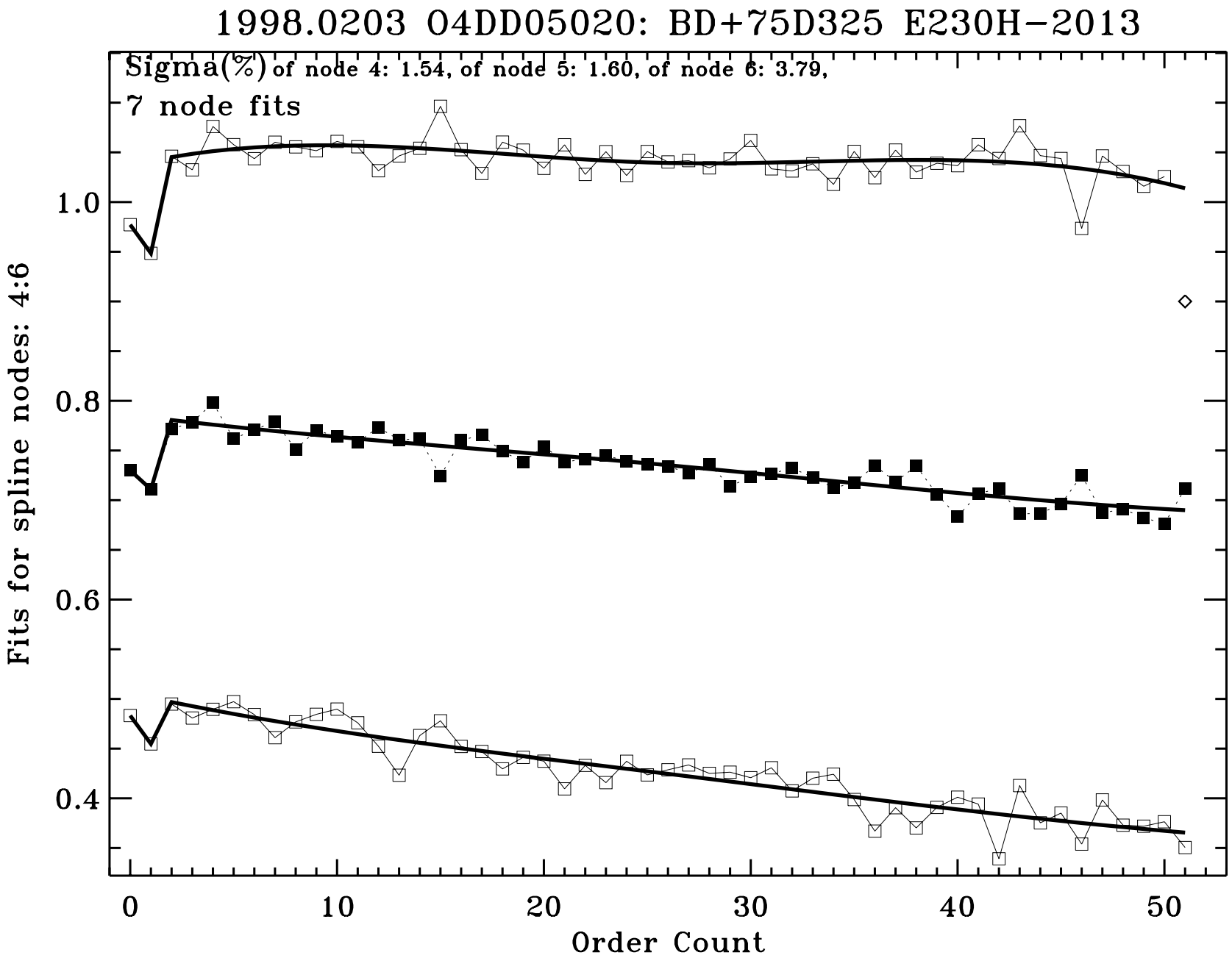
1998.0203 04DD05020: BD+75D325 E230H-2013
Sigma(%) of node 4: 1.54, of node 5: 1.60, of node 6: 3.79,
7 node fits
Fits for spline nodes: 4:6
1.0
0.8
0.6
0.4
0
10
20
30
40
50
Order Count
BOHLIN: echsens 3-Jun-1998 15:00

Fig. 4 (cont.)

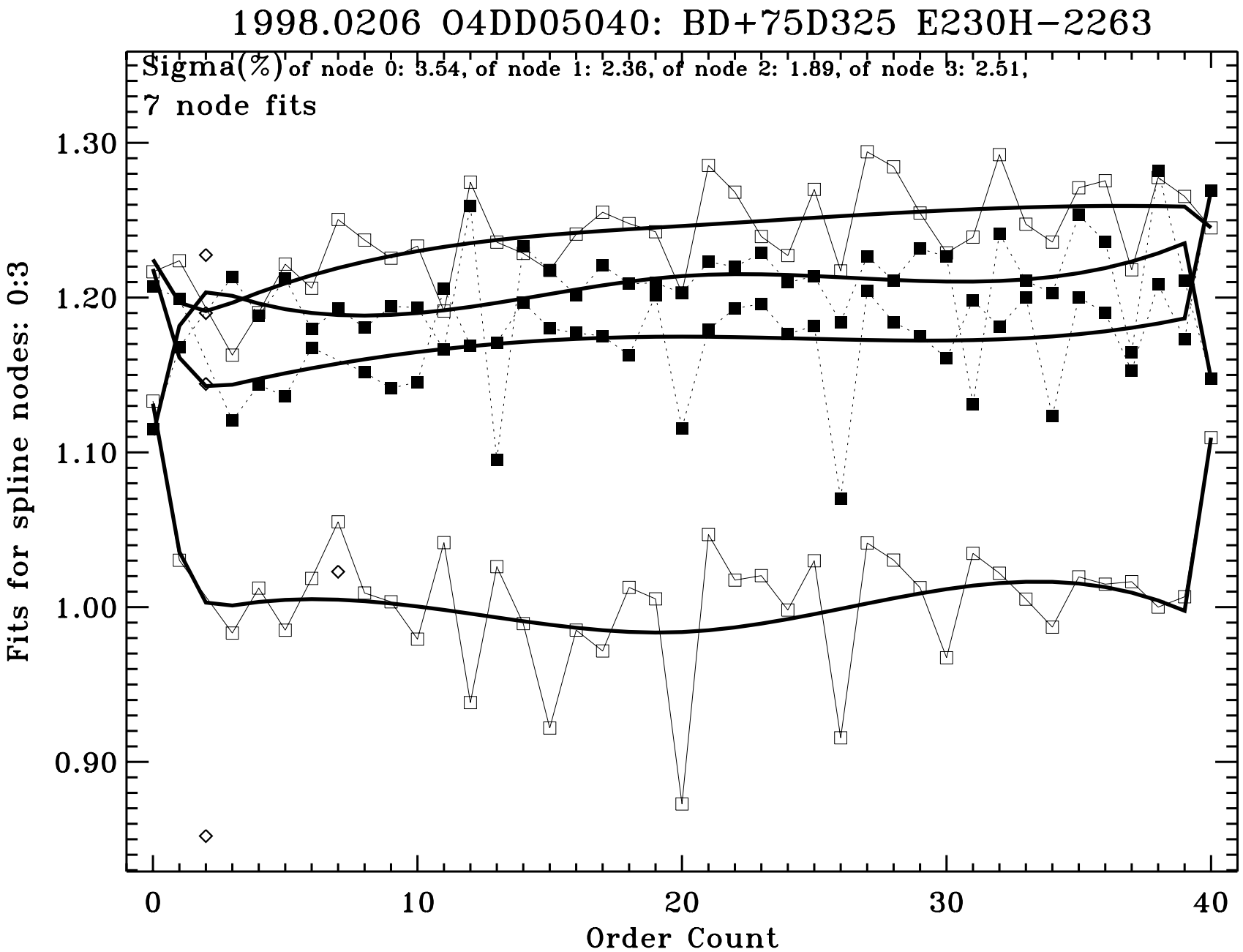
1998.0206 04DD05040: BD+75D325 E230H-2263
Sigma(%) of node 0: 3.54, of node 1: 2.36, of node 2: 1.89, of node 3: 2.51,
7 node fits
Fits for spline nodes: 0:3
1.30
1.20
1.10
1.00
0.90
0
10
20
30
40
Order Count
BOHLIN: echsens 3-Jun-1998 15:01

Fig. 4 (cont.)

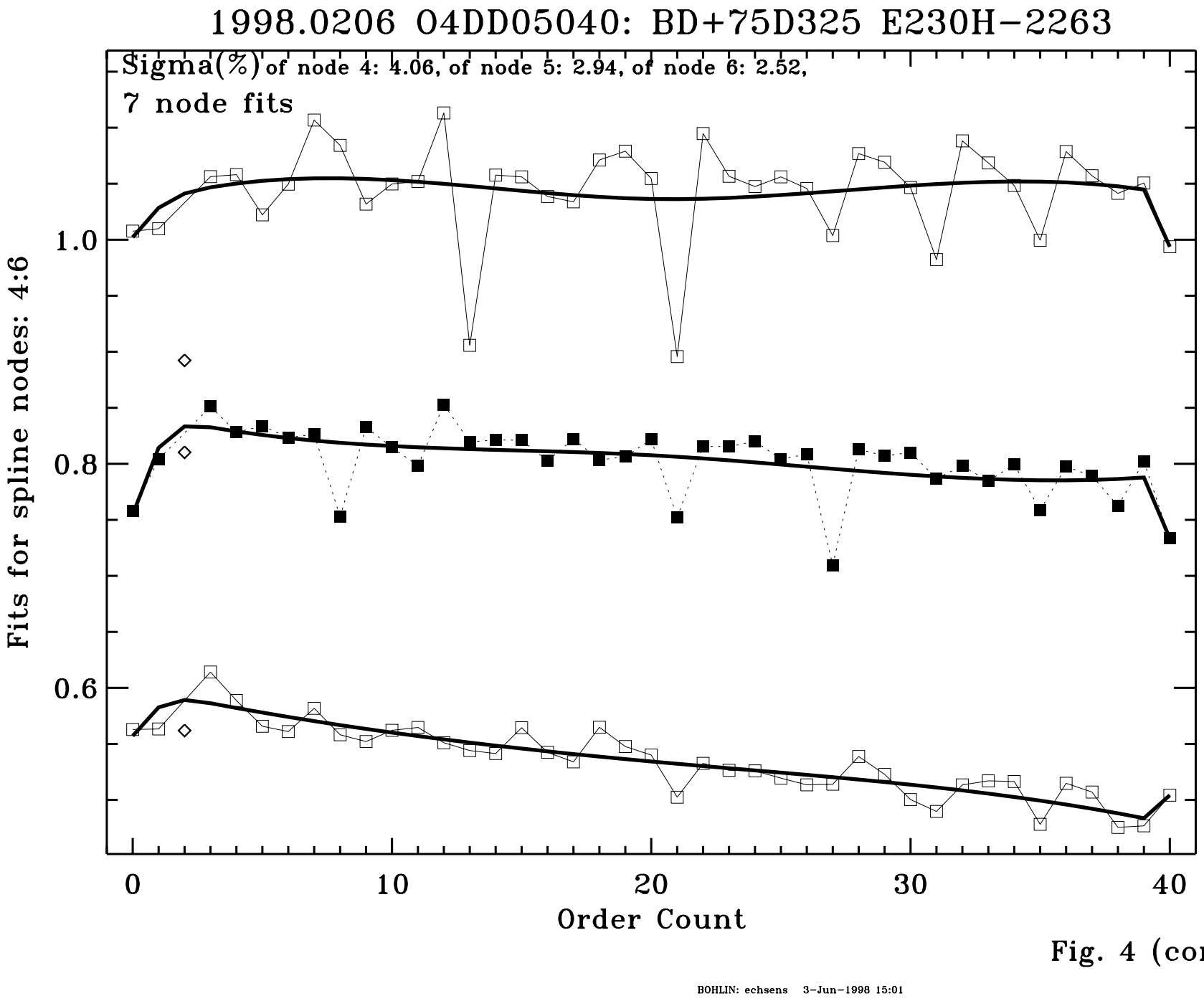
1998.0206 04DD05040: BD+75D325 E230H-2263
Sigma(%) of node 4: 4.06, of node 5: 2.94, of node 6: 2.52,
7 node fits
Fits for spline nodes: 4:6
1.0
0.8
0.6
0
10
20
30
40
Order Count
BOHLIN: echsens 3-Jun-1998 15:01

Fig. 4 (cont.)

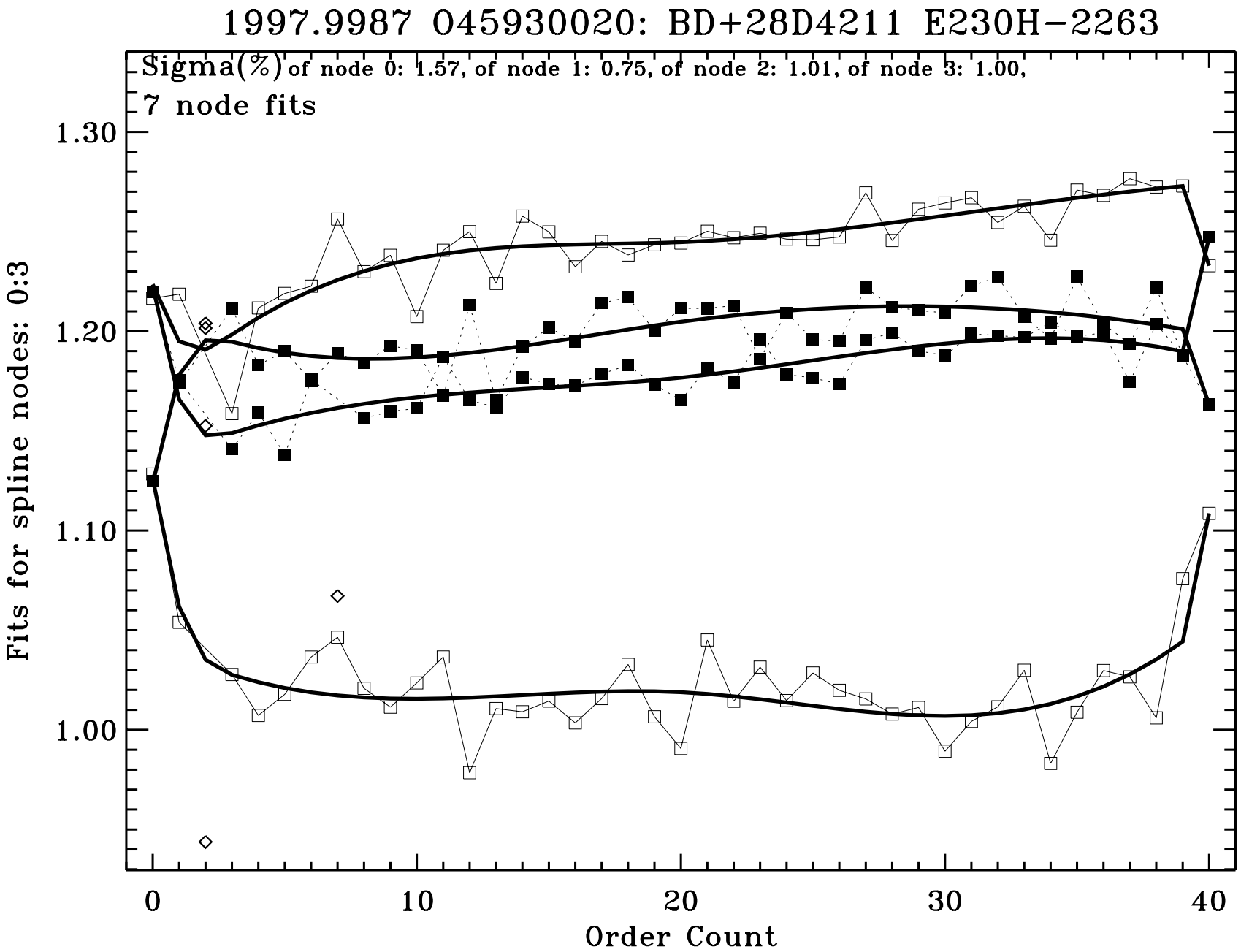
1997.9987 045930020: BD+28D4211 E230H-2263
Sigma(%) of node 0: 1.57, of node 1: 0.75, of node 2: 1.01, of node 3: 1.00,
7 node fits
Fits for spline nodes: 0:3
1.30
1.20
1.10
1.00
0
10
20
30
40
Order Count
BOHLIN: echsens 3-Jun-1998 15:01

Fig. 4 (cont.)

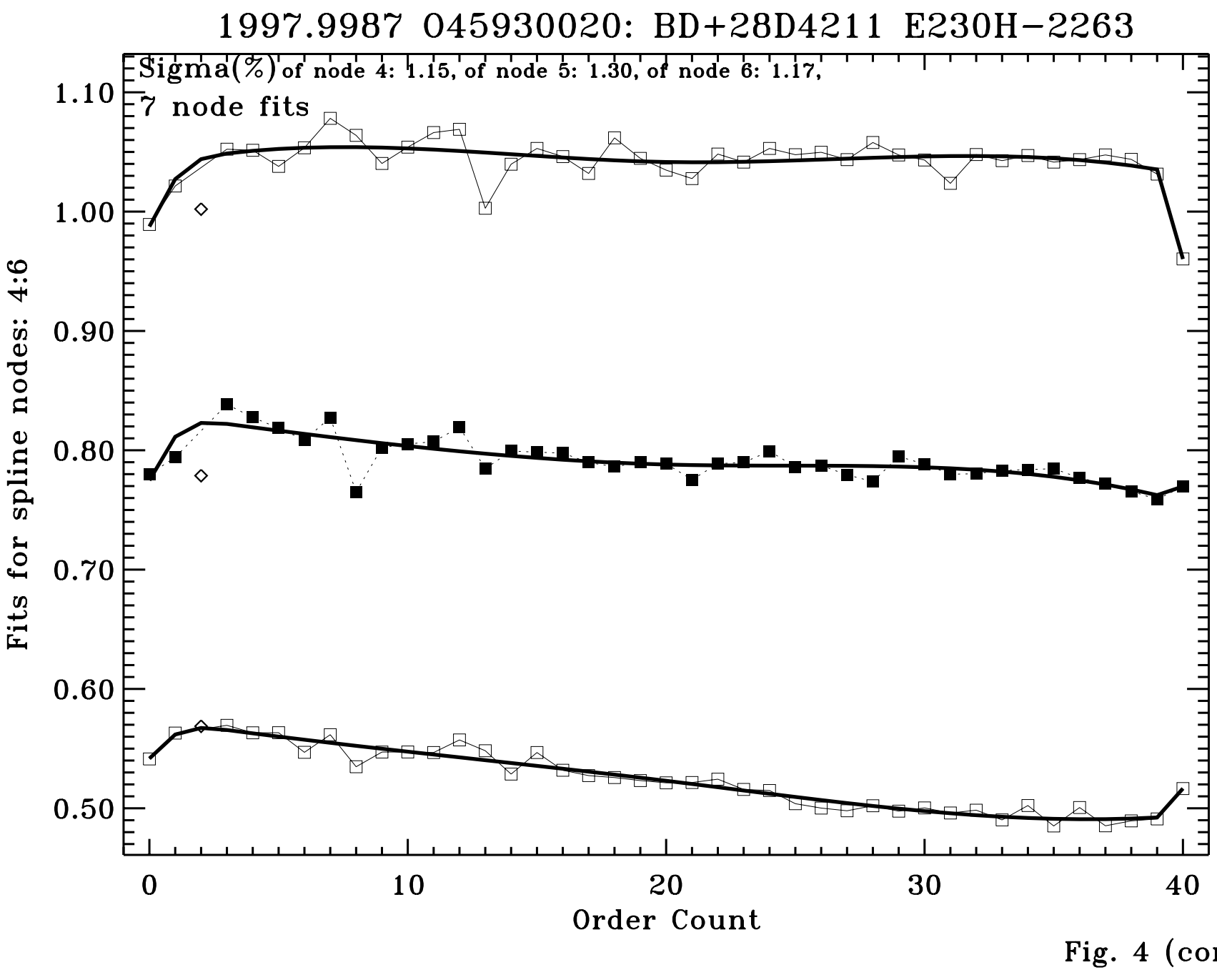
1997.9987 045930020: BD+28D4211 E230H-2263
Sigma(%) of node 4: 1.15, of node 5: 1.30, of node 6: 1.17,
7 node fits
Fits for spline nodes: 4:6
1.10
1.00
0.90
0.80
0.70
0.60
0.50
0
10
20
30
40
Order Count
BOHLIN: echsens 3-Jun-1998 15:01

Fig. 4 (cont.)

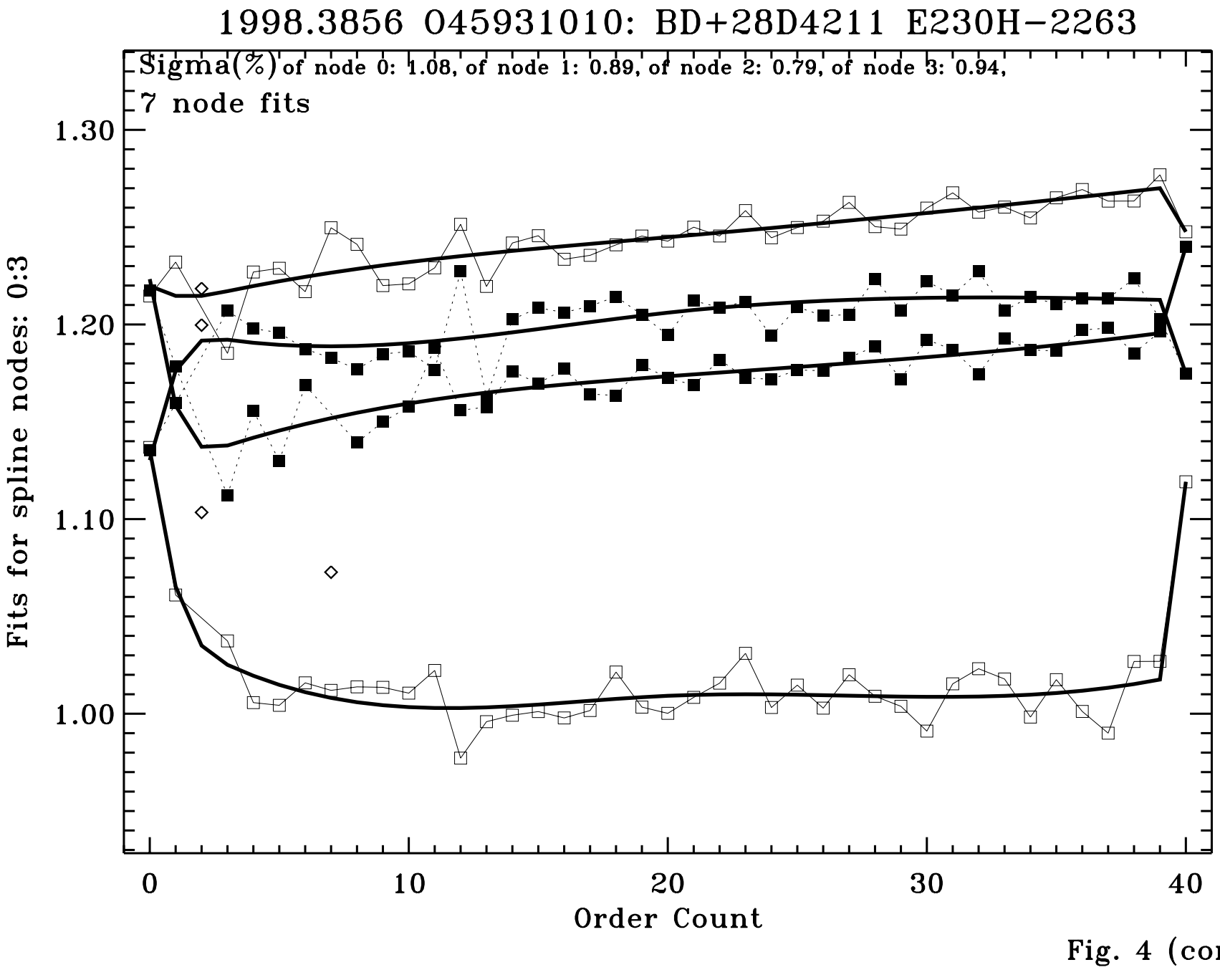
1998.3856 045931010: BD+28D4211 E230H-2263
Sigma(%) of node 0: 1.08, of node 1: 0.89, of node 2: 0.79, of node 3: 0.94,
7 node fits
Fits for spline nodes: 0:3
1.30
1.20
1.10
1.00
0
10
20
30
40
Order Count
BOHLIN: echsens 3-Jun-1998 15:01

Fig. 4 (cont.)

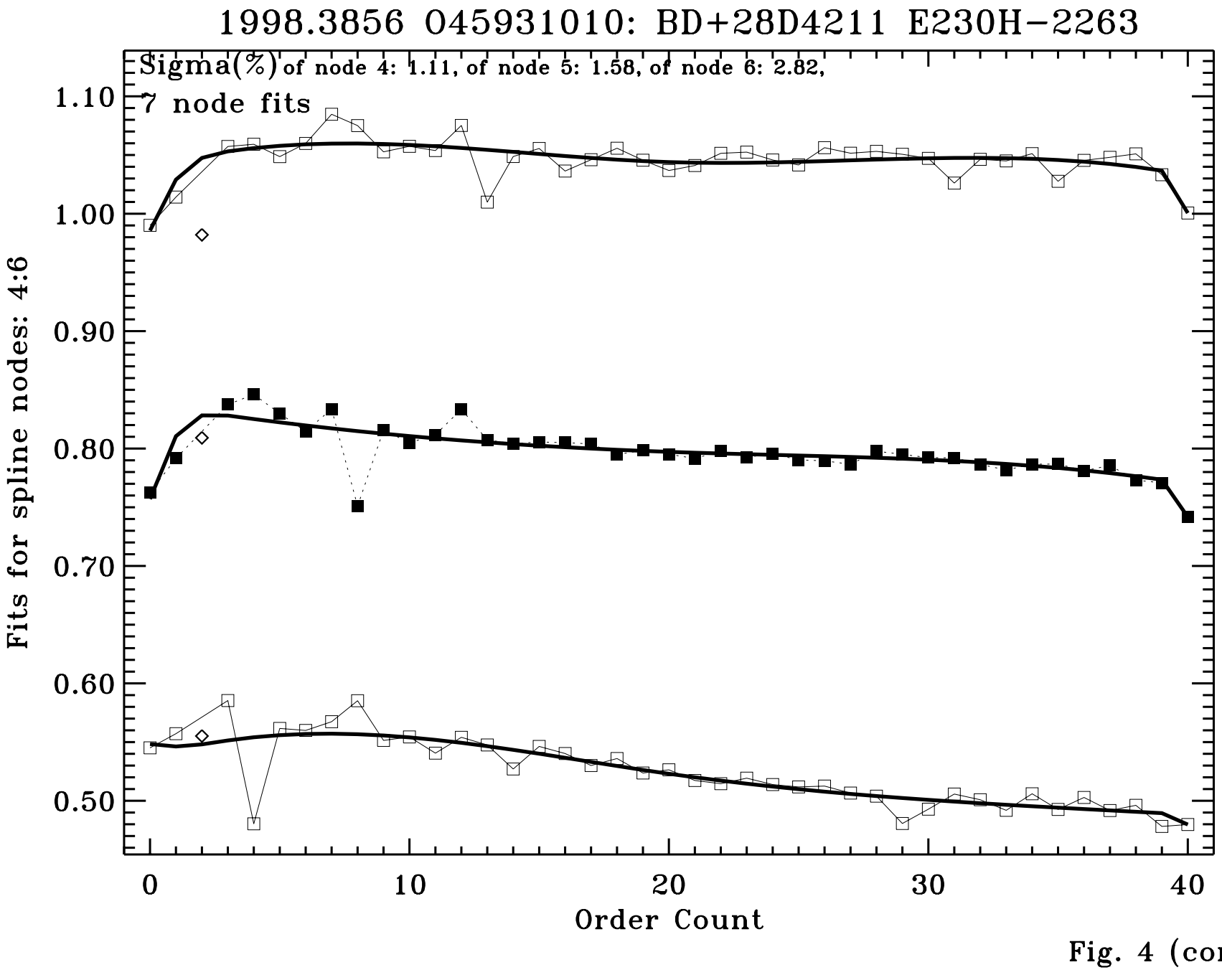
1998.3856 045931010: BD+28D4211 E230H-2263
Sigma(%) of node 4: 1.11, of node 5: 1.58, of node 6: 2.82,
7 node fits
Fits for spline nodes: 4:6
1.10
1.00
0.90
0.80
0.70
0.60
0.50
0
10
20
30
40
Order Count
BOHLIN: echsens 3-Jun-1998 15:01

Fig. 4 (cont.)

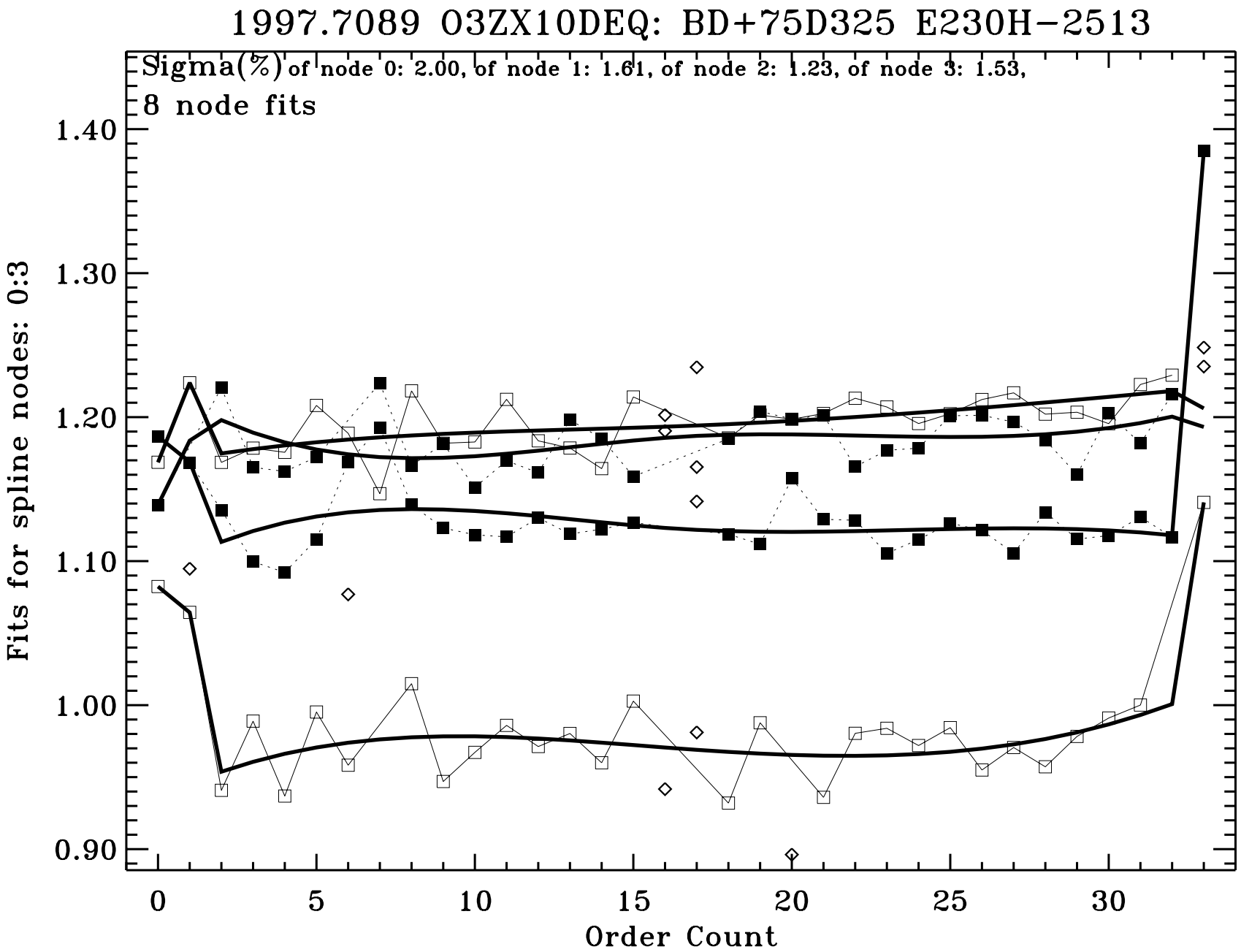
1997.7089 03ZX10DEQ: BD+75D325 E230H-2513
Sigma(%) of node 0: 2.00, of node 1: 1.61, of node 2: 1.23, of node 3: 1.53,
8 node fits
Fits for spline nodes: 0:3
1.40
1.30
1.20
1.10
1.00
0.90
0
5
10
15
20
25
30
Order Count
BOHLIN: echsens 3-Jun-1998 15:01

Fig. 4 (cont.)

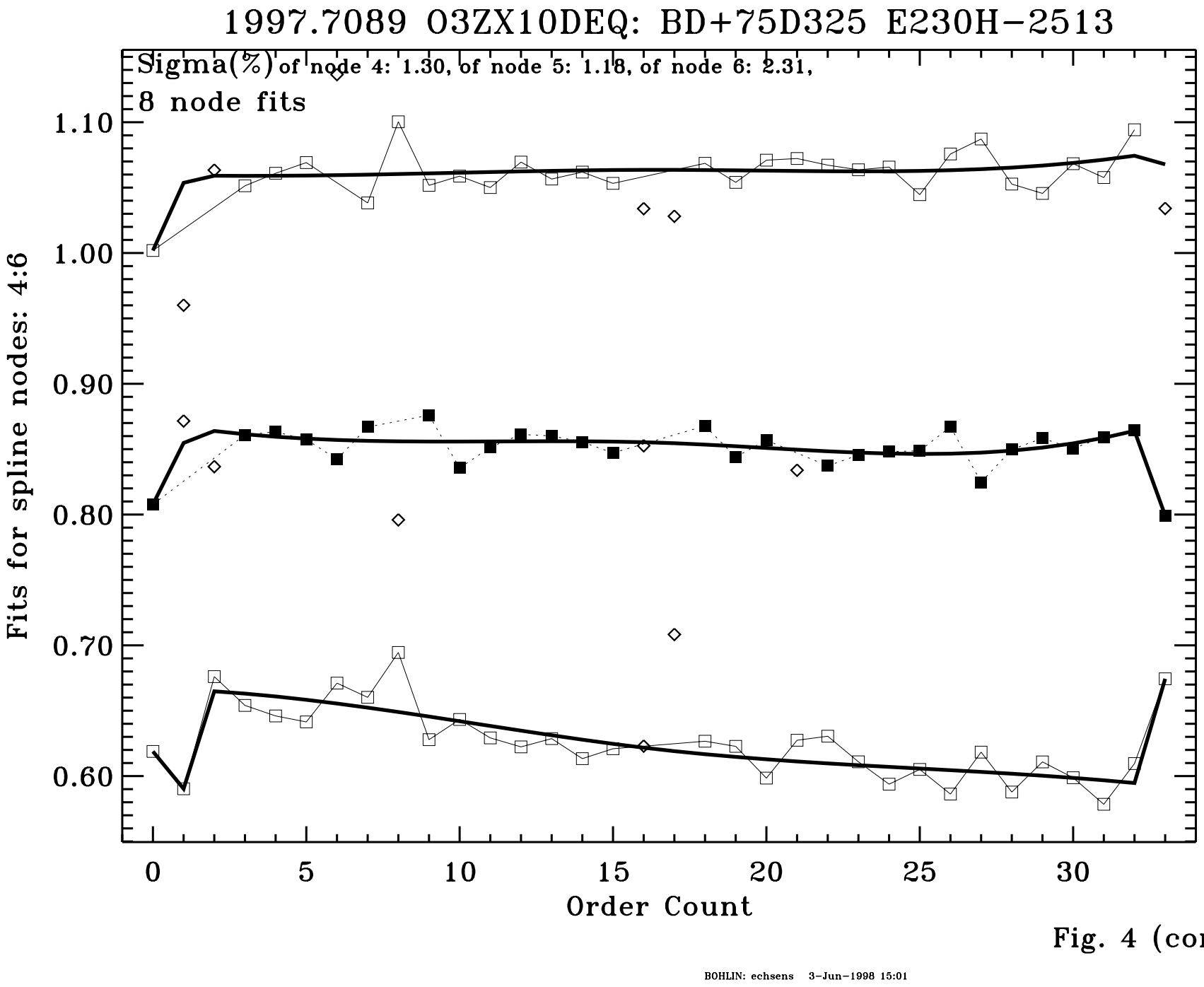
1997.7089 03ZX10DEQ: BD+75D325 E230H-2513
Sigma(%) of node 4: 1.30, of node 5: 1.18, of node 6: 2.31,
8 node fits
Fits for spline nodes: 4:6
1.10
1.00
0.90
0.80
0.70
0.60
0
5
10
15
20
25
30
Order Count
BOHLIN: echsens 3-Jun-1998 15:01

Fig. 4 (cont.)

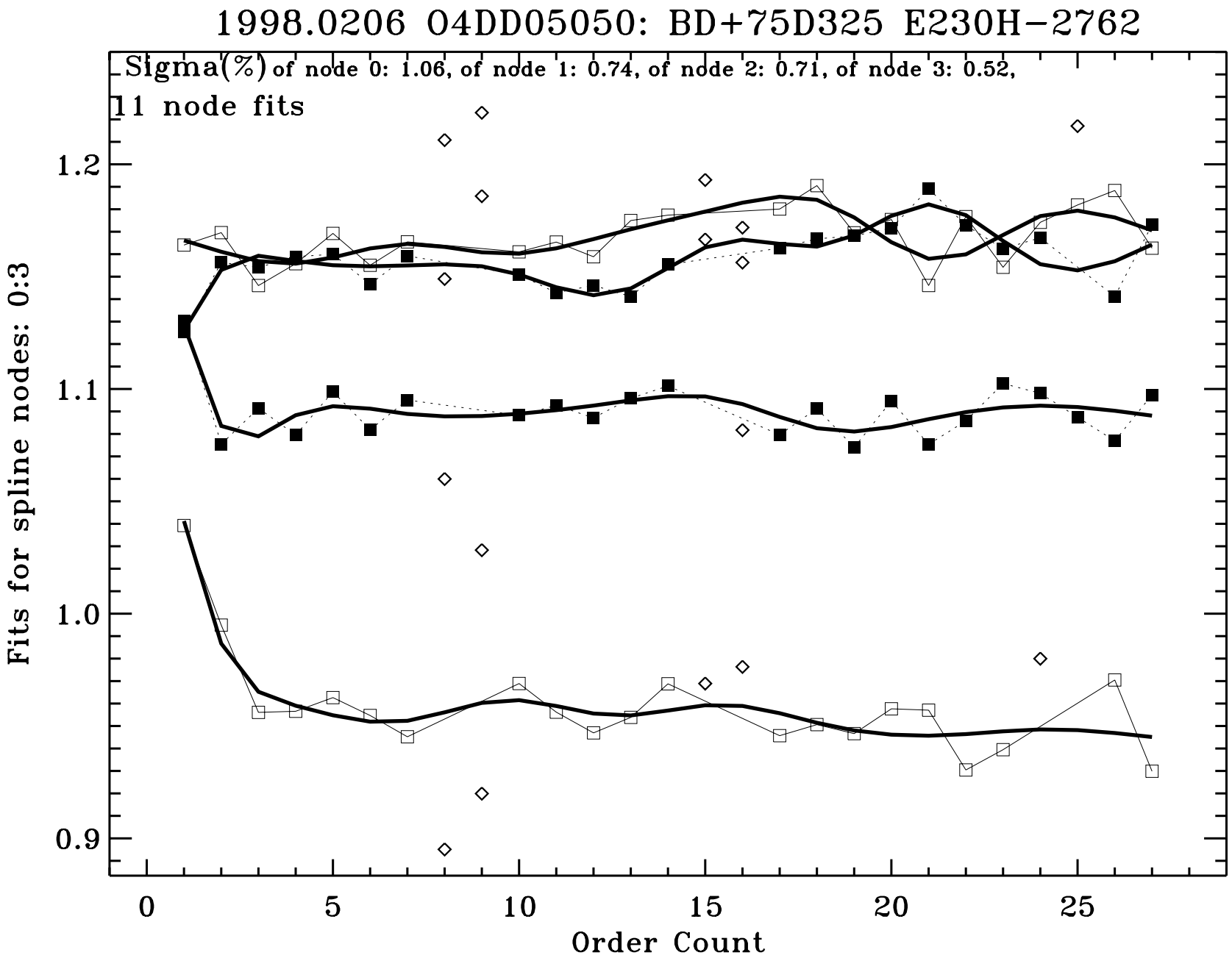
1998.0206 04DD05050: BD+75D325 E230H-2762
Sigma(%) of node 0: 1.06, of node 1: 0.74, of node 2: 0.71, of node 3: 0.52,
11 node fits
Fits for spline nodes: 0:3
1.2
1.1
1.0
0.9
0
5
10
15
20
25
Order Count
BOHLIN: echsens 3-Jun-1998 15:01

Fig. 4 (cont.)

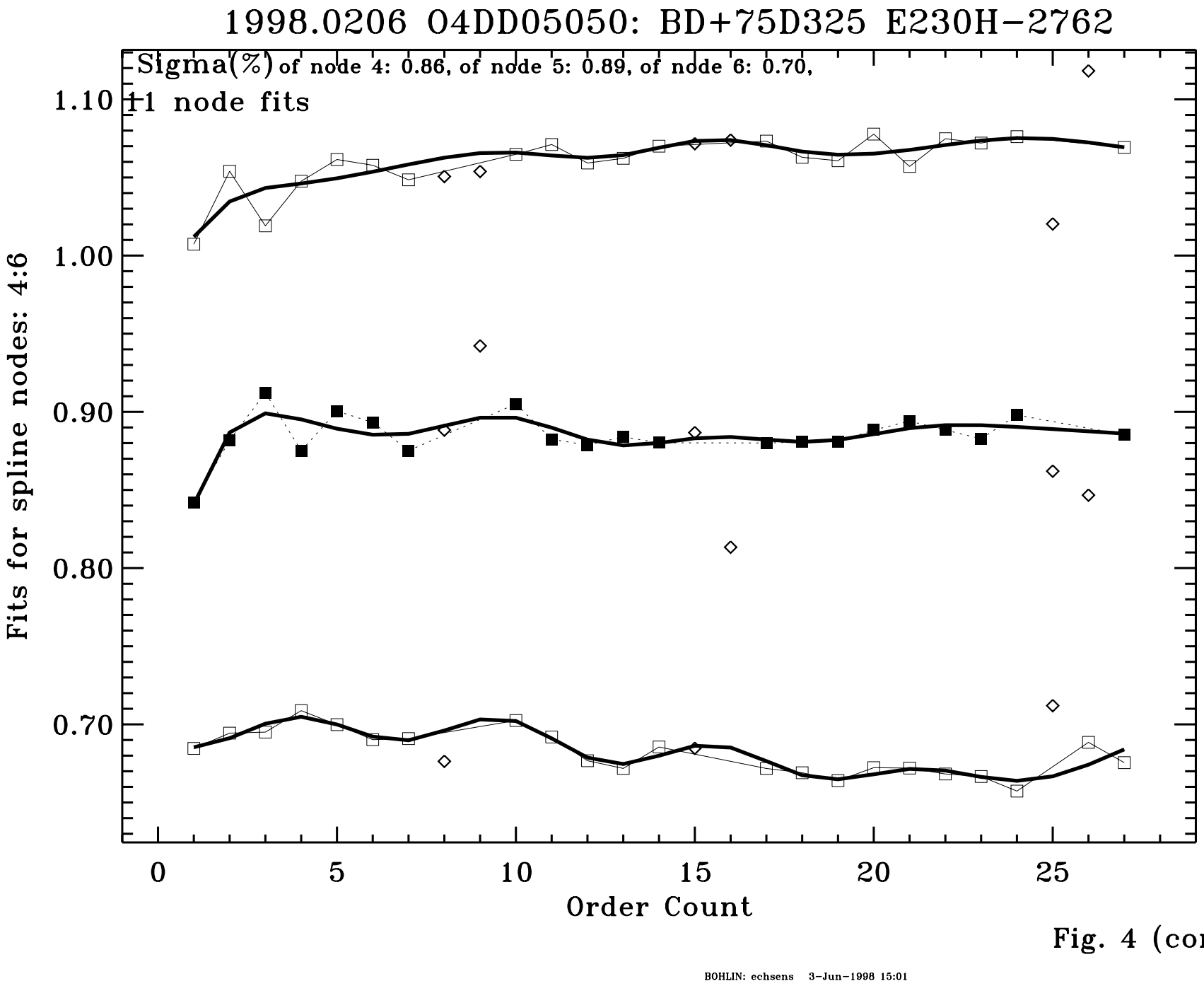
1998.0206 04DD05050: BD+75D325 E230H-2762
Sigma(%) of node 4: 0.86, of node 5: 0.89, of node 6: 0.70,
1+1 node fits
Fits for spline nodes: 4:6
1.10
1.00
0.90
0.80
0.70
0
5
10
15
20
25
Order Count
BOHLIN: echsens 3-Jun-1998 15:01

Fig. 4 (cont.)

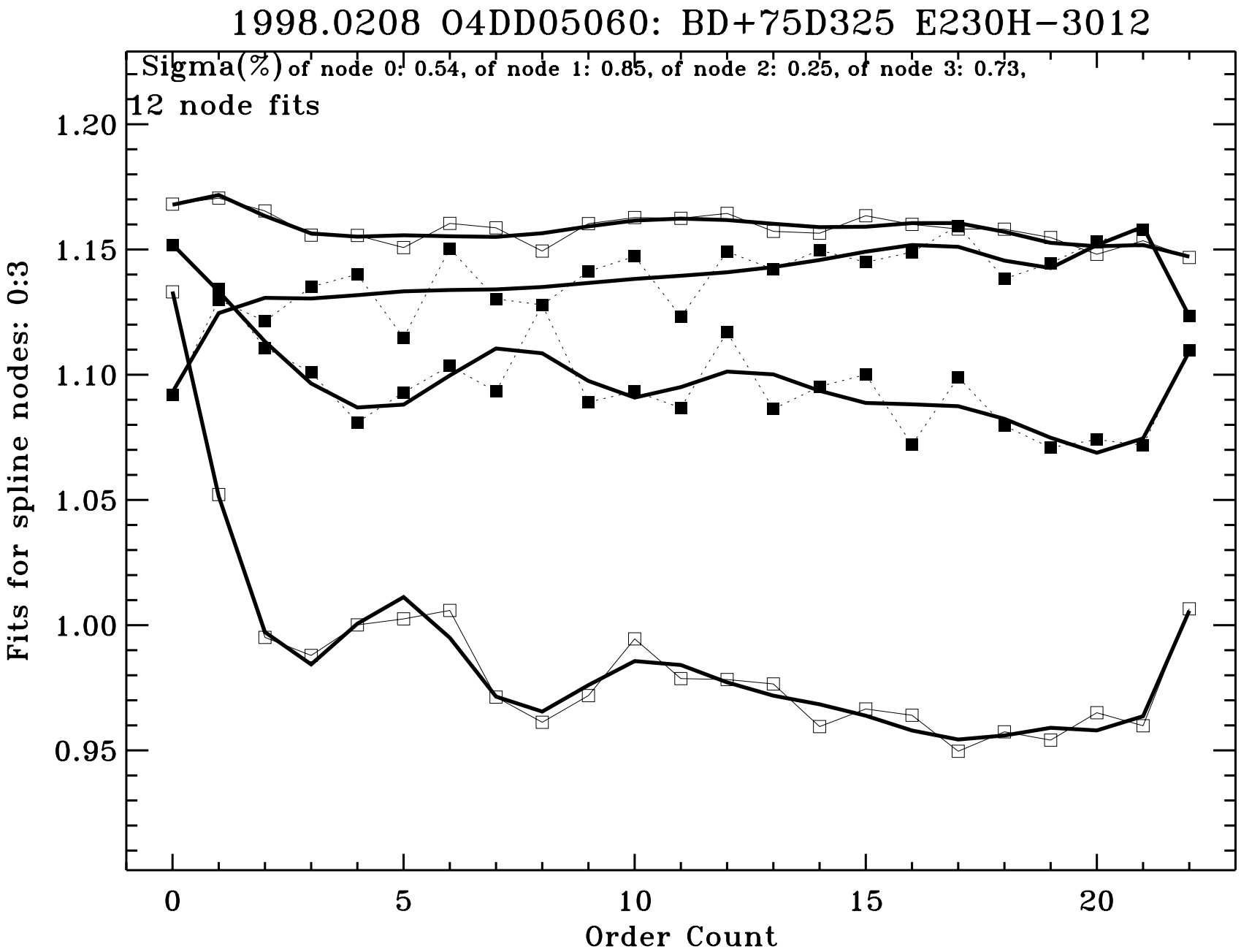
1998.0208 04DD05060: BD+75D325 E230H-3012
Sigma(%) of node 0: 0.54, of node 1: 0.85, of node 2: 0.25, of node 3: 0.73,
12 node fits
Fits for spline nodes: 0:3
1.20
1.15
1.10
1.05
1.00
0.95
0
5
10
15
20
Order Count
BOHLIN: echsens 3-Jun-1998 15:01

Fig. 4 (cont.)

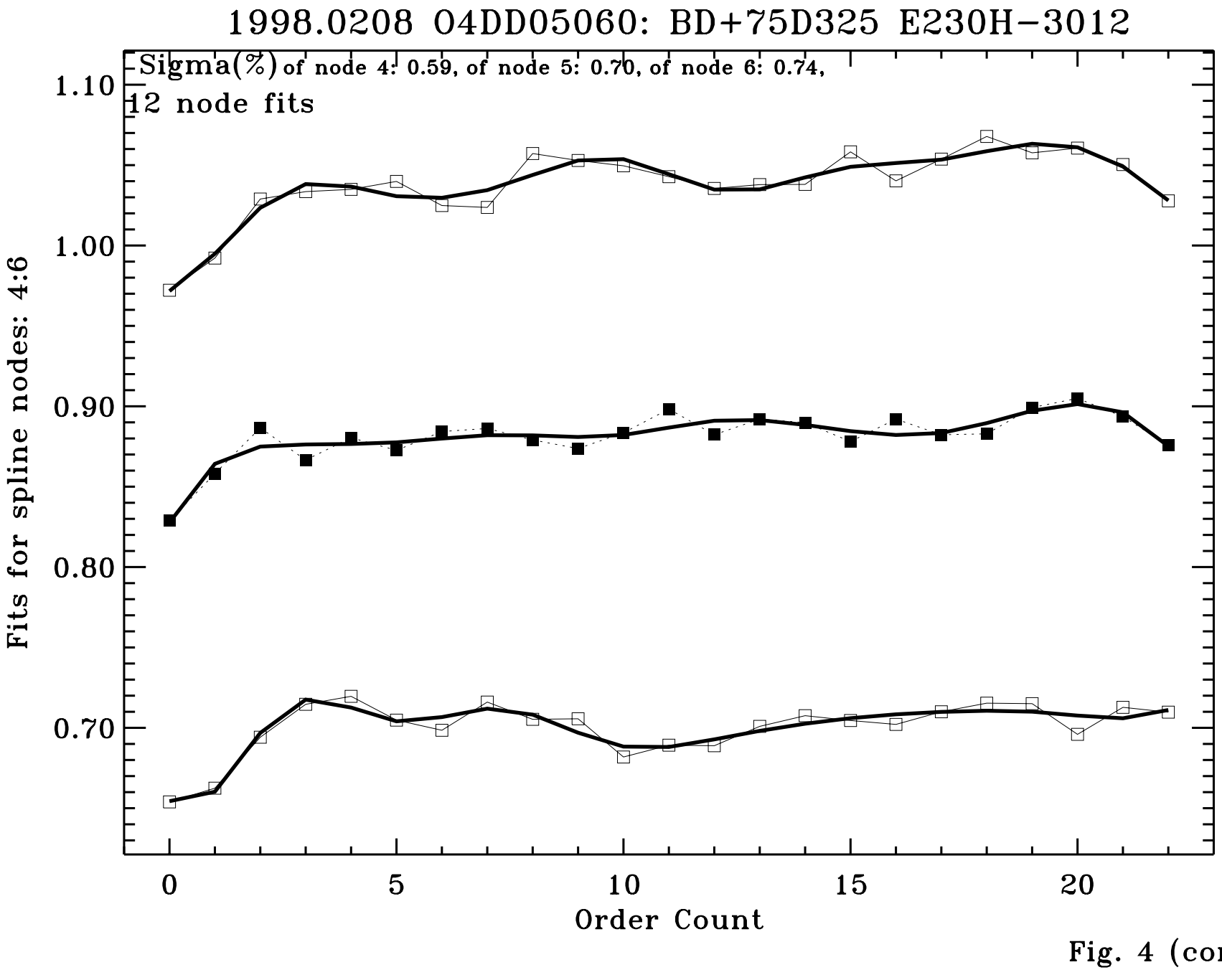
1998.0208 04DD05060: BD+75D325 E230H-3012
Sigma(%) of node 4: 0.59, of node 5: 0.70, of node 6: 0.74,
12 node fits
Fits for spline nodes: 4:6
1.10
1.00
0.90
0.80
0.70
0
5
10
15
20
Order Count
BOHLIN: echsens 3-Jun-1998 15:01

Fig. 4 (cont.)

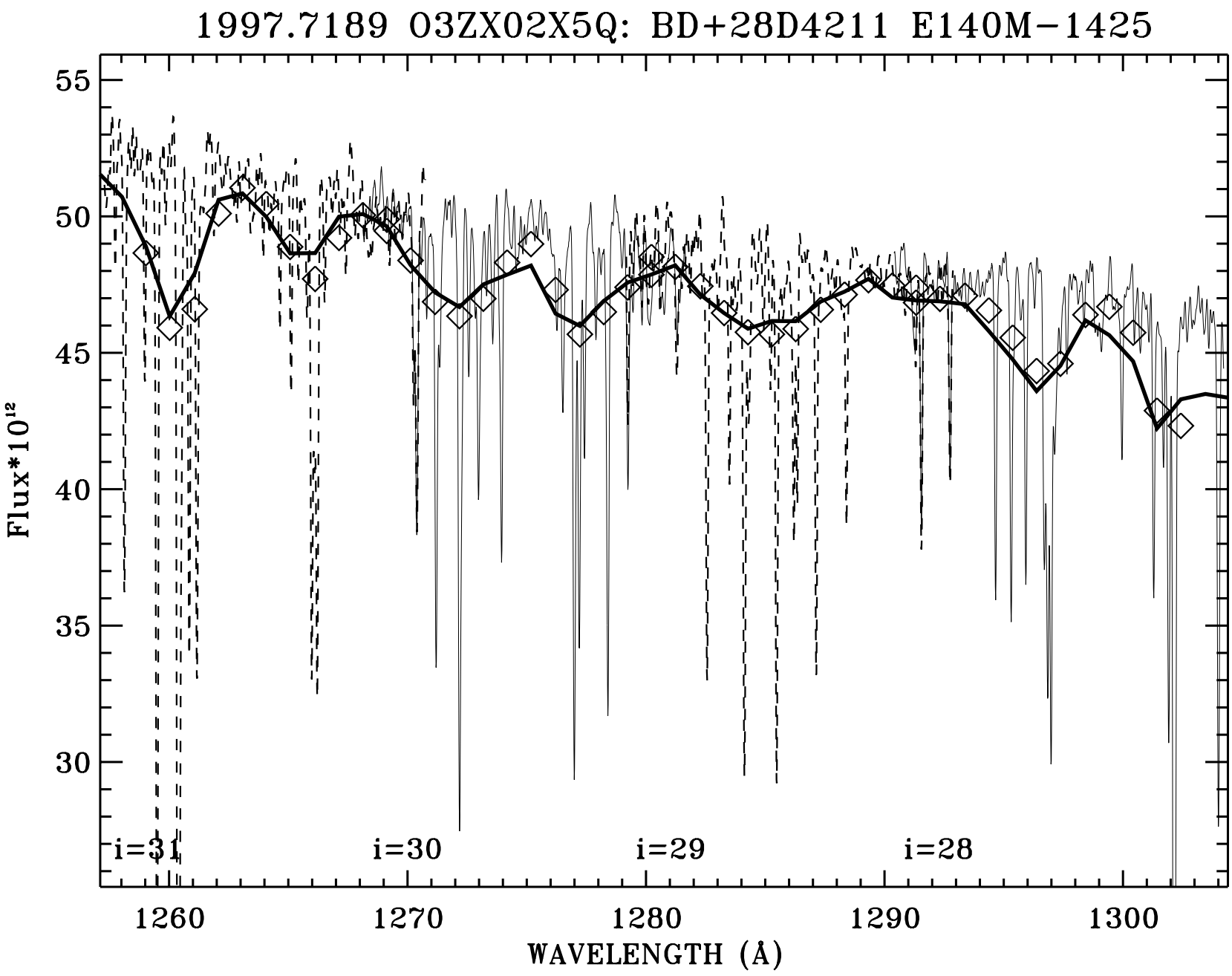

Fig. 5

BOHLIN: echsens 3-Jun-1998 15:15

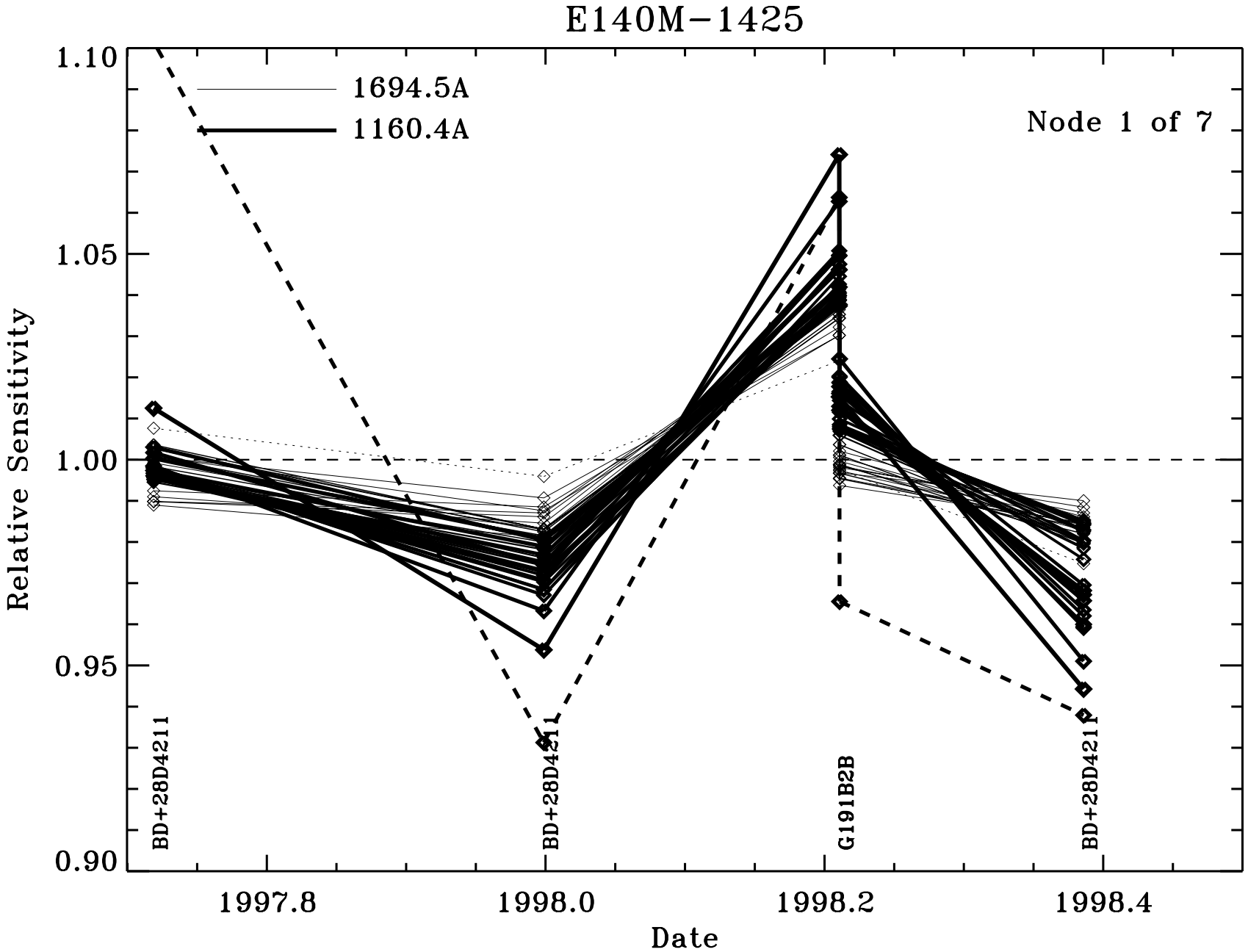

Fig. 6

BOHLIN: echsnsall 3-Jun-1998 15:19

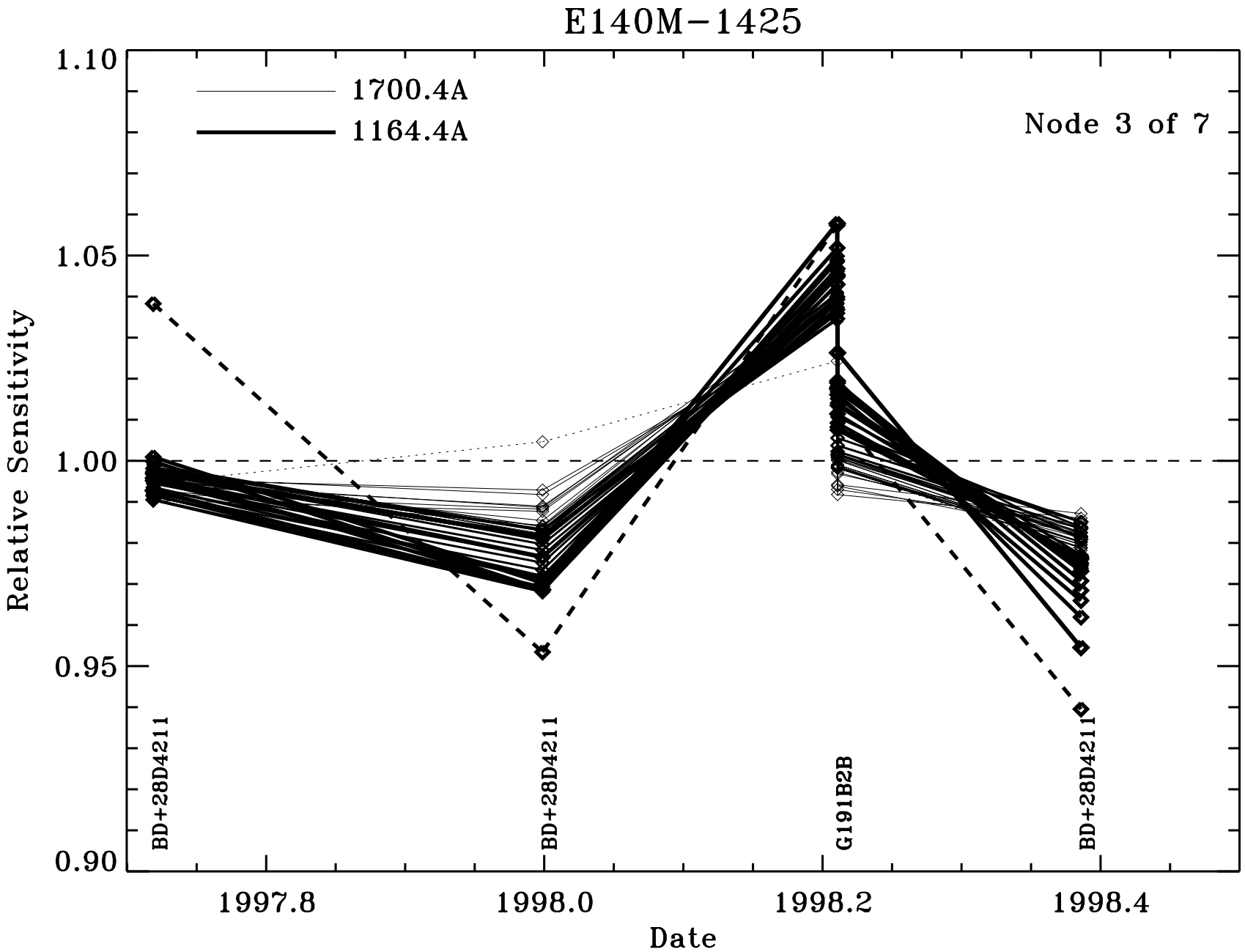

Fig. 6 (cont.)

BOHLIN: echsnsall 3-Jun-1998 15:19

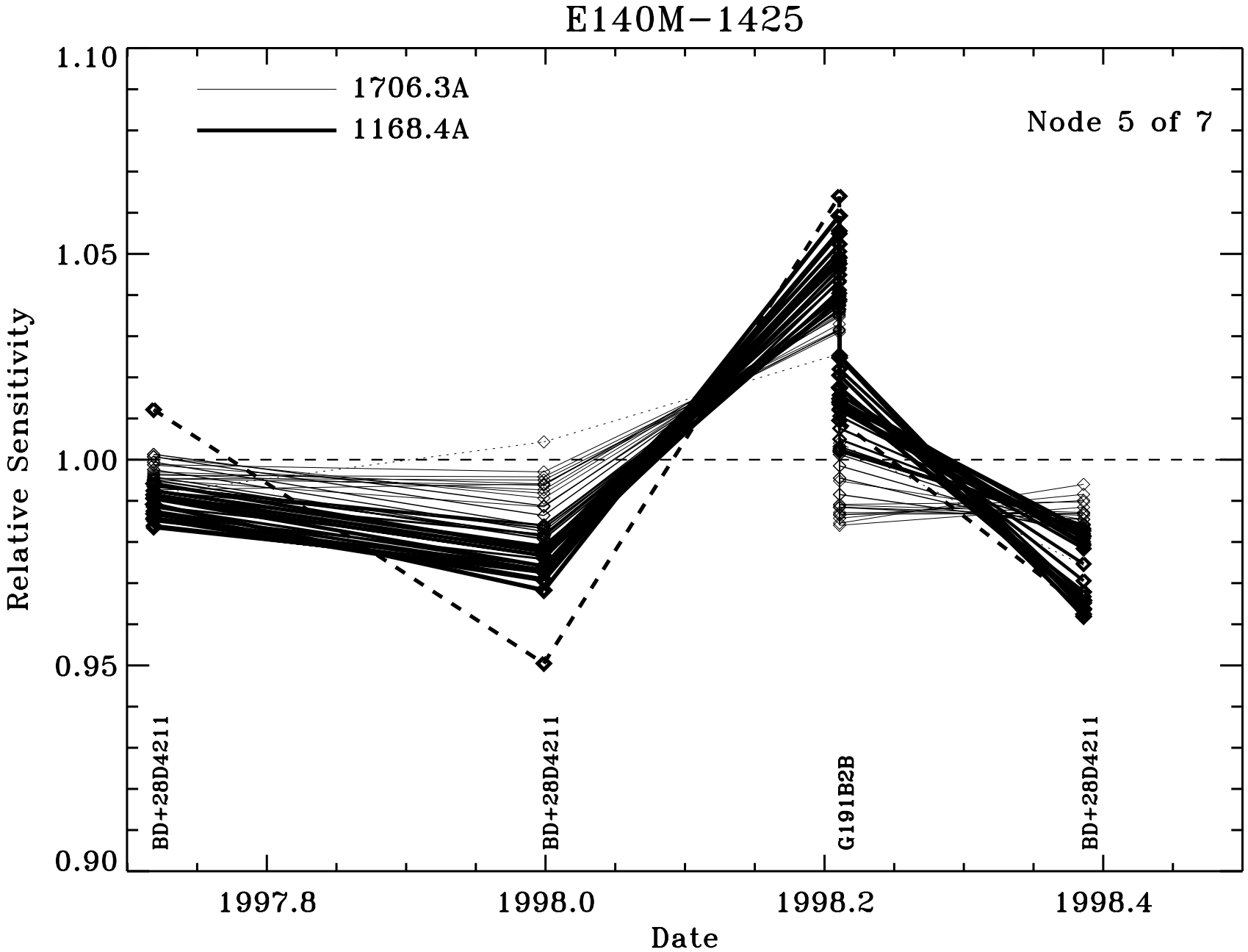
E140M−1425
1706.3A
1168.4A
Node 5 of 7
Relative Sensitivity
1.10
1.05
1.00
0.95
0.90
BD+28D4211
BD+28D4211
G191B2B
BD+28D4211
1997.8
1998.0
1998.2
1998.4
Date
BOHLIN: echsnsall 3-Jun-1998 15:19

Fig. 6 (cont.)

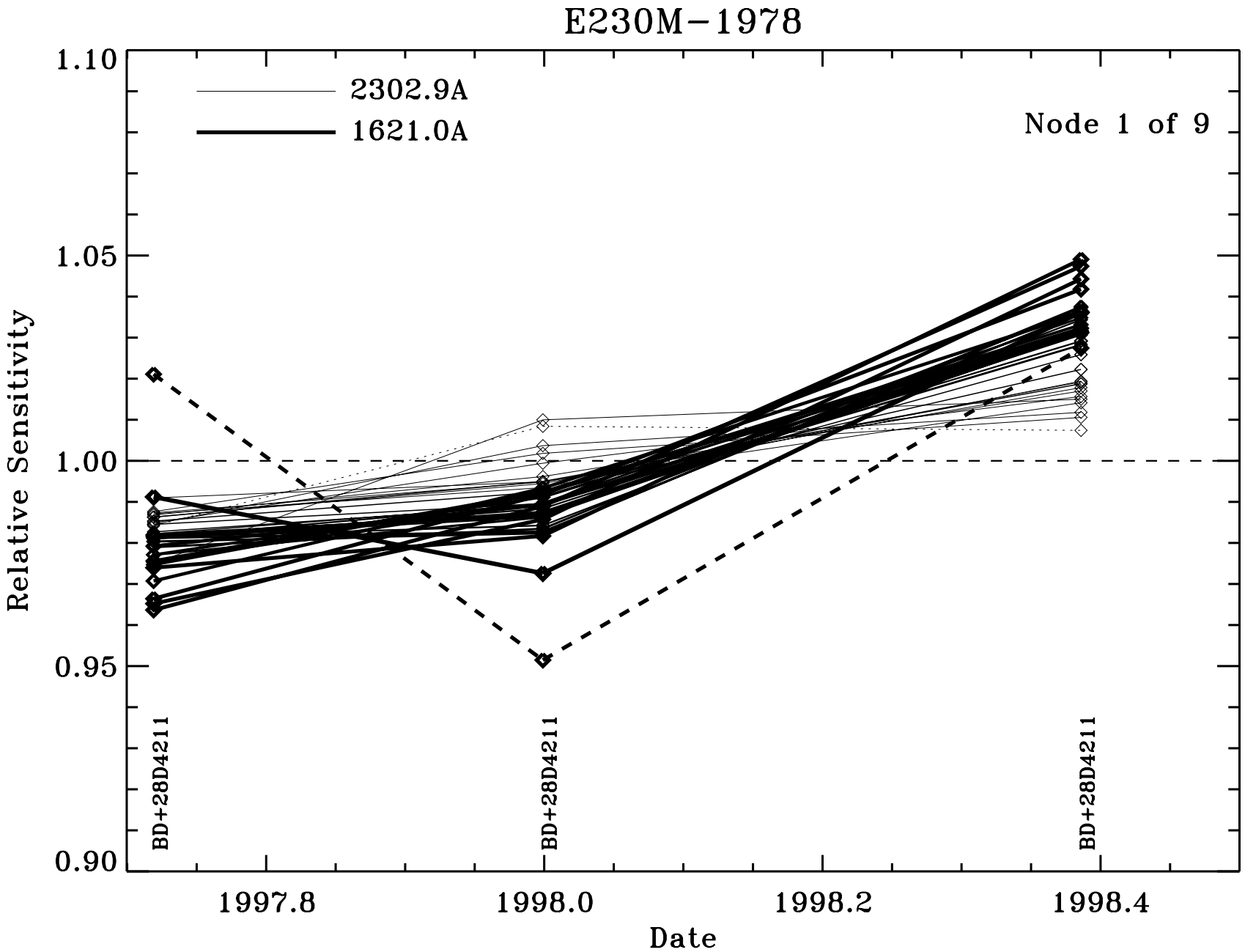

Fig. 6 (cont.)

BOHLIN: echsnsall 3-Jun-1998 15:19

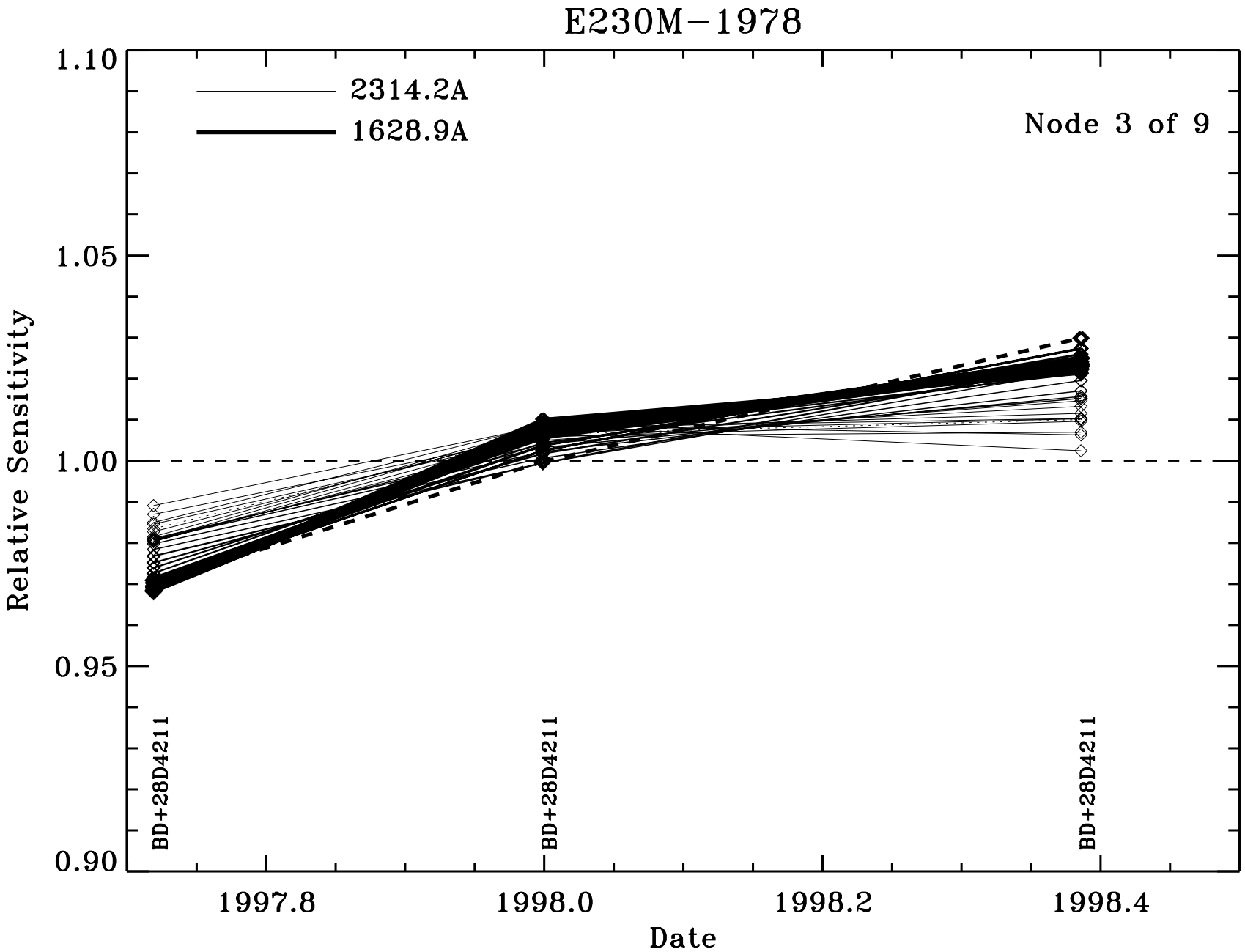

Fig. 6 (cont.)

BOHLIN: echsnsall 3-Jun-1998 15:19

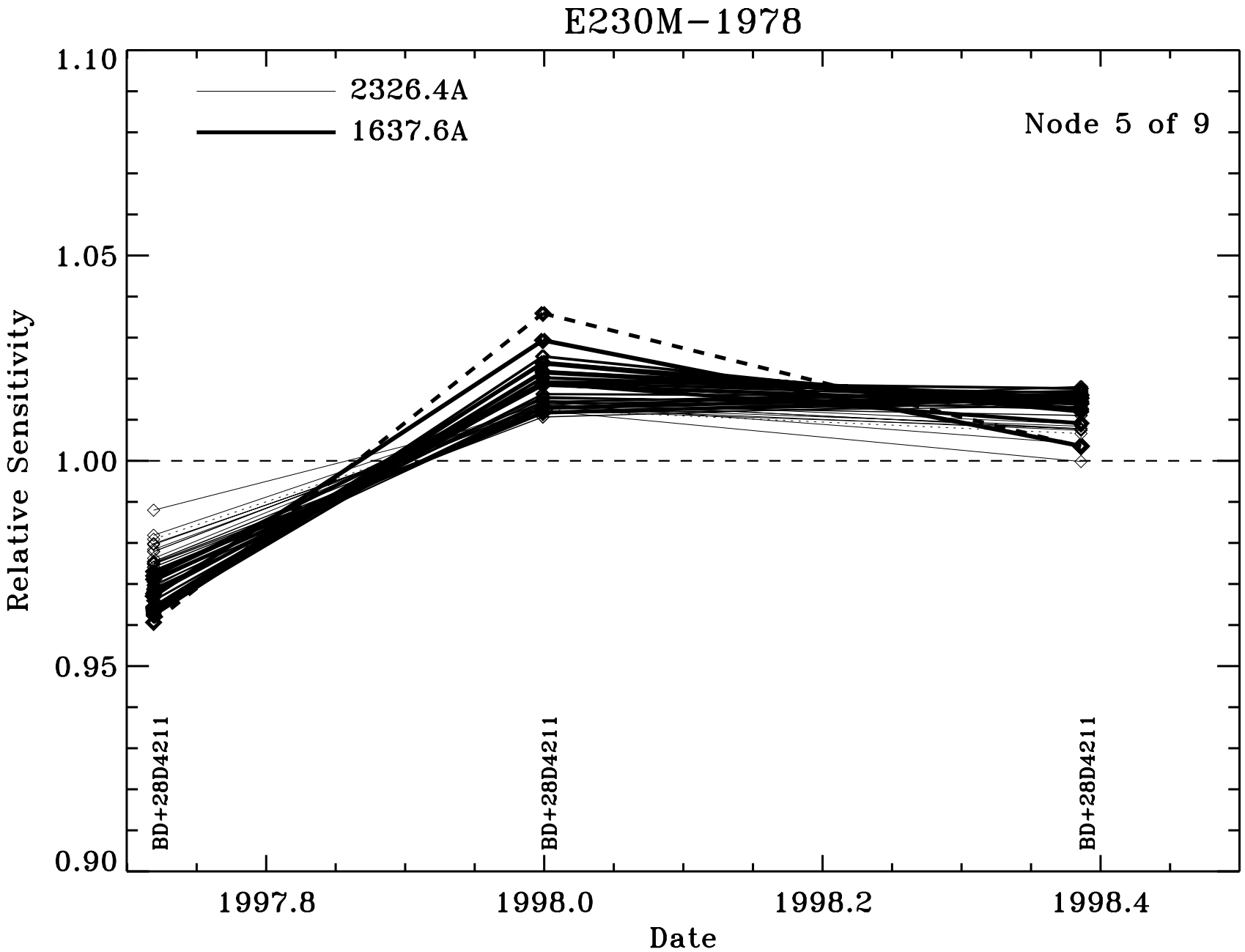

Fig. 6 (cont.)

BOHLIN: echsnsall 3-Jun-1998 15:19

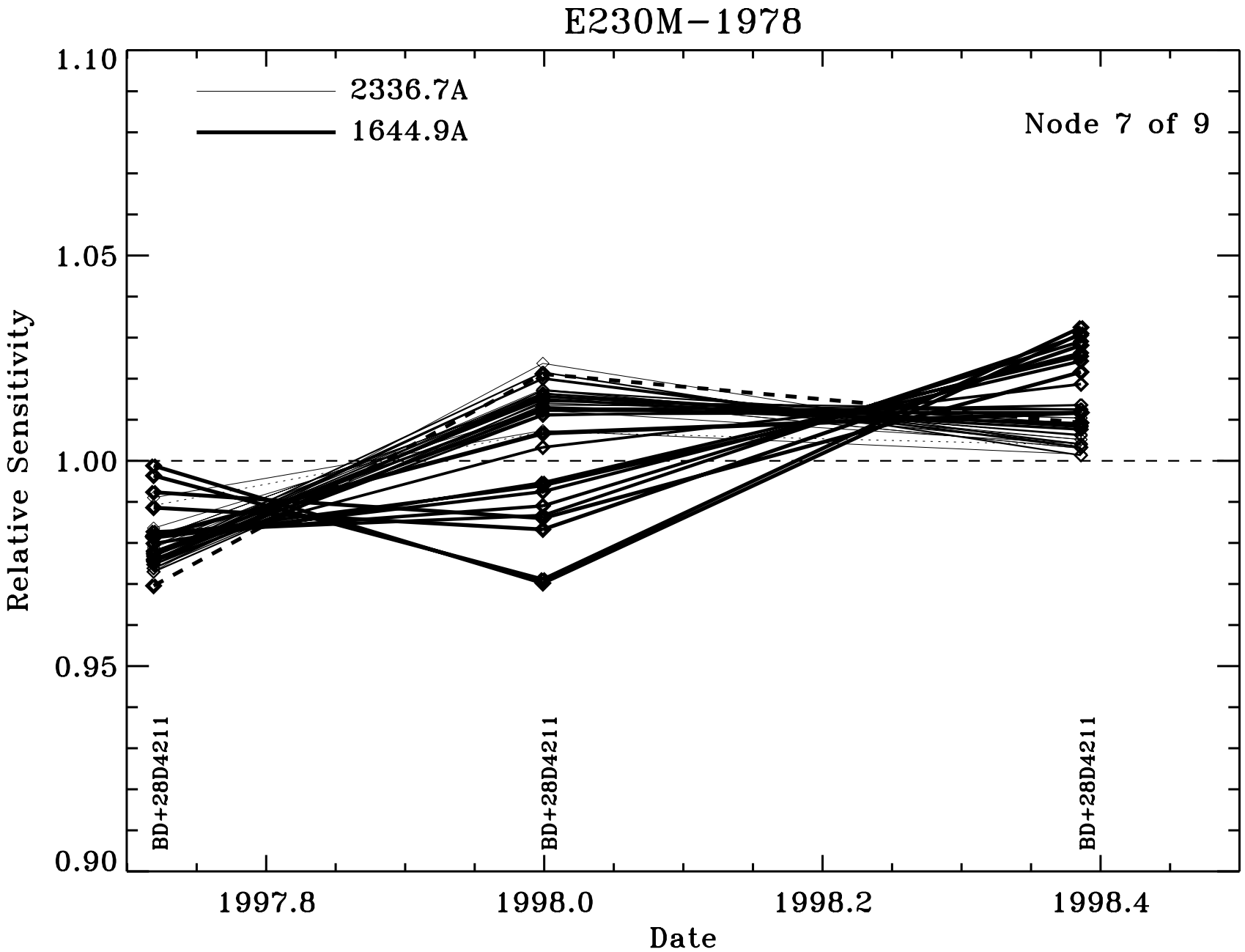

Fig. 6 (cont.)

BOHLIN: echsnsall 3-Jun-1998 15:19

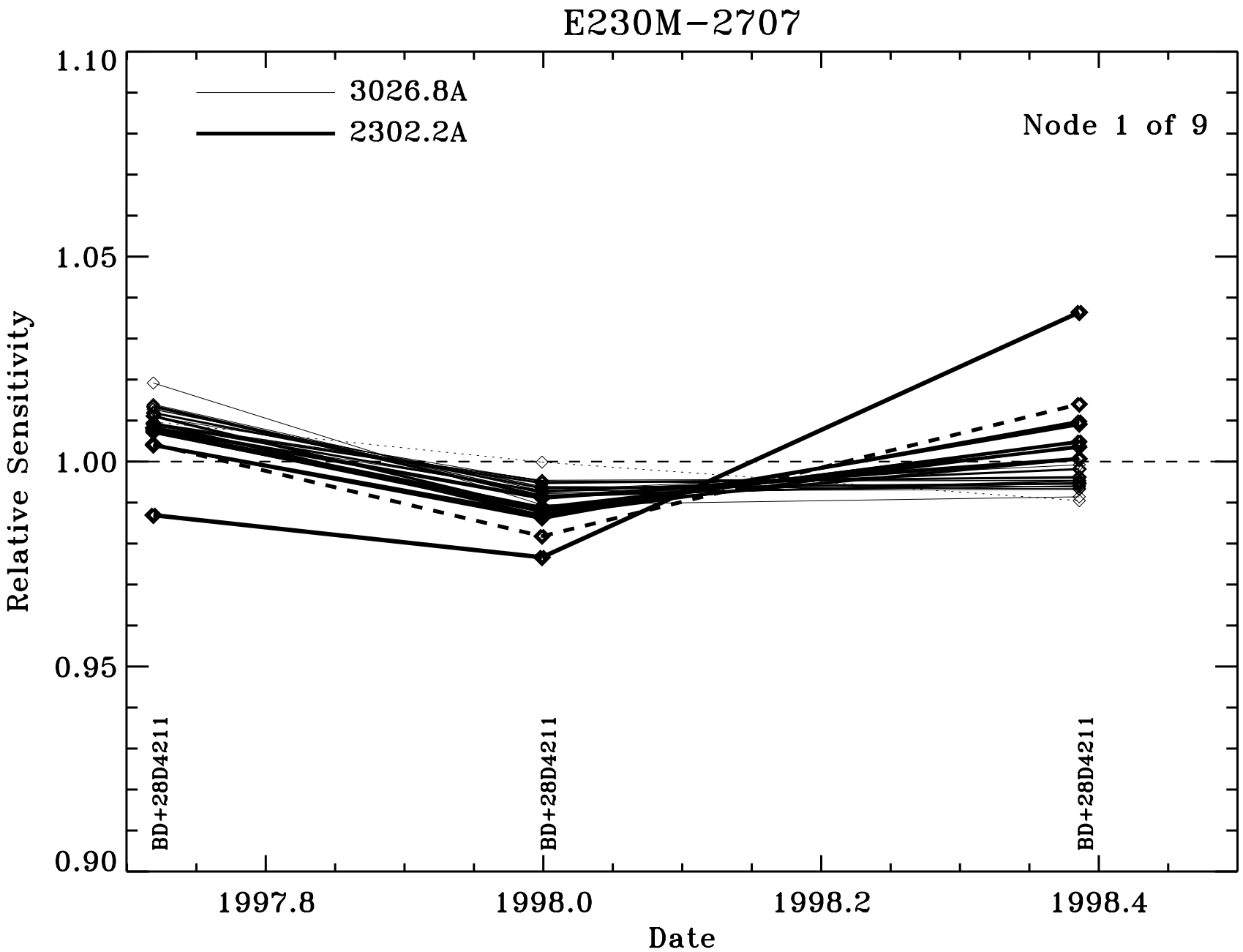

Fig. 6 (cont.)

BOHLIN: echsnsall 3-Jun-1998 15:19

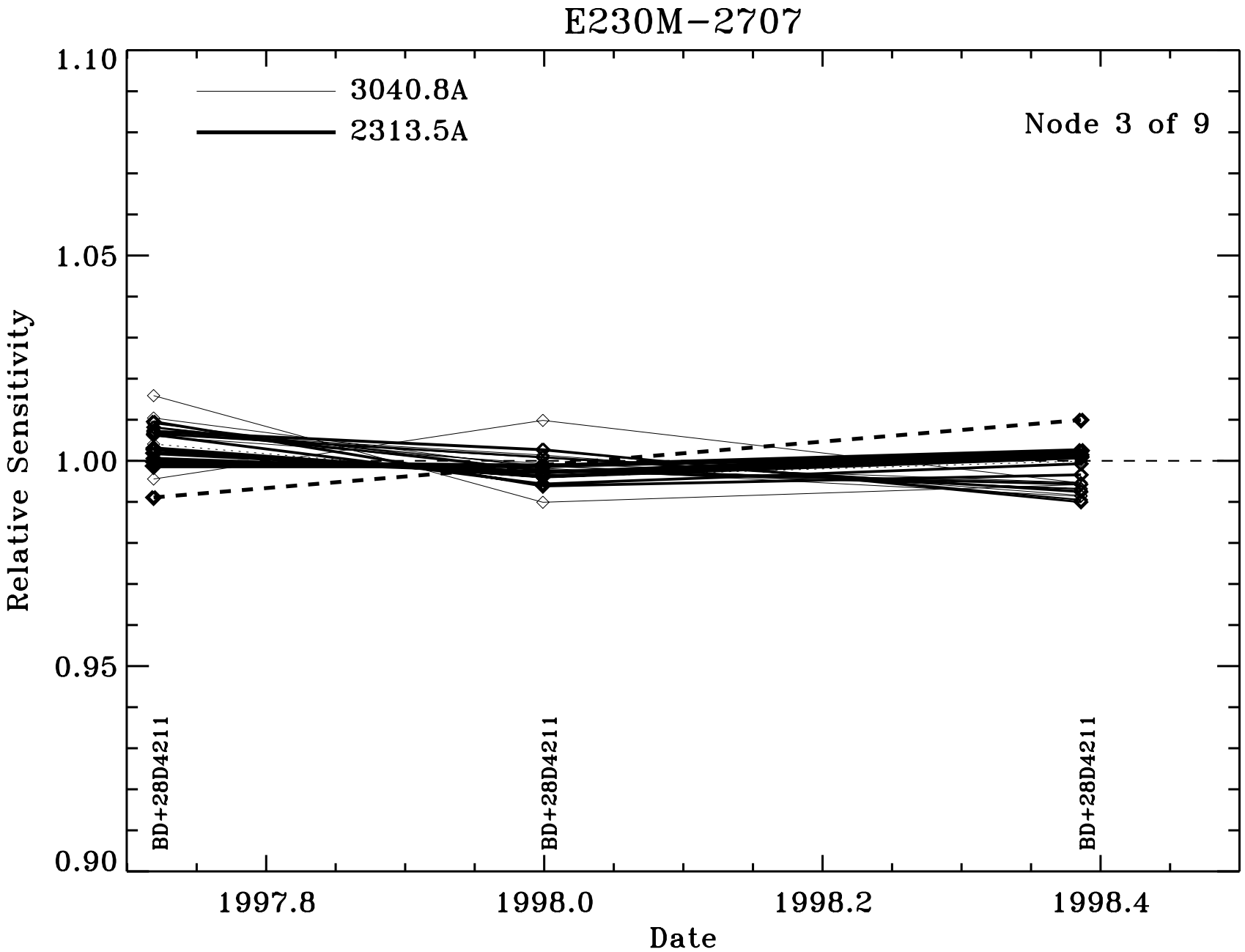

Fig. 6 (cont.)

BOHLIN: echsnsall 3-Jun-1998 15:19

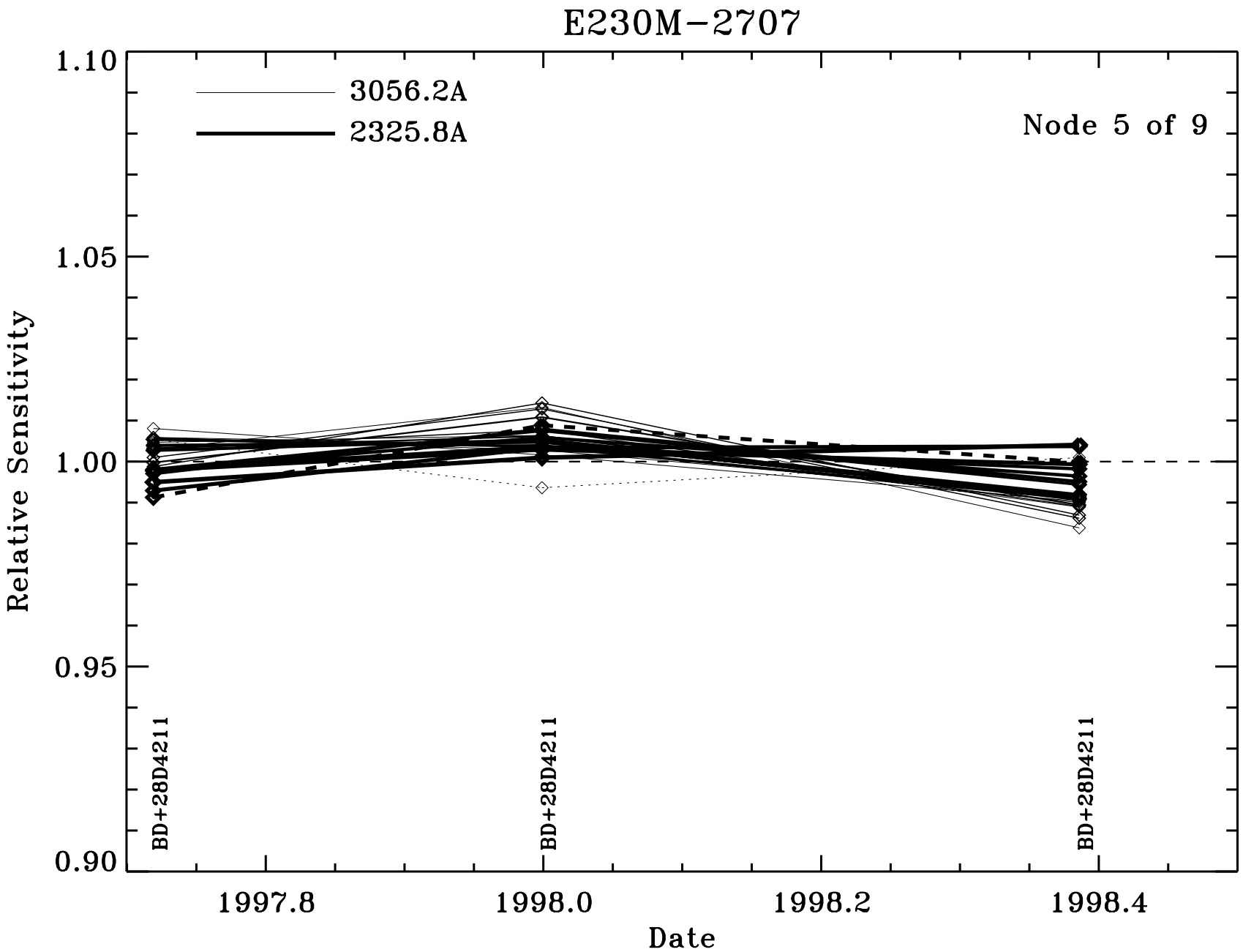

Fig. 6 (cont.)

BOHLIN: echsnsall 3-Jun-1998 15:19

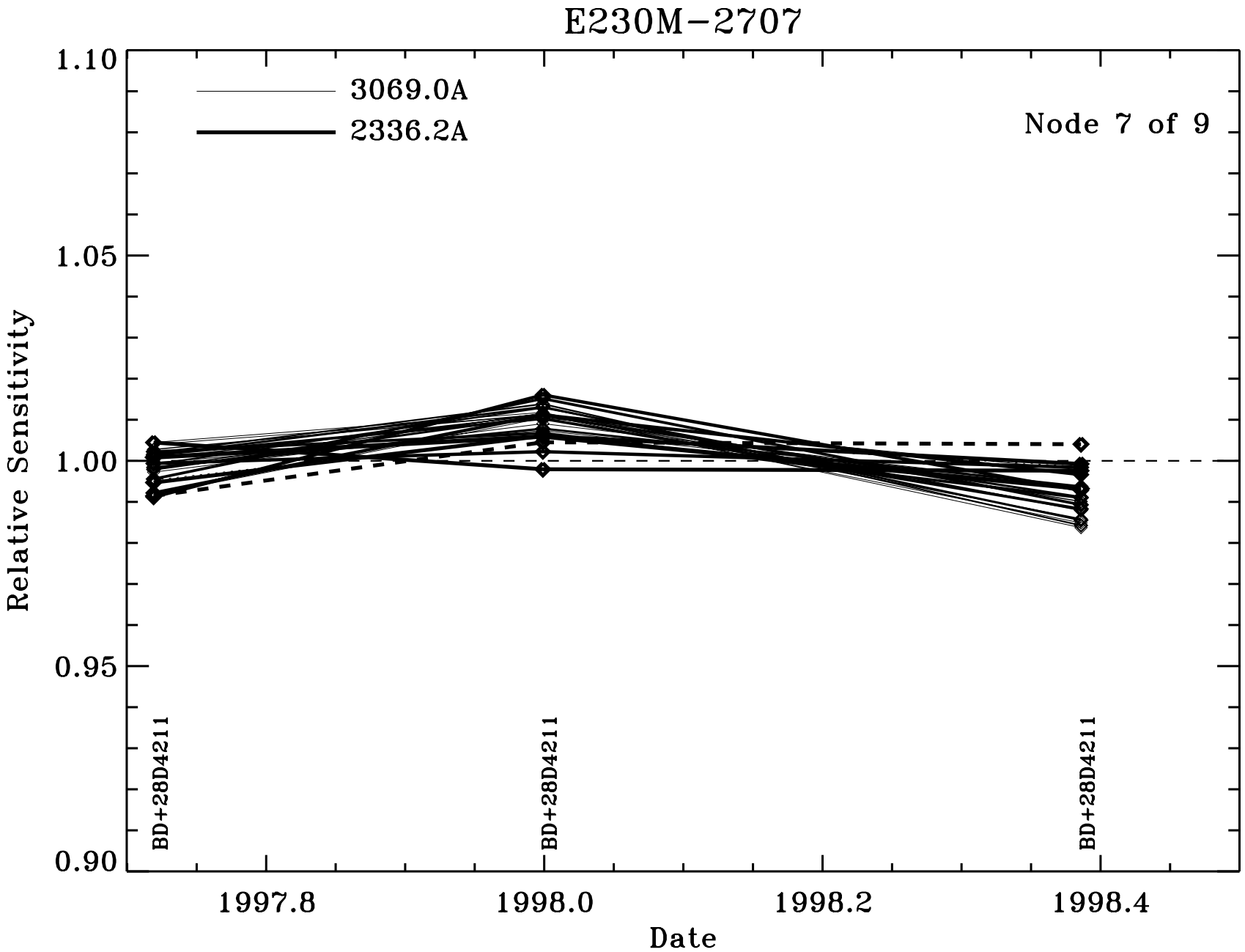

Fig. 6 (cont.)

BOHLIN: echsnsall 3-Jun-1998 15:19

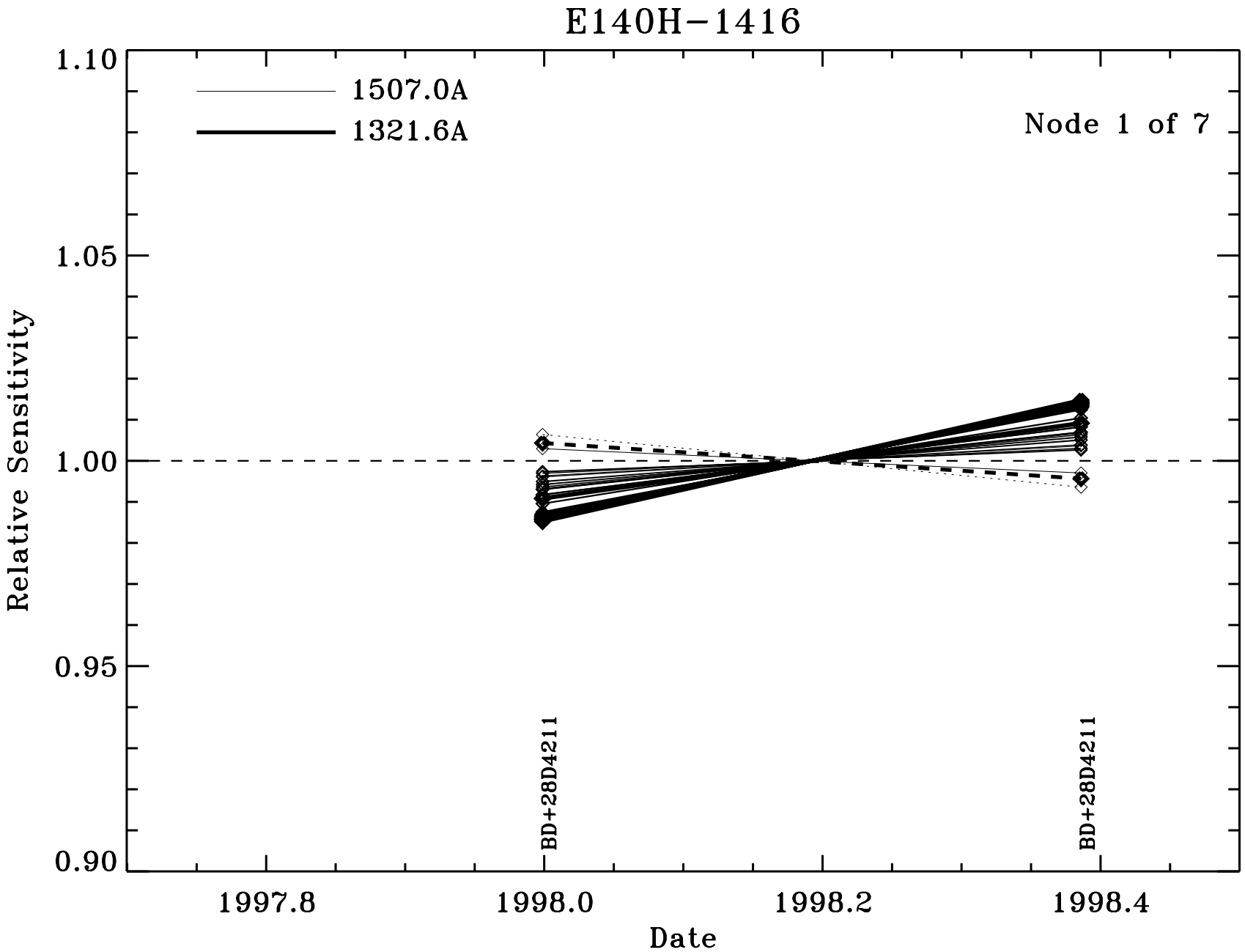

Fig. 6 (cont.)

BOHLIN: echsnsall 3-Jun-1998 15:19

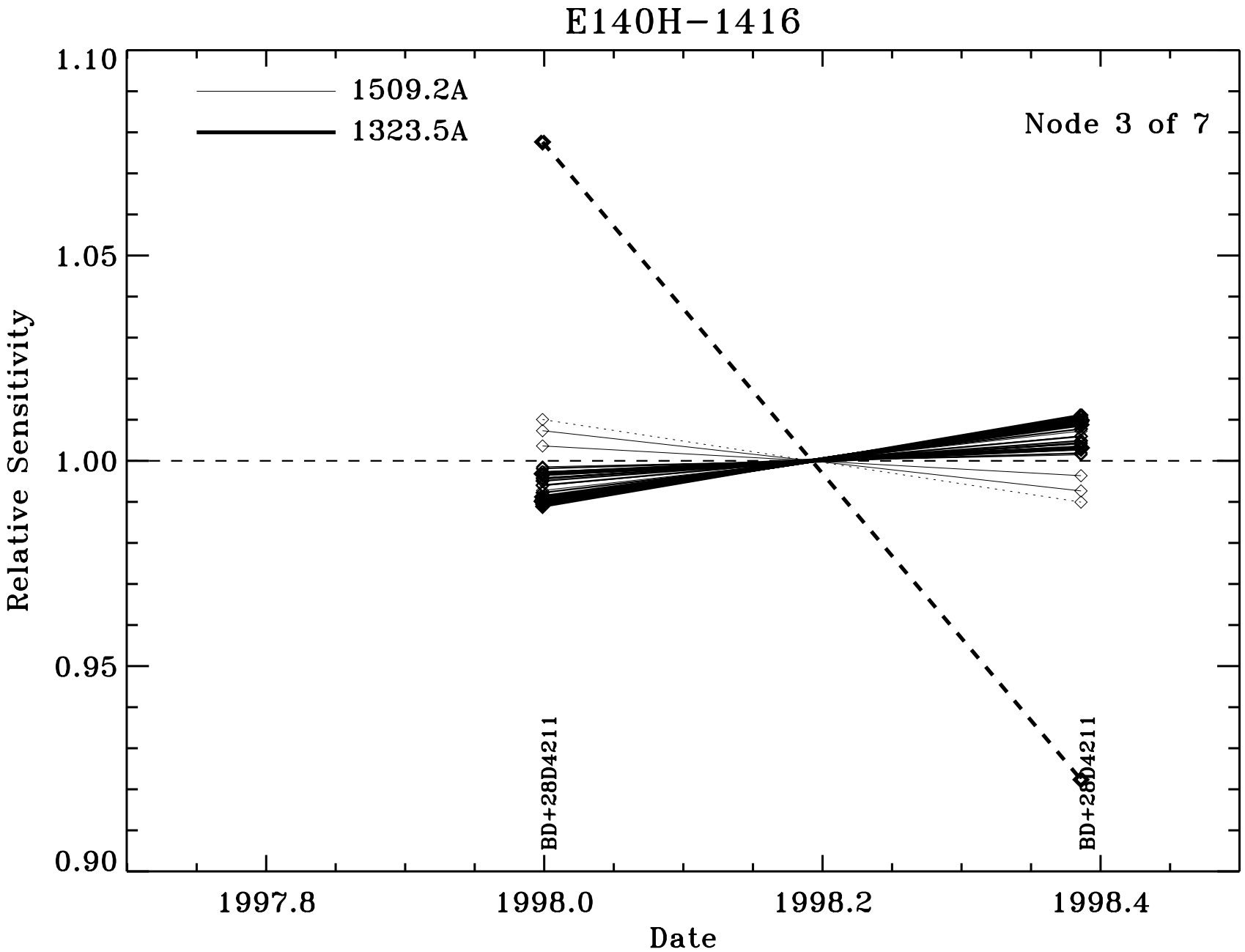
E140H-1416
1509.2A
1323.5A
Node 3 of 7
Relative Sensitivity
1.10
1.05
1.00
0.95
0.90
1997.8
1998.0
1998.2
1998.4
Date
BD+28D4211
BD+28D4211
BOHLIN: echsnsall 3-Jun-1998 15:19

Fig. 6 (cont.)

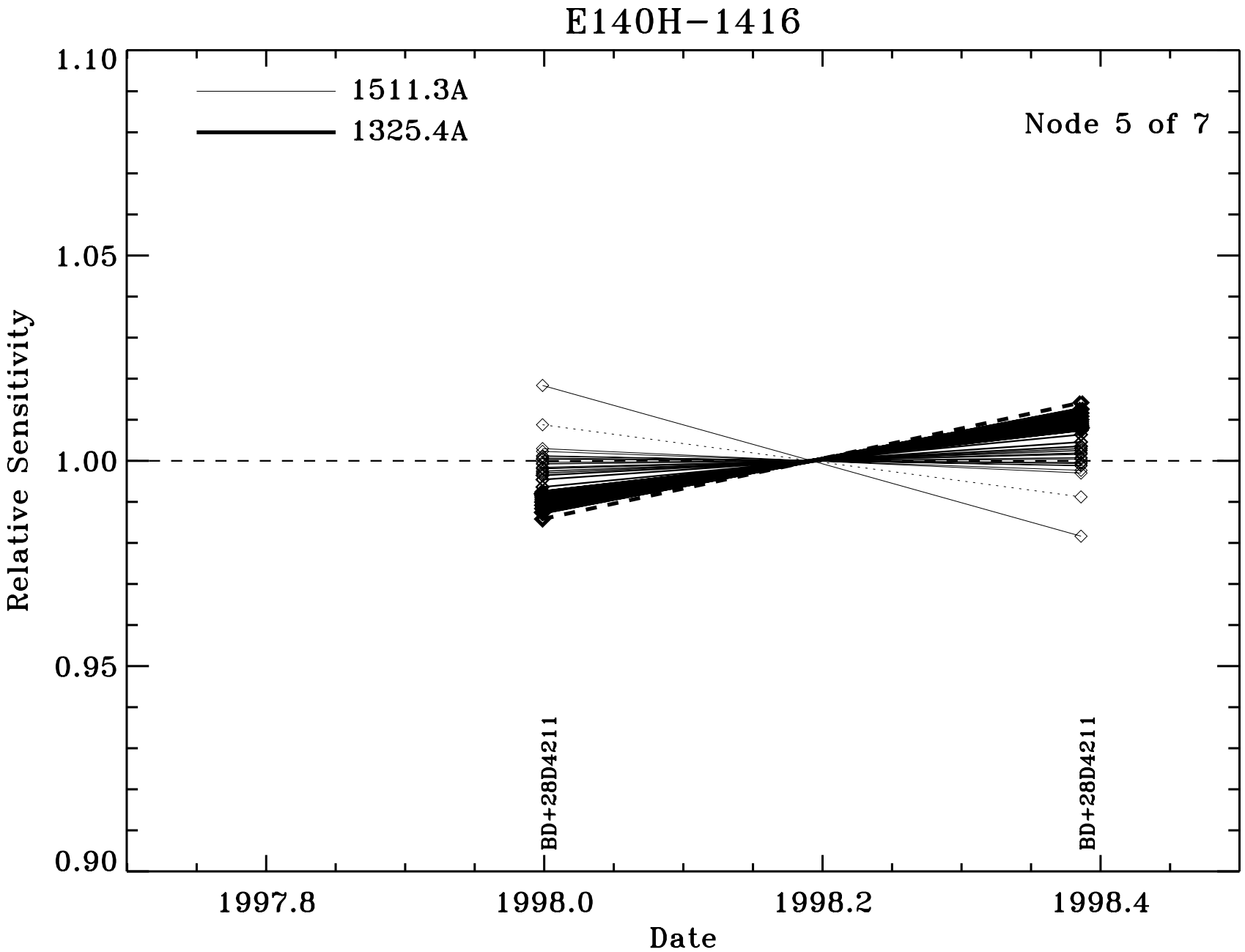

Fig. 6 (cont.)

BOHLIN: echsnsall 3-Jun-1998 15:19

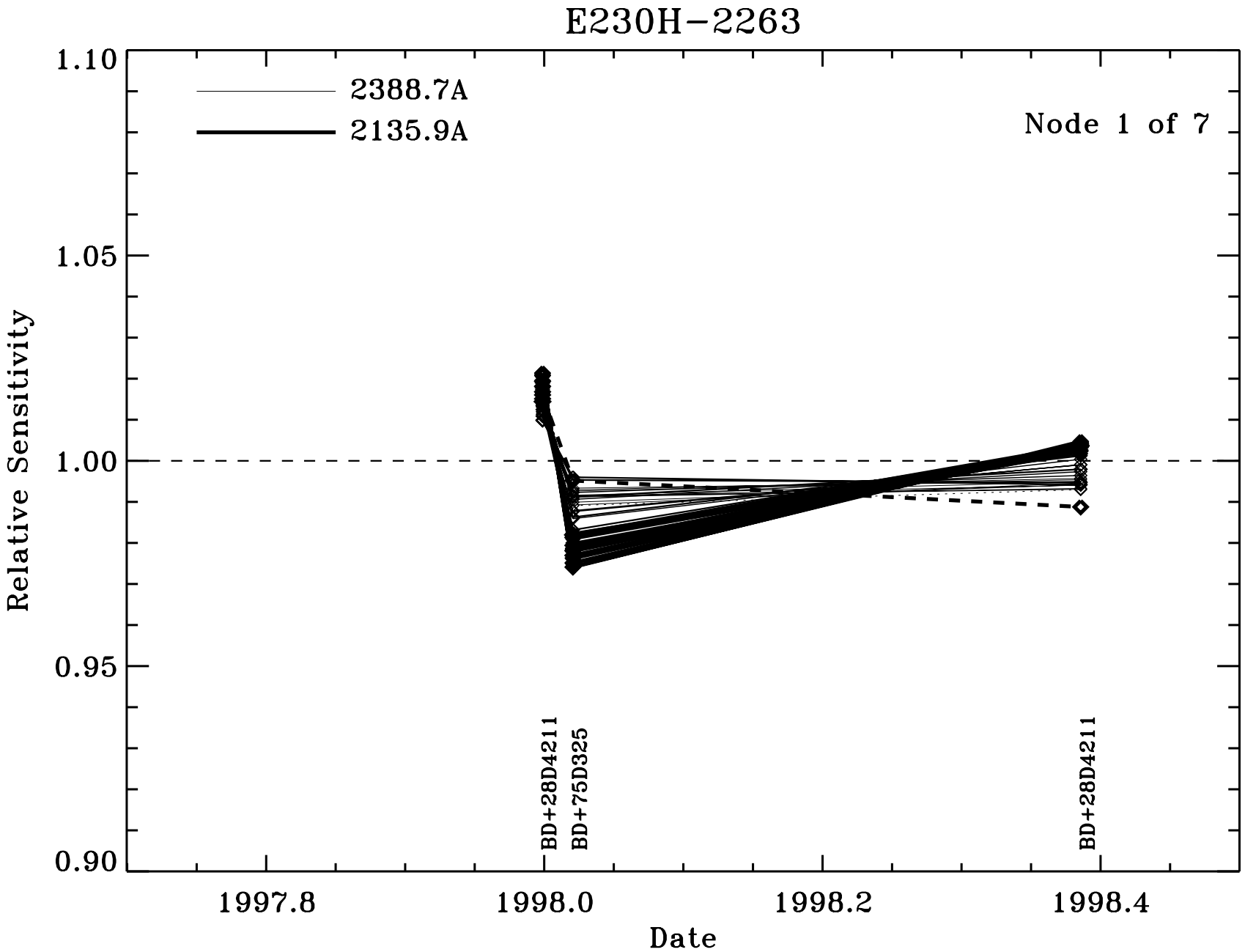

Fig. 6 (cont.)

BOHLIN: echsnsall 3-Jun-1998 15:19

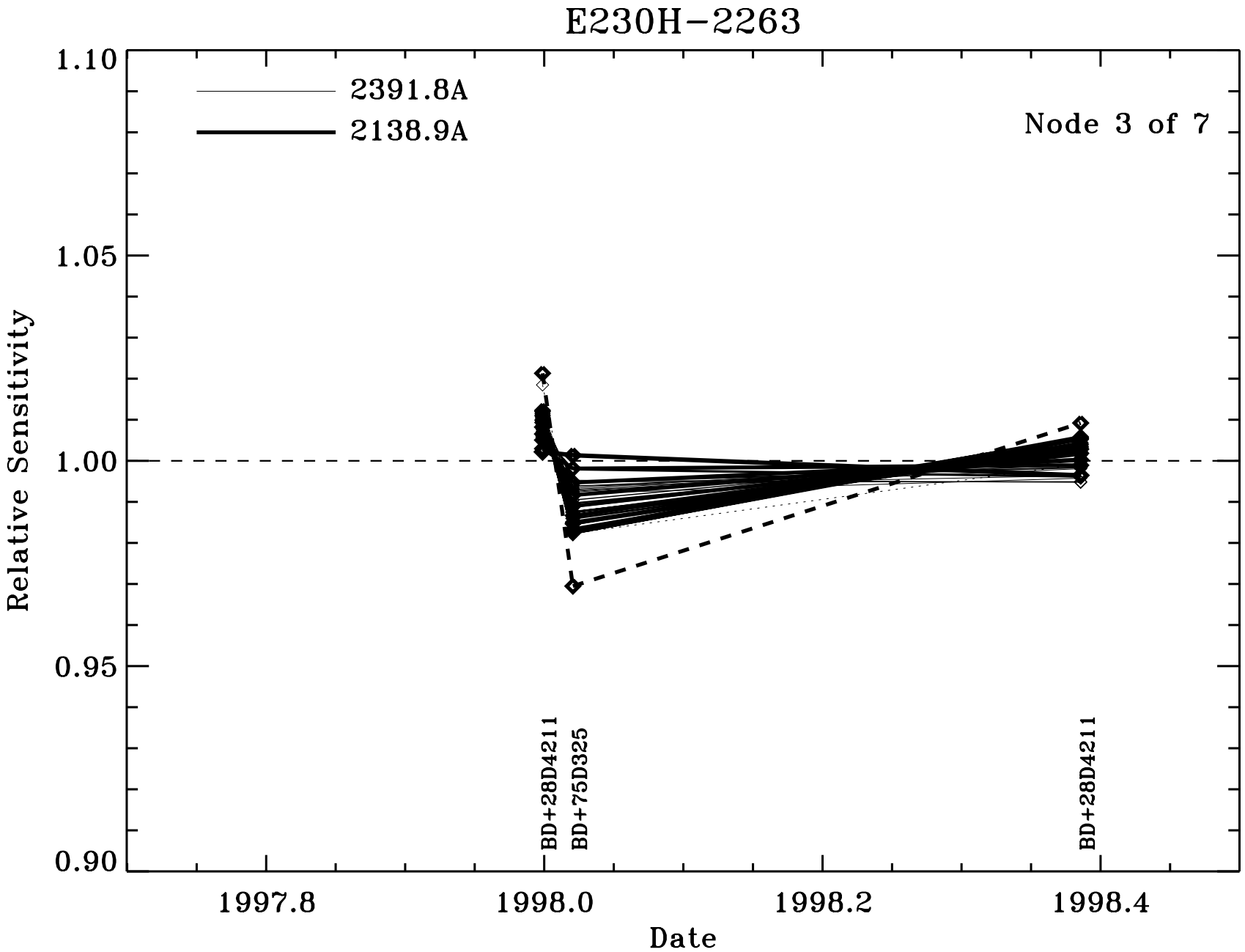
E230H-2263
2391.8A
2138.9A
Node 3 of 7
Relative Sensitivity
1.10
1.05
1.00
0.95
0.90
BD+28D4211
BD+75D325
BD+28D4211
1997.8
1998.0
1998.2
1998.4
Date
BOHLIN: echsnsall 3-Jun-1998 15:19

Fig. 6 (cont.)

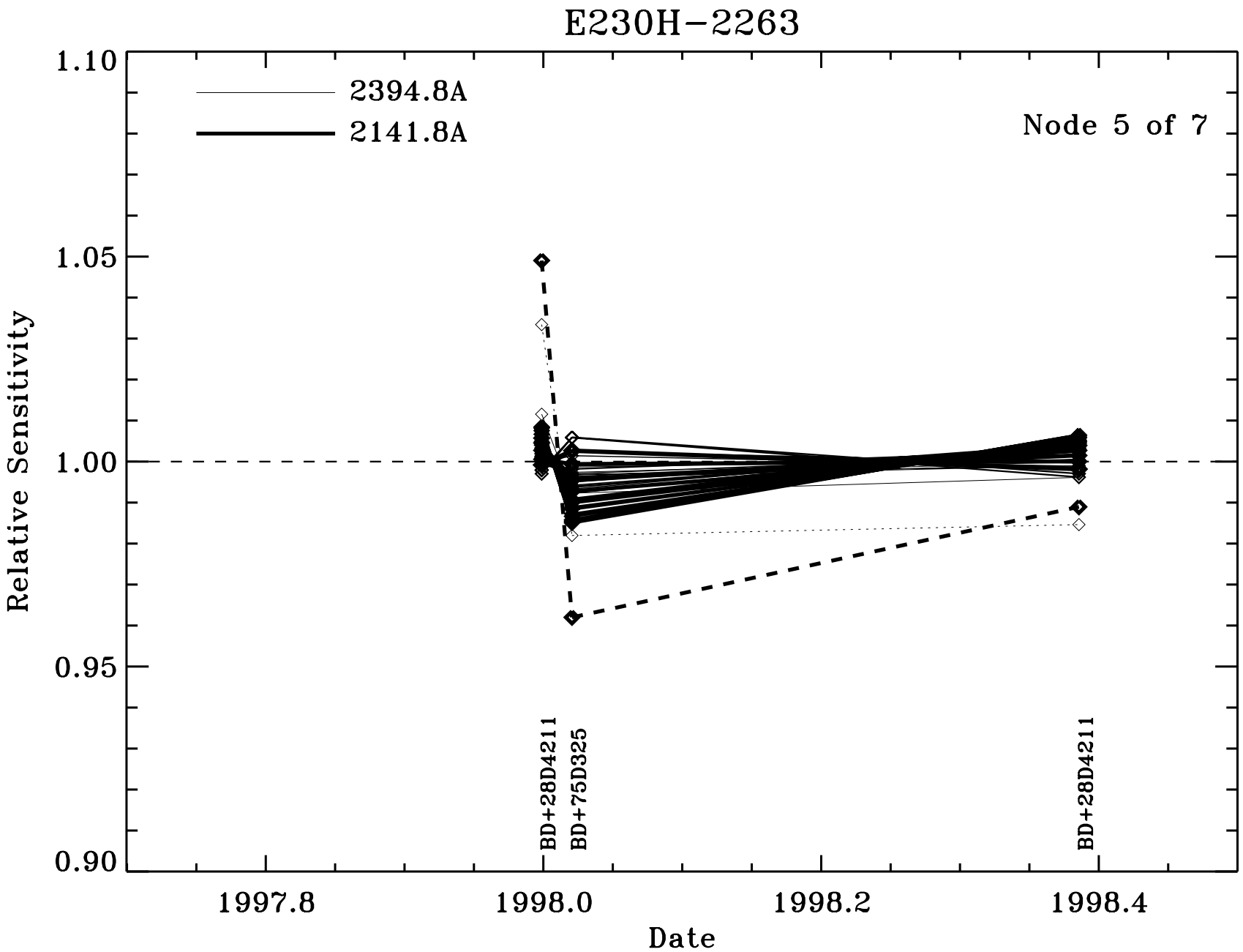
E230H-2263
2394.8A
2141.8A
Node 5 of 7
Relative Sensitivity
1.10
1.05
1.00
0.95
0.90
1997.8
1998.0
1998.2
1998.4
Date
BD+28D4211
BD+75D325
BD+28D4211
BOHLIN: echsnsall 3-Jun-1998 15:19

Fig. 6 (cont.)